# Solar Total Energy Program
# Semiannual Report
# April 1975 - September 1975

Solar Energy Projects Division, 5712

Sandia Laboratories
energy report

# SOLAR TOTAL ENERGY PROGRAM SEMIANNUAL REPORT

## April 1975 - September 1975

Edited by Roscoe L. Champion and
Michael W. Edenburn
Solar Energy Projects Division, 5712
Sandia Laboratories
Albuquerque, NM 87115

Approved:

J. A. Leonard

G. E. Brandvold

## ABSTRACT

This report describes the activites of the Sandia Laboratories
Solar Total Energy Program during the 6-month period,
April 1975 through September 1975. Included are highlights
of the period, descriptions of the system and its components,
including recent modifications, and the results of systems
analyses and component testing.

CONTENTS

CONTENTS (cont.)

TABLES

FIGURES

FIGURES (Cont.)

SOLAR TOTAL ENERGY PROGRAM SEMIANNUAL REPORT
April - September 1975

## SECTION I. INTRODUCTION

The Solar Total Energy Program is the outgrowth of a series of exploratory system studies, conducted at Sandia Laboratories since 1972, concerning potential uses of solar energy.

The studies have coalesced into the concept of a cascaded system in which solar energy collected at a central area is used to provide electrical power, heating, air-conditioning, and hot water to a wide spectrum of users. A comprehensive hardware program designed to demonstrate the solar total energy concept is being conducted concurrently with systems analyses performed to investigate various additional means of implementing solar total energy concepts.

The primary objective of the Solar Total Energy Program is to determine and demonstrate the technical and economic feasibility of solar total energy systems for a variety of sites and loads. In support of the primary objective additional objectives of the program are (1) to construct a system (Solar Total Energy Test Facility) which is sufficiently versatile to be used as an engineering evaluation center or test bed, for further development of individual components or other solar energy subsystems, (2) to encourage private sector participation in the program and in the development of components for the system, (3) to determine those areas of research and development that offer the greatest payoffs, and (4) to develop and validate a systems analysis computer program capable of evaluating the great number of possible combinations of total energy system configurations.

The Solar Total Energy System, depicted in block diagram form in Figure 1.1 and as an artist's concept in Figure 1.2 (also in a photo, Figure 3.1), will operate as follows: A heat transfer fluid is heated in the receiver tubes of the solar collectors by reflected and focused solar radiation. This fluid is pumped to the high-temperature storage tank. On a demand basis, fluid is extracted from this storage and pumped to the boiler which produces superheated toluene vapor to power the turbine/generator. The boiler can also be operated from a fossil-fuel-fired heater to insure continuity of operation during extended cloudy periods. Turbine condenser coolant is stored in the low-temperature stratified fluid tank and, on a demand basis, fluid is extracted to power heating, air-conditioning, and hot-water-heating components.
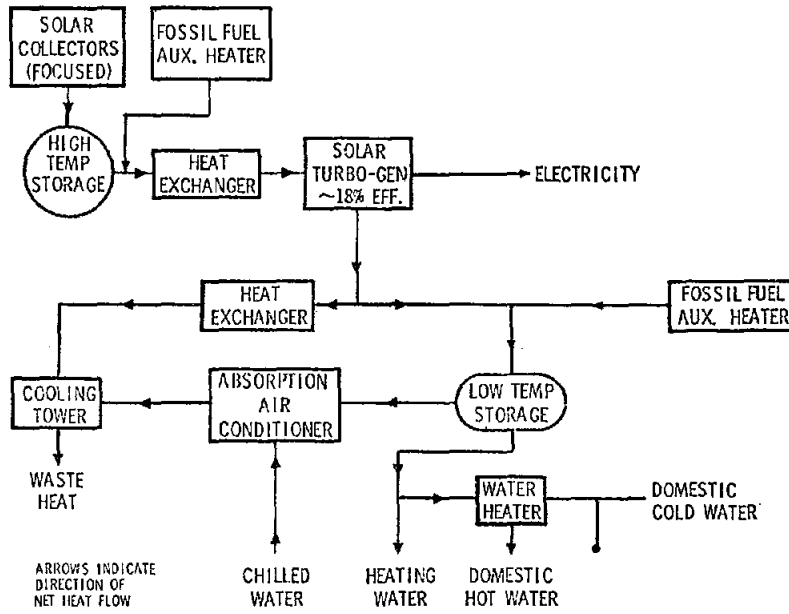
Figure 1.1 Solar Total Energy System Simplified Schematic
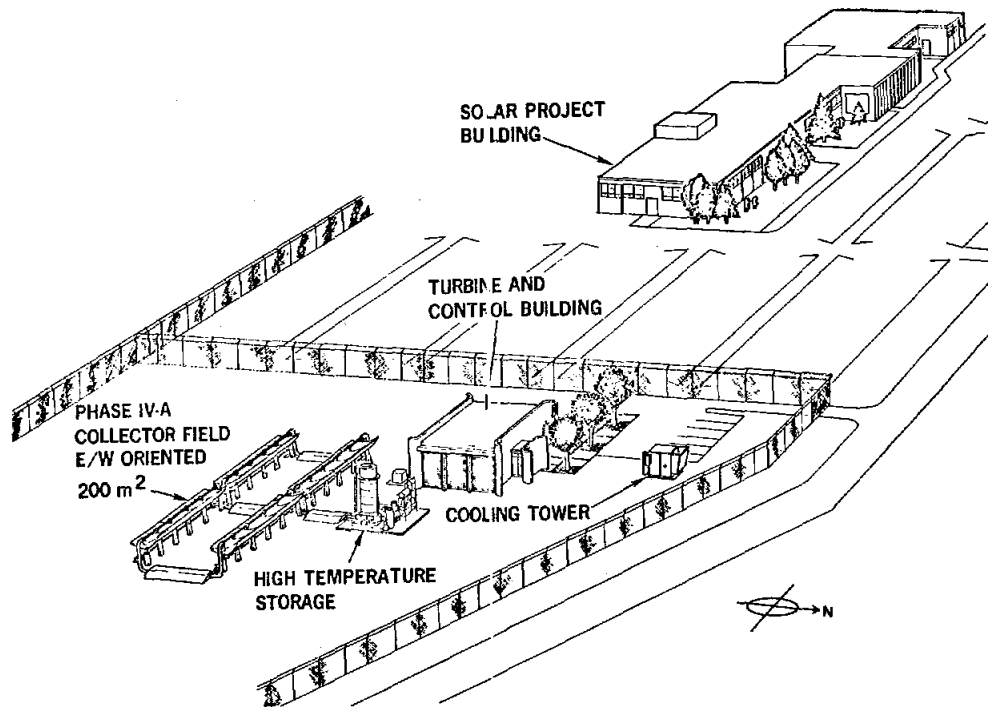


Figure 1.2 Solar Total Energy Test Facility

The overall Solar Total Energy Program consists of seven phases with the work reported in this document being part of Phase IV. The program, which began in 1972 with background research and exploratory analysis, has progressed to the present hardware stage in which the Solar Total Energy Test Facility is being built to provide energy for an 1100 m$^2$ office building, the Solar Project Building. The program will conclude with the construction and operation of a solar total energy pilot plant, which is expected to be done in cooperation with commercial interests.

Phase I, II, and III, which emphasized preliminary studies and designs, have been completed. Phase IV-A began in July 1974 and will end late in 1976. Phase IV-A is the pivotal phase in that it marks the transition from the analysis and design effort to the hardward and construction effort. About 25% of the high-temperature, solar-to-electric portion of the system is to be put into operation during this phase. Data collection in the high-temperature regime is of primary importance because little operating experience in this area has been accumulated.

During Phase IV-B, which started in July 1975, the remainder of the collector field and storage capacity will be added, and the cascaded low-temperature portion of the system (heating, air-conditioning, and hot water) will be installed. Much of the Phase IV-B effort will be subcontracted.

Phase V will consist of operating the test bed under various conditions to gather and analyze engineering data which can provide a basis for the design of the pilot plant and for future solar energy systems. During this phase, the feasibility of supplying electric power, heat, and cooling to the Solar Project Building will also be demonstrated.

Phases VI and VII will consist of the design, construction, and operation of a pilot commercial solar total energy power plant. These phases will involve substantial private sector participation. The overall Solar Total Energy Program plan and major milestones are illustrated in Figure 1.3.

SOLAR TOTAL ENERGY PROGRAM

Fiscal Year

| Phase | 73 | 74 | 75 | 76 | 76a | 77 | 78 |
|---|---|---|---|---|---|---|---|
| I. Background Phase | ▼1 | | | | | | |
| II. Exploratory Study | | ▼ 2,3 | | | | | |
| III. Exploratory Development | | | ▼ ▼ ▼▼8 4 5 6,7 | | | | |
| IV. Development Model Installation | | | | | | | |
| A. Solar-to-Electric Components | | | ▼9 | ▼ 10, 11 | | ▼ ▼ 13 | 13a |
| B. Cascaded Components | | | | | | | |
| V. System Operation | | | | ▼ ▼ 12 14 | | ▼ 16 | ▼ 15 |
| VI. Pilot Plant Design and Construction | | | | | | | ▼17 |
| VII. Pilot Plant Operation | | | | | | | |
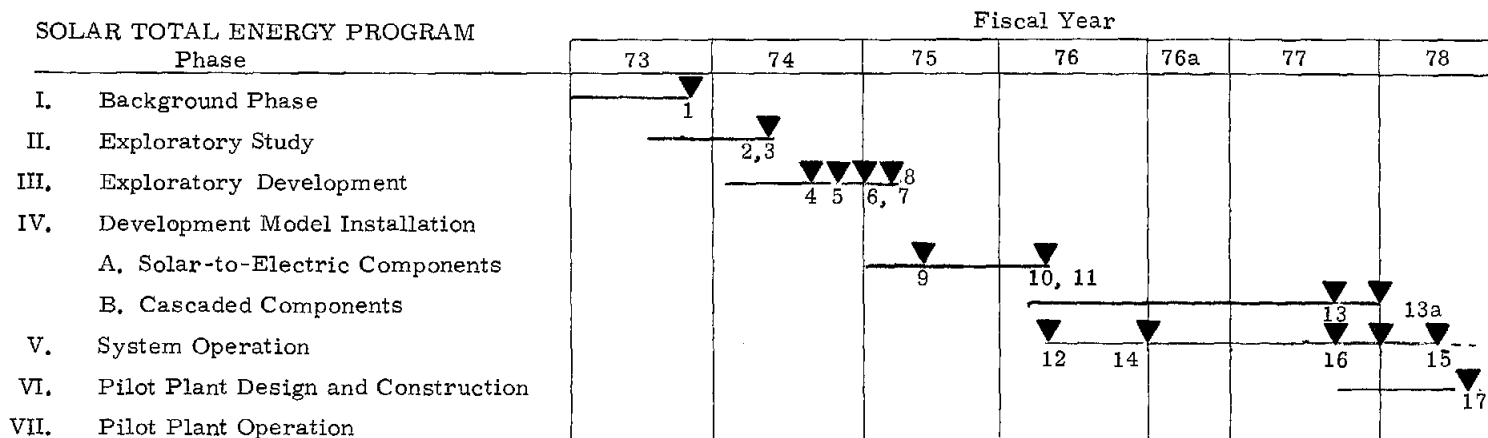
Milestones:

1.  Completion of Phase I
2.  Preliminary system design complete
3.  Economic evaluation complete
4.  Collector evaluation facility complete
5.  System analysis program operational
6.  Baseline system design complete
7.  Phase IV-A proposal submitted
8.  Phase IV-A supplementary proposal submitted
9.  System analysis program loads profiles established
10.  Partial collector field, storage, and turbine-generator test bed complete
11.  Solar and weather input data established
12.  Initial operation of partial Solar Total Energy test bed
13.  Remainder of Solar Total Energy System completed
13a.  Subcontracted collector subsystems completed
14.  System analysis program refined and revalidated
15.  Operation of complete Solar Total Energy System
16.  Demonstration of Solar Project Building
17.  Pilot plant preliminary design

Figure 1-3.  Solar Total Energy Program Schedule and Milestones

# SECTION II. OVERVIEW OF ACTIVITIES

## Highlights

The following activities and milestones highlighted this reporting period:

- RFP for Collector Field Subsystems Released in September
- Solar Total Energy Symposium Hosted in July
- Collector Test Facility Relocated Outside Tech Area
- Installation of Reflector Structures 75% Complete
- Delivery of Aluminized Mylar and Teflon Reflectors From Sheldahl 50% Complete
- All Receiver Tubes Delivered From BKC and Being Assembled in Glass Shop
- Black Chrome Process Spec Developed by SLA and BKC Proving Adequate
- High-Temperature Storage Tank Delivered from SLL--Plumbing and Instrumentation Underway
- Turbine Generator Accepted at Sunstrand and Delivered
- Turbine and Control Building Completed
- All Instrumentation and Control System Hardware on Hand-- Installation Underway.

## Reports, Presentations and Patent Disclosures
### April 1 to September 30, 1975

### Publications

B. W. Marshall, "Analysis of a 1000-Home Solar Total Energy Community Using Clear Air Solar Intensity," SAND75-0097, Sandia Laboratories, May 1975.

G. W. Treadwell, "Selection of Parabolic Solar Collector Field Arrays," SAND74-0375, Sandia Laboratories, May 1975.

L. N. Ernst and R. S. Rusk, "Solar Collector Test Facility," SAND74-0405, Sandia Laboratories, June 1975.

M. W. Edenburn and N. R. Grandjean, "Energy System Simulation Computer Program-SOLSYS," SAND75-0048, Sandia Laboratories, June 1975.

R. B. Pettit, "Total Hemispherical Emittance Measurement Apparatus for Solar Selective Coatings," SAND75-0079, Sandia Laboratories, June 1975.

M. W. Edenburn, "Building 832 and Small Neighborhood Applications for Sandia Laboratories Solar Energy System Test Bed," SAND75-0202, July 1975.

Solar Community System Analysis Projects (final report to NSF), Solar Energy Systems Division 5717, SAND75-0250, July 1975.

R. W. Harrigan, Solar Total Energy Program Semiannual Report, October 1974-March 1975, Solar Energy Projects Division 5712 and Solar Energy Systems Division 5717, SAND75-0278, July 1975.

D. M. Mattox, et al., "Selective Solar Photothermal Absorbers," SAND75-0361, Sandia Laboratories, July 1975.

M. W. Edenburn and N. R. Grandjean, "Brief Description of SOLSYS-Energy System Simulation Computer Program," SAND75-0388, September 1975.


Presentations


R. P. Stromberg, "The Sandia Project and Alternative Systems," Solar Total Energy Technology Symposium, Sandia Laboratories, Albuquerque, New Mexico, July 10, 1975.

R. H. Braasch, "Intermediate Temperature Solar Collector Subsystems," Solar Total Energy Technology Symposium, Sandia Laboratories, Albuquerque, New Mexico, July 11, 1975.

B. J. Petterson, "Materials and Controls for Solar Collectors," New Mexico Solar Energy Society, July 12, 1975.

E. C. Boes, "Estimating the Direct Component of Solar Radiation," presented at 1975 International Solar Energy Society Conference, Los Angeles, California, July 28, 1975.

R. W. Harrigan, "Photochemical Solar Energy Conversion," presented at 1975 ISES, Los Angeles, California, July 29, 1975.

B. W. Marshall, "Analysis of a Solar Total Energy System," presented at 1975 ISES, Los Angeles, California, July 30, 1975.

M. W. Edenburn, "Sandia Laboratories Energy System Simulation Computer Program, presented at 1975 ISES, Los Angeles, California, July 30, 1975.

R. B. Pettit and P. R. Sowell, "Solar Absorptance and Emittance Properties of Several Solar Coatings," presented at 1975 ISES conference, Los Angeles, California, July 30, 1975.

G. W. Treadwell, "Test Results from a Parabolic-Cylindrical Solar Collector," presented at 1975 ISES, Los Angeles, California, July 31, 1975.

M. W. Edenburn, "Performance Analysis of a Cylindrical Parabolic Focusing Collector and Comparison with Experimental Results," presented at 1975 ISES, Los Angeles, California, July 31, 1975.

J. A. Leonard, "Solar Total Energy Project," Interagency Mechanical Operations Group Conference, Albuquerque, New Mexico, October 8, 1975.

J. A. Leonard, "ERDA Solar Energy Programs," Air National Guard Civil Engineering Conference, St. Louis, Missouri, October 9, 1975.

J. A. Leonard, "Sandia's Solar Total Energy Program," presented at Society for Advancement of Materials and Process Engineering Conference, Albuquerque, New Mexico, October 15, 1975.

R. L. Champion, "Approaches to Fabrication of Parabolic Trough Reflectors," presented at SAMPE Conference, Albuquerque, New Mexico, October 15, 1975.

E. C. Boes, "Sandia's Solar Data Research," Geophysical Monitoring and Resource Assessment Program Planning Meeting, ERDA/Hq Solar Energy Division, Washington, D. C., April 1975.

R. W. Harrigan, "Solar Total Energy," Sandia Kiwanis Club, Albuquerque, New Mexico, April 1, 1975.

R. W. Harrigan, "Solar Energy Research at Sandia Laboratories," Rio Rancho Civic Association, Albuquerque, New Mexico, April 15, 1975.

R. P. Stromberg and B. W. Marshall, "Solar Process Heat," Southern California Gas, Los Angeles, California, April 22, 1975.

B. W. Marshall, "A Look at Solar Energy Activities in the United States," Science Now Program, Nevada Operations Office, ERDA, Las Vegas, Nevada, April 25, 1975.

R. P. Stromberg and R. H. Braasch, "Solar Total Energy," Solar Thermal Semiannual Review, Houston, Texas, April 29, 1975.

R. W. Harrigan, "Solar Total Energy," University of New Mexico, Department of Mechanical Engineering, Albuquerque, New Mexico, May 2, 1975.

B. W Marshall, "Solar Energy Research at Sandia," Instrument Society of America, Las Vegas Section, Las Vegas, Nevada, May 6, 1975.

B. W. Marshall, "Solar Energy Research in the United States," Community School, Albuquerque Public Schools, Albuquerque, New Mexico, May 27, 1975.

R. P. Stromberg, "Solar Total Energy," American Nuclear Society, New Orleans, Louisiana, June 12, 1975.

R. H. Braasch, R. P. Stromberg, G. E. Brandvold and J. A. Leonard, Solar Total Energy Program Review, ERDA/Hq Solar Energy Division, Washington, D. C., July 1, 1975.

R. P. Stromberg and B. W. Marshall, "Solar Process Heat," Monsanto Research Corporation, Dayton, Ohio, July 15, 1975.

R. W. Harrigan, "Solar Energy," Rio Grande Kiwanis Club, Albuquerque, New Mexico, July 21, 1975.

J. A. Leonard, "Solar Total Energy Project," Org. 3600 Technical Symposium, Albuquerque, New Mexico, August 7, 1975.

B. J. Petterson, "Solar Heating and Cooling," Sierra Club, Albuquerque, New Mexico, August 14, 1975.

R. H. Braasch, "Sandia's Solar Total Energy Test Facility," NATO-CCMS tour, Albuquerque, New Mexico, August 15, 1975.

B. W. Marshall, "Sandia Solar Total Energy Program," Belen Rotary Club, Belen, New Mexico, August 20, 1975.

R. H. Braasch, "Solar Energy and Sandia's Involvement in this Endeavor," Marine Corps Reserve Officers Association, Interagency Mechanical Operations Group, KAFB, New Mexico, September 8, 1975.

M. W. Edenburn, "Solar Energy Applications for Residential Construction," New Mexico Association of Building Design, Albuquerque, New Mexico, September 11, 1975.

R. W. Harrigan, "Solar Energy Research at Sandia," Reserve Officers Association, KAFB, New Mexico, September 16, 1975.

R. H. Braasch, "Solar Total Energy Program and Tour of Sandia's Test Facilities," IEEE Meeting, Albuquerque, New Mexico, September 23, 1975.

A. F. Veneruso, "Power Conditioning, Control and Storage," ERDA/Hq Photovoltaics Branch, Washington, D. C., September 25, 1975.

J. A. Leonard, "Solar Total Energy and Tour of Test Facility," New Mexico Pueblo Governors, Albuquerque, New Mexico, September 26, 1975.

R. P. Stromberg, "Solar Total Energy Program," Environmental Editors Tour, sponsored by Mobil Oil, Albuquerque, New Mexico, October 3, 1975.

R. W. Harrigan, "Solar Total Energy," Building Contractors Association, Albuquerque, New Mexico, October 16, 1975.


Patent Disclosures


G. L. McCoach and J. A. Leonard, "180° Field of View Sun Sensor," June 6, 1975.

# SECTION III. PROGRAM DESCRIPTION AND STATUS

## Task 1. Program Management

Phase IV of the Solar Total Energy Program has been organized into a work breakdown structure of tasks and subtasks. The complete work breakdown structure is given in the Contents (page 5). The responsibilities of Program Manager of the Solar Total Energy Program were assigned to James A. Leonard, effective September 1, 1975. A chart illustrating complete program staffing is shown in Appendix D. This section presents the detailed status of each program task.

## Task 2. System Management

### 2.1 System Engineering

Future Quadrants of the Collector Field -- With the initial quadrant of 200 $m^2$ under construction, system engineering efforts have expanded to include procurement of the remaining three quadrants to be incorporated under Phase IV-B. To this end, a Request for Proposal (RFP) has been prepared and sent to a broad range of companies who have indicated interest in design, development and, in subsequent phases, fabricating and installing a quadrant of the collector field. Nationwide advertising space was also purchased in the Wall Street Journal on September 9, 1975, and in Commerce Business Daily on September 4, 1975, inviting contacts by qualified firms. A total of 52 RFP's have been sent to respondents to the advertising and to interested companies in the solar industry.

The RFP requested proposals for 200 $m^2$ of concentrating distributed solar collector field subsystems including design, construction and preliminary operation. The work is to be divided into two phases. Phase I will include system analysis, configuration selection, collector array analysis, economic analysis, preliminary design plus bench model and component testing. Initial contracts will be for Phase I only. Phase II, presently planned for FY 78, will consist of final collector field development and detailed design, fabrication and procurement, full-size collector testing, and construction, installation and initial operation of the collector field.

System Schematic -- The latest Solar Total Energy Program system schematic is shown in Figure 2-1. Only minor changes have been made in the system design or operating parameters during this reporting period. With this stability in system definition, the project effort has been directed toward integration of the components into a functional system.
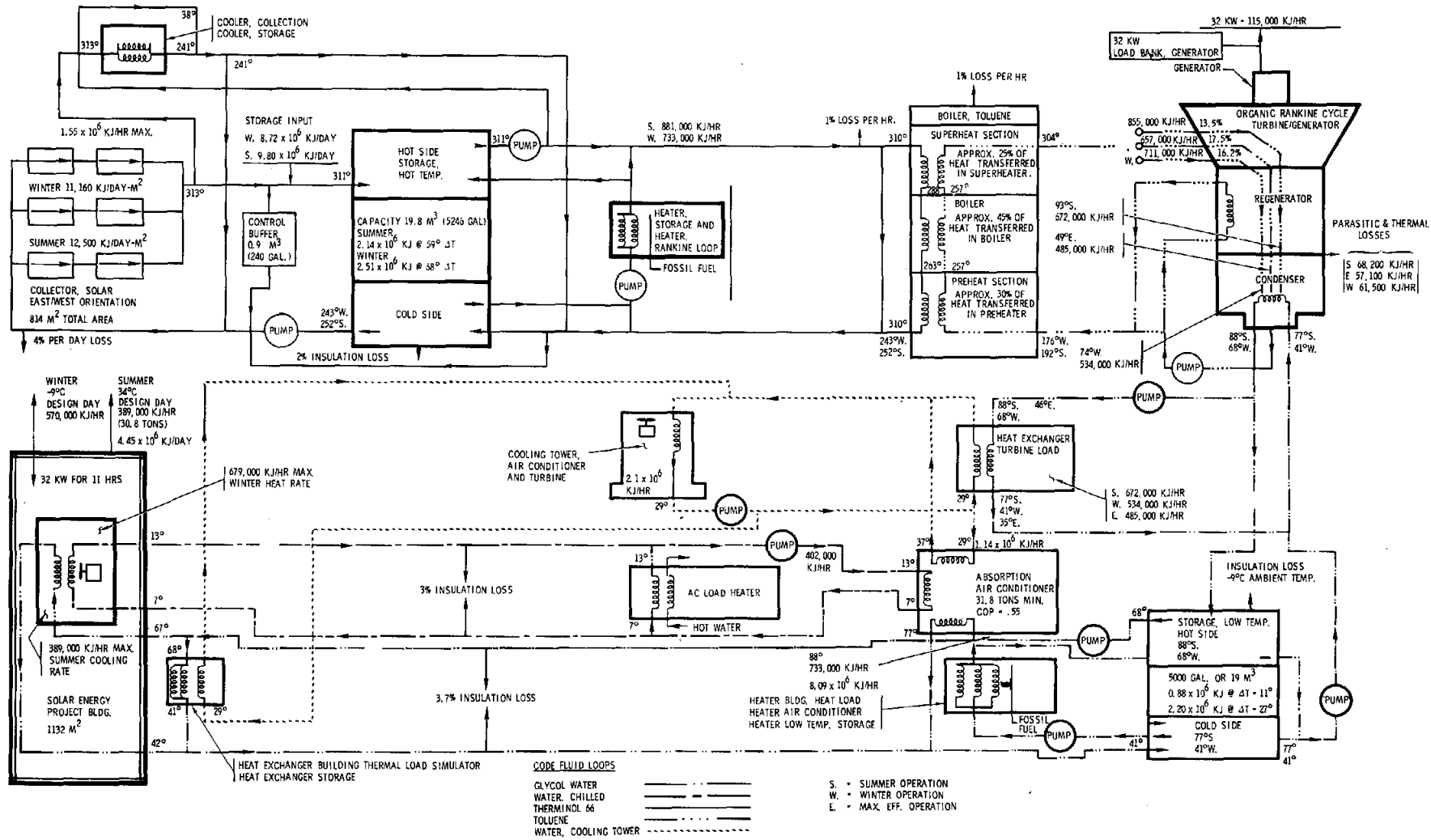
Figure 2.1. Solar Total Energy System Schematic

Rankine Cycle Turbine Performance -- As noted in our last semiannual report, the performance of the Rankine cycle turbine has been lower than anticipated. The turbine/generator system has been operated at Sundstrand Aviation for a total of 237 hours, during which measurements were made of system performance. Results indicate cycle efficiencies lower than expected.

As a result of the lower turbine performance, a system analysis has been conducted to determine the effects on the rest of the solar total energy system. These effects are discussed below. Alternative courses of action have been investigated but no changes will be made until the operating efficiencies are confirmed by operation of the Rankine cycle system at Sandia.

Table 2-I compares the predicted cycle efficiencies with the actual efficiencies. The original performance goals were to generate 35 kW with 32 kW for the Solar Total Energy Project Building load and 3 kW for the Rankine cycle auxiliary components (parasitic load). The efficiencies of Table 2-I are calculated by dividing the electrical output by the turbine input power for conditions with and without parasitic loads. Generation of 35 kW (or 32 kW) can be achieved by increasing the design boiler input by 27% (or 16%).

TABLE 2-I

Rankine Cycle Efficiencies and Effects

| Cycle Temperature Limits | | Efficiencies (%) | | |
|---|---|---|---|---|
| | | Predicted w/parasitics | Actual | |
| ($^{\circ}$C) | ($^{\circ}$F) | | w/parasitics (35 kW) | w/o parasitics (32 kW) |
| 296/93 | 565/200 | 13.6 | 10.6 to 10.9 | 11.6 to 11.9 |
| 296/74 | 565/165 | 16.2 | 12.2 to 13.3 | 13.3 to 14.5 |
| 296/59 | 565/138 | | 13.0 | 14.2 |
| 296/49 | 565/120 | 17.5 | | |

If the 32-kW turbine/generator output remains a goal, the following changes in the system may be required:

Collector Area -- Required area would be increased by 16% or 130 m$^2$ (1400 ft$^2$). Since Phase IV-A only calls for 25% of the field, this effect can be temporarily ignored. When the remaining field is constructed, it can be increased by 16% if initial system operation confirms the need.

Storage Capacity -- For Phase IV-A the effect is to decrease the maximum operating time of the turbine from 48 to 41 minutes, which is acceptable.

19

Boiler -- The boiler is currently rated at 955,800 kJ/hr (906,000 Btu/hr). The new demand rate would be about 1,076,100 kJ/hr (1,020,000 Btu/hr). The boiler may meet the new load either because of the manufacturer's conservatism or by increasing the T-66 flow rate (at the expense of storage ΔT). This component presently represents the major constraint to heat flow in the system. However, because of the cost, it will not be replaced.

Storage Fluid Transfer System -- The system pump has a 151 ℓ/min (40 gpm) capability and the new requirement is 170 ℓ/min (45 gpm). Consequently, the system is marginal. In order to prevent this item from being the bottleneck, a new motor, gear box, and motor controller capable of 170 ℓ/min would need to be ordered for incorporation later. Initially, the system will be operated with the present pump.

Condenser Fluid Transfer System -- Present pump capacity is 284 ℓ/min (75 gpm) at a $359 \times 10^3$ Pa (52 psi) head. The new requirement is 333 ℓ/min (88 gpm) at a $359 \times 10^3$ Pa head to accommodate a 19% increase in heat flow from the condenser. This pump would need to be modified by using a larger, higher speed motor and a new impeller.

Heat Exchanger, Turbine Load -- The heat exchanger was not sized for maximum heat flow conditions, i.e., summer operation. It was sized for a minimum driving ΔT between the cooling water and condenser water, i.e., equinox operation. The new requirement is about 608,000 kJ/hr (577,000 Btu/hr) -- the exact value is not known as the turbine was not tested for equinox operation -- and the unit is sized for 527,500 kJ/hr (500,000 Btu/hr). The required heat rate can be achieved either by increasing the cooling water flow rate or by operating when the dew point is below 29°C (85°F) (most of the year in Albuquerque).

Cooling Tower System -- The cooling tower is large enough to handle operation of the turbine and air conditioner simultaneously as required; the tower rating is $2.11 \times 10^6$ kJ/hr ($2 \times 10^6$ Btu/hr) and the new requirement is $2.05 \times 10^6$ kJ/hr ($1.94 \times 10^6$ Btu/hr). However, the pump may not be big enough to handle the increased flow rate to the turbine-load heat exchanger. Since the system is available, it will be tested to determine its capability, and if it is not satisfactory, 6.1 m (20 feet) of pipe and 3 control valves in the turbine-load heat-exchanger loop could be changed in Phase IV-B.

20

## 2.2 System Analysis

Program SOLSYS -- The solar energy system simulation computer program SOLSYS is essentially the same as at the end of the last reporting period. New electric load and solar intensity data are available to the program and these are described under Task 8. Reports describing SOLSYS briefly[1] and in detail[2] have been published, and a description of SOLSYS was presented at the 1975 International Solar Energy Society conference in Los Angeles.[3]

SOLSYS is presently being packaged and will be submitted to the ERDA computer code dissemination center at Argonne National Laboratory.

Economic Analysis -- The computer program and various economic factors employed in the computation of levelized annual revenue requirements for solar total energy systems have been described in previous progress reports.[4,5] No changes have been made in the program except for adding the option to choose one of three depreciation methods: straight line, sum-of-years digit, and double-declining balance. The computer program computes the total present value of the solar total energy plant, as well as the level annual revenue requirement. The plant is assumed to be constructed at the start of the study period with no time period allowed for construction.

Mixed Community Cascaded vs Noncascaded Systems -- In this study a cascaded solar energy system and a noncascaded system were compared. Both were applied to the thermal and electric loads of the mixed community described in the last semiannual report,[5] and in Section 8.1 of this report.

Both systems used east-west-axis, focusing collectors to heat Therminol 66, which was stored in a stratified tank and subsequently removed to preheat, boil, and superheat the working fluid in a Rankine power generation cycle. In the cascaded system, water extracted heat from the power cycle's condenser at 62°C (143°F) during the winter and spring, and at 102°C (215°F) during the summer and fall. The hot water was stored in a stratified unit and distributed for space heating, air conditioning, and water heating. The power cycle in the noncascaded system had a condenser temperature of 32°C (89°F), and rejected condenser heat was not used. The noncascaded system used flat-plate collectors at the site of the thermal load to provide heat for space heating, air conditioning, and water heating.

---

[1] M. W. Edenburn and N. R. Grandjean, "Brief Description of SOLSYS-Energy System Simulation Computer Program," SAND75-0388, Sandia Laboratories, September 1975.

[2] M. W. Edenburn and N. R. Grandjean, "Energy System Simulation Computer Program - SOLSYS," SAND75-0048, Sandia Laboratories, June 1975.

[3] M. W. Edenburn, "Sandia Laboratories Energy System Simulation Computer Program," 1974 ISES conference, July 29, Los Angeles.

[4] J. A. Leonard and S. Thunborg, "Solar Total Energy Program Quarterly Report, July-September 1975," SAND74-0398, Sandia Laboratories, December 1974.

[5] R. W. Harrigan, "Solar Total Energy Program Semiannual Report, October 1974-March 1975," SAND75-0278, Sandia Laboratories, July 1975.

The systems were simulated using SOLSYS and were run for four representative one-week periods in each of the four 1962 Albuquerque seasons. System specifications are summarized in Table 2-II. Table 2-III shows some initial capital costs for the two systems. Both systems require the same fossil fuel augmentation, so fuel costs are equal.

TABLE 2-II

Cascaded and Noncascaded System Specifications

|  | Cascaded | Noncascaded |
|---|---|---|
| Focusing Collector | | |
| Area (m2) | 81,300 | 70,100 |
| Flat-Plate Collector | | |
| Area (m$^2$) | 0 | 30,600 |
| High-Temperature Storage | | |
| Volume (m$^3$) | 3,700 | 2,500 |
| Low-Temperature Storage | | |
| Volume (m$^3$) | 2,700 | 2,900 |
| Power Cycle Efficiency (%): | | |
| Winter and Spring | .239 | .274 |
| Summer and Fall | .189 | .274 |
| Fuel Saved (%) | 69 | 68 |

TABLE 2-III

Capital Costs, Cascaded and Noncascaded Systems
(millions of dollars)

|  | Cascaded | Noncascaded |
|---|---|---|
| High-Temperature Storage | 3.56 | 2.35 |
| Low-Temperature Storage | .55 | 1.01 |
| Distribution System | 2.50 | 0 |

Figure 2-2 shows collector cost plus storage cost plus distribution cost for the noncascaded system divided by the cost for the cascaded system. Assuming that flat-plate collectors are less expensive than focusing collectors, per unit area, flat-plate collector cost must exceed $175/m$^2$ ($16.25/ft$^2$) if the cascaded system is to be competitive with the noncascaded system.

Flat-plate collectors cost significantly less than $175/m$^2$. Therefore, the total energy system is less attractive than the noncascaded system with separate electrical and thermal subsystems when applied to a whole community. But the fact that the cascaded system is inappropriate for a whole community does not mean that it is also inappropriate for small segments of a community (which may have a density and a thermal-to-electrical load ratio favorable to such use).
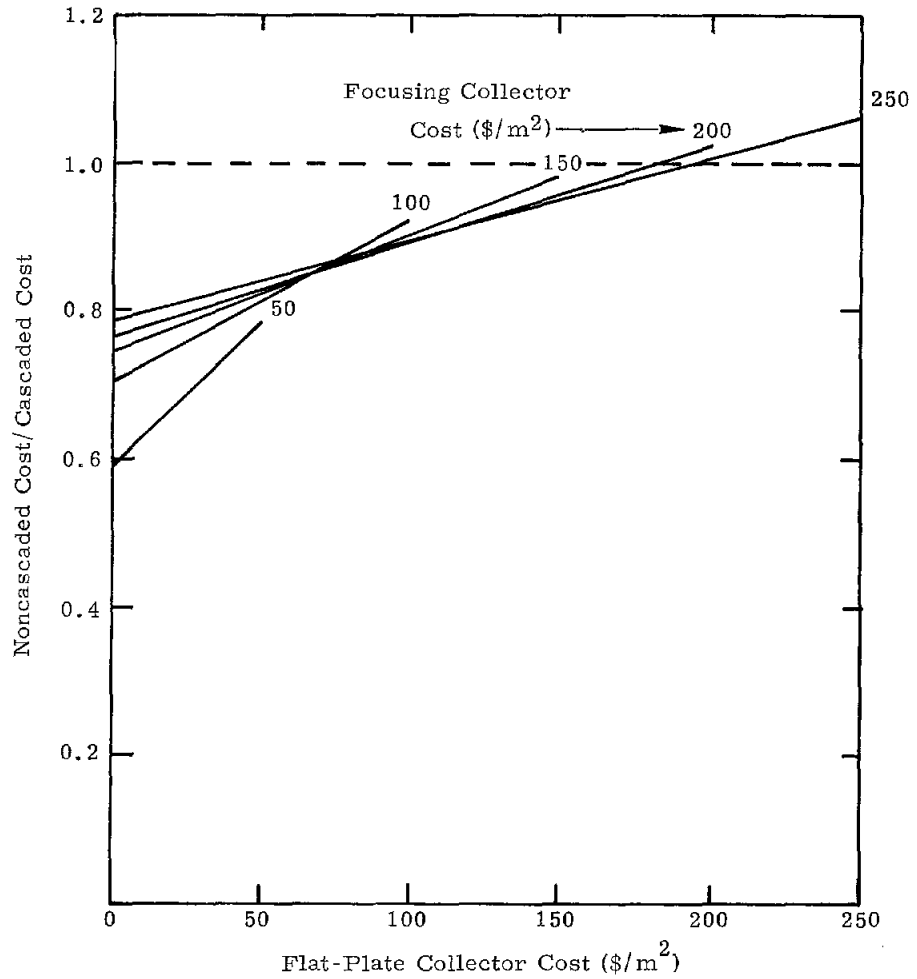
Figure 2-2.   Collector, Storage, Distribution System Costs for
Cascaded and Noncascaded Systems

Our hypothetical community contains four density zones of residential dwellings as well as
three schools and a commercial complex. The economics of a solar total energy system sized
to meet the community electrical demands have been evaluated; proper system sizing was ex-
amined as well as the effect of dwelling-unit density on economics. Table 2-IV reproduces
part of Table 2-II and adds component sizing for a high-density subset of the community. A
report will be published describing the life-cycle cost analysis in detail,[1] and those results are
summarized here.

---

[1] R. W. Harrigan, "Application of Solar Total Energy to a Mixed-Load Community," SAND75-0542,
Sandia Laboratories, December 1975.

TABLE 2-IV


Solar Energy System Component Descriptions
(For 1962 Albuquerque solar intensity and weather data)

| | Entire 2000-Dwelling Community | | High-Density Area Only | |
|---|---|---|---|---|
| | Cascaded | Noncascaded | Cascaded | Noncascaded |
| Collector Area, $m^2$ | 81,300 | 70,100 | 32,500 | 28,000 |
| High-Temp Storage, $m^3$ [a] | 3,700 | 2,500 | 1,400 | 950 |
| Peak Electric Demand, $MW_e$ | 4.0 | 4.0 | 1.5 | 1.5 |
| Low-Temp Storage, $m^3$ [b] | 2,300 | -- | 1,500 | -- |
| Fuel Burned, $10^9$ kJ/year [c] | 153.3 | 92.0 | 54.8 | 32.9 |
| Average Turbine Effectiveness, % | 21.5 | 27.0 | 21.5 | 27.0 |

Note [a] One $m^3$ of high-temperature storage equals 0.22 GJ at $\Delta T = 115°C$.

[b] One $m^3$ of low-temperature storage equals 0.086 GJ at $\Delta T = 20°C$.

[c] Extrapolated from results of typical one-week computations in each of the four seasons.


The effects of providing for distribution of low-temperature thermal energy are reflected in Table 2-V, which indicates that cascading is advantageous in a high-density-load situation where the distribution system is compact. The extra cost of distributing thermal energy from an on-site solar power plant must be compared to the revenues from the sale of that energy to determine the cost effectiveness of cascading but, for the entire community, the cost of such distribution is $786,500/yr while the revenues generated are only $616,400/yr. However, for the high-density subcommunity, a system cost of $269,100/yr generates $295,300/yr in revenues from the sale of thermal energy. Thus, not only would a thermal distribution system for the high-density areas be profitable, it would help pay for the electric generation system which does not break even. The economic assumptions used for this analysis are given in Table 2-VI.

TABLE 2-V

Summary of Annual Revenue Requirements
for Solar Total Energy Systems

| Community | Solar Plant Annual Revenue Requirements [a] ($x10^3$) | | | | | Cascading Cost | Solar Plant Annual Revenues [b] ($x10^3$) | | |
|---|---|---|---|---|---|---|---|---|---|
| | Electrical Plant | Thermal Distribution | Electrical Distribution | General Plant | Total | | Thermal | Electric | Total |
| Entire 2000: | | | | | | | | | |
| Cascaded | 1,935.4 | 413.2 | 79.6 | 197.6 | 2,625.8 | 786.5 | 616.4 | 901.0 | 1,517.4 |
| Noncascaded | 1,570.6 | 0.0 | 79.6 | 189.1 | 1,839.3 | | 0 | 901.0 | 901.0 |
| High-Density: | | | | | | | | | |
| Cascaded | 791.4 | 120.7 | 61.9 | 175.9 | 1,149.9 | 269.1 | 295.3 | 339.2 | 634.5 |
| Noncascaded | 645.2 | 0.0 | 61.9 | 173.7 | 880.8 | | 0 | 339.2 | 339.2 |

Notes: a Based on collector cost of $107/m^2$.

   b Based on $4/GJ levelized cost for fossil fuel and $10.60/GJ electric cost at residence.

TABLE 2-VI

Economic Parameters for Solar Total Energy Analysis

● Capital Financing

| | % Holdings | Required Rate of Return (%) | | |
|---|---|---|---|---|
| | | Inflation | Plus | Total |
| Debt (bonds) | 60 | 7 | 2.5 | 9.5 |
| Equity (stocks) | 40 | 7 | 4.5 | 11.5 |

● Capital Recovery Factor Before Taxes

   System Life = 29 years

   Income Tax Rate = .50

   Effective Interest Rate

   $(0.025) (0.60) + 2(0.045) (0.40) = 0.051$

   Capital Recovery Factor

   CRF (for 29 yr @ 0.051) = 0.06678

● Levelized Annual Fuel Costs

   At city gate    $1.50/GJ

   At residence    $4.00/GJ

● Collector Cost - $107/m^2$

An additional outcome of the study was the realization that optimum system size is determined by maximum use of both high- and low-temperature energy. Since only about 20% of the total cost of electricity is due to fuel cost, increases in future fuel prices should not affect electricity prices as much as residential fuel prices. Thus, the sale of low-quality thermal energy, which would compete directly with fossil fuel for heating and cooling, is very beneficial to an on-site solar power generation plant. In fact, the solar system which maximizes solar energy use in the 2000-dwelling-unit load is one designed to generate only enough low-temperature thermal energy to meet the average winter heating and hot-water demands. Such a system would meet 67% of the electric load, which represents most of the constant base load and all peak loads; the remaining 33% represents a small constant portion of the base load which must be obtained from other sources.

An additional feature pointed out by Table 2-V is the penalty paid by the smaller system designed to service the high-density subcommunity. While this system generates less than one-half the power of the 2000-dwelling-unit system, the general plant costs are almost equal to those of the larger system, indicating that both systems require essentially the same support personnel and structure.

The results of this analysis indicate that, with a levelized residential value of $4/GJ ($4.22/MBtu) for thermal energy, the solar total energy plant's revenues do not equal its revenue requirements. For a system designed around the winter thermal load, as described above, a levelized value of approximately $6.30/GJ ($6.65/MBtu) for thermal energy would be necessary for the solar plant's revenues to equal its revenue requirements. Figure 2-3 shows the relationship between 1975 fuel prices and 29-year levelized fuel prices. To give a perspective: $6.30/GJ energy is equivalent to the cost of propane increasing, on the average, about 3.5% above inflation for 29 years; $6.30/GJ is also less than the 1975 cost of electrical energy at $0.025/kWh.
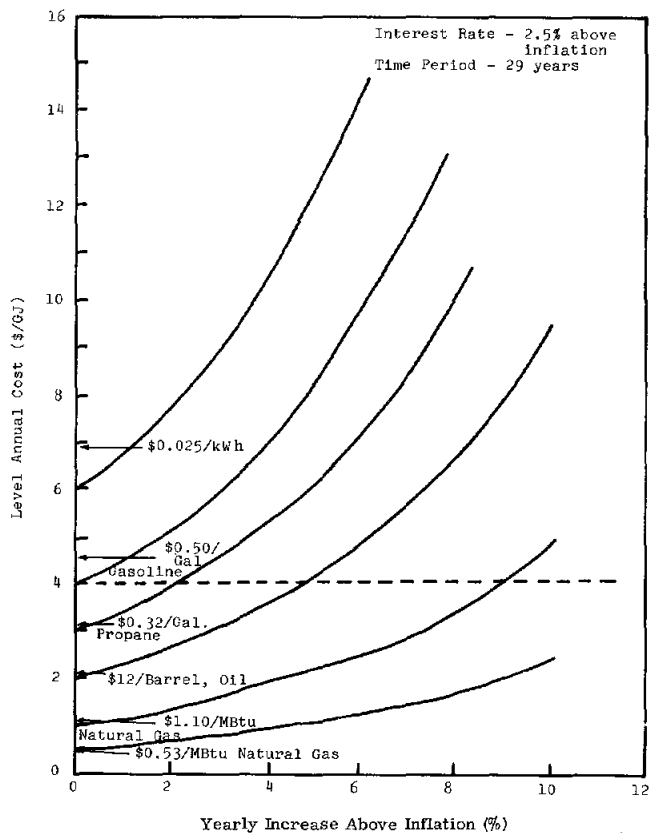
Figure 2-3. Levelized Fuel Prices

Cascaded Solar Total Energy System With Flywheel Storage -- A comparative analysis was made of various solar total energy system configurations serving a mixed-load community. One was a cascaded solar total energy system using a flywheel for kinetic energy storage. The principle components distinguishing the flywheel system from the other systems are:

- A 93,797-m$^2$ field of parabolic-trough, focusing collectors

- A 47,500-kWh flywheel system for energy storage to meet the electrical load outside of sunshine hours. (Storage capability was established to meet overnight electric load requirements of the community. The energy exchange process for the input and output from the flywheel were both assumed to be at 90% conversion efficiency.)

- A low-temperature storage capability consisting of a 4500-m$^3$ volume for hot fluid storage.

A performance evaluation of this system based upon real solar and weather data from 1962 Albuquerque Weather Service tapes indicates that a fossil fuel savings of about 62% would be realized for the mixed-load community.

An economic evaluation of the flywheel in comparison with other solar energy storage systems was conducted. The costs of the flywheel storage components for this system include a capital cost of $38.25 per kWh of capacity and an annual operating and maintenance cost of one mil per kWh of capacity. The evaluation indicates the flywheel storage results in a slightly higher levelized cost of energy than the other systems which store thermal energy in the form of hot fluid.

Combined PVT Collection for an Average House in Albuquerque -- A comprehensive system study was conducted on a combined photovoltaic-thermal (PVT) system for a 140-m$^2$ (1500-ft$^2$) house. The object was to design a PVT system which would provide all the heating and hot water needs and all or part of the electrical needs for an average house. A number of PVT options are being considered:

- E-W collectors with temperature-sensitive solar cells
- E-W collectors with optimized high-temperature solar cells
- N-S collectors with optimized high-temperature solar cells and several collector tilt angles.

Two cooling-load options are also being analyzed:

- Absorptive air conditioning which requires 105°C (221°F) water
- Evaporative cooling which requires only cool water.

In all of the analysis the collectors are parabolic cylinders with a 90° rim angle, 2-m width, and a geometric concentration ratio of 50 to 1. The solar cells are assumed to be mounted on the exposed area of the solar receiver. Water is used as the coolant fluid which always remains below boiling.

Electrical storage is provided by high-quality lead/acid batteries, and hot water is stored in a stratified tank.

When the combined PVT system is sized to provide daily heating and hot water needs the electrical energy produced is about 70% of the load requirement.

Preliminary estimates on the capital costs of a combined PVT system in Albuquerque, assuming evaporative cooling is used, are about $5000 per peak electrical kilowatt, using actual solar insolation data. Some estimates on levelized annual payment requirements for a PVT system financed for 30 years show that, if fuel costs escalate as predicted, PVT system costs are competitive with levelized annual fuel costs.

The overall annual fuel savings of a PVT system in Albuquerque on a 140-m$^2$ home could be as high as 85%. Thus far in the analysis the use of evaporative cooling (common in Albuquerque) allows the thermal design of the PVT system to be dependent on winter conditions. Collector cooling-water temperature does not have to be increased during the summer to accommodate an absorptive air conditioner. Higher cooling-water temperature would result in reduced thermal efficiency.

Data recently obtained on seasonal, one-house electrical loads are more realistic than earlier load data. Despite the new electric loads, the system cost is still minimized by designing for thermal requirements. If the cost of electricity should become much higher, the picture might change.

Because the combined PVT system is designed for a temperature of 77°C (170°F), little difference was noted between the output of temperature-dependent solar cells with $\eta_{27°C}$ = 15% and non-temperature-dependent cells with $\eta_{100°C}$ = 12%. These differences are still being studied.

Because of the low operating temperatures (compared to a solar turbine system) there is little difference between the collector area required for a house using oriented E-W collectors and one using N-S collectors. Thus far the results indicate as little as a 2-m$^2$ reduction in collector area from E-W to N-S, which represents about 6% of the collector area required. Tilting N-S collectors to optimize them for seasonal loads is under study.

Solar Total Energy College Campus -- Authorization to proceed with a study phase on the Dallas Community College Campus Project during FY 76 was granted by the Division of Solar Energy, ERDA. Total funding for the study phase was established at $98,000 with ERDA contributing $93,000 and the Dallas County Community College District providing $5,000. Construction of the Northlake Campus for the DCCCD was begun in Irving, Texas, during the past summer and first occupancy is scheduled for the fall of 1977. The study phase of the project will investigate the application of solar total energy systems to the Northlake Campus. A conceptual design of the solar energy system recommended for the Northlake Campus will conclude the study phase of the project.

Preliminary consideration of the Application of solar energy systems for the Northlake Campus has resulted in the selection of three primary system options for further detailed study.

    Cascaded solar total energy system

    Noncascaded solar energy system

    Heating and air conditioning only.

These options have been presented for evaluation to the DCCCD and to Envirodynamics, Inc., the principle architect for the Northlake Campus. Envirodynamics and Sandia have agreed on both a list of tasks to be undertaken in conducting the study and a division of responsibility for them.

Envirodynamics has provided Sandia with thermal-load profiles for the first phase of the Northlake Campus. These data consist of twelve 24-hour load profiles covering each month of the year. The profiles were calculated using data taken from 1962 Fort Worth Weather Service tapes. A correlation has been developed relating the campus thermal load variation to ambient temperature; this information is being incorporated into the SOLSYS computer program. Then the addition of load profiles for electricity and hot-water demand will permit a comparative performance evaluation of the solar system options selected for detailed study.

Analysis of a 10-MW System for a Southwestern Military Base -- As an outgrowth of the system analyses on the 1000-home community reported previously, a brief study was undertaken to examine the potential use of the solar total energy concept for a military base. For this purpose the cascaded total energy system had focusing parabolic collectors, a Rankine power generation cycle, stratified liquid thermal storage units, absorption air conditioners, and hot water heating . The loads, taken from a study by SRI,[1] were for days of high heating, moderate heating, no heat or cooling, moderate cooling, and high cooling. Table 2-VII presents the system loads and a summary of the results for 174,120 m$^2$ (1.874 x 10$^6$ ft$^2$) of north-south collectors. The portion of the total energy requirements supplied by solar energy varies from 46 or 47% for high heating and high cooling days to 100% for no-heating-or-cooling days, with an average of 71% for the five types of days. During high heating and high cooling days a significant amount of fossil fuel is required to meet the thermal demands and no energy is wasted in the cooling towers. For days with no heating and no cooling, no fossil fuel is required and significant energy must be dissipated in the cooling tower. Daily performance of different components of the system was calculated. These results illustrate the ability of solar total energy systems to meet such demands and also indicate the use of the SOLSYS computer analysis program as a means to compute the performance of a wide range of energy systems and loads.

TABLE 2-VII

Operation of 10-MW Solar System for Military Base

Located in Southwest USA

(all values in J/day x 10$^{-12}$)

| Day | Solar Input* | Fossil Fuel Consumed | | Percent Solar | Cooling Tower Operation | | System Loads | | |
| | | High-Temp. | Low-Temp. | | High-Temp. | Low-Temp. | Electric | Heating | Cooling |
|---|---|---|---|---|---|---|---|---|---|
| High Heating | 2.7 | 1.1 | 2.1 | 46 | 0.0 | 0.0 | 0.74 | 5.1 | 0.0 |
| Moderate Heating | 2.7 | 0.4 | 0.03 | 87 | 0.01 | 0.04 | 0.60 | 2.5 | 0.0 |
| No Heating or Cooling | 2.7 | 0.0 | 0.0 | 100 | 0.4 | 1.5 | 0.49 | 0.5 | 0.0 |
| Moderate Cooling | 2.93 | 0.0 | 1.02 | 74 | 0.14 | 0.3 | 0.56 | 0.5 | 1.3 |
| High Cooling | 2.93 | 0.07 | 3.18 | 47 | 0.0 | 0.0 | 0.5 | . | |

[1] Assessment of Total Energy Systems for the Department of D. Institute, Project EGU-2513, November 1973.

*North-South collectors, area = 174,120 m$^2$

30

Collector - Power Cycle Optimization -- In Sandia's solar total energy test facility, a collector field outlet temperature and a Rankine cycle peak superheat temperature of 316°C (600°F) and 310°C (590°F), respectively, were chosen. The following study was conducted to determine if system economics could be improved by using either higher or lower temperatures.

To determine the economically optimum peak superheat temperature, two variables were considered: peak superheat temperature (collector outlet temperature was assumed to be 5°C above peak superheat temperature), and boiler pressure. As peak superheat temperature increases, collector efficiency decreases and power generation cycle efficiency increases. For a fixed superheat temperature, as boiler pressure decreases (amount of superheat increases), the temperature difference, $\Delta T$, between the heating fluid entering the power cycle's superheater and the fluid leaving the power cycle's preheater increases. The increased $\Delta T$ reduces required storage volume and increases collector efficiency.

Figure 2-4 shows the yearly clear-day-average electricity generated per square meter of collector for a combined east-west axis, parabolic, focusing collector and toluene Rankine power generation cycle. The maximum electrical output is obtained with a peak superheat temperature of 362°C (683°F).



Superheat Temperatures (°C)

A. 219    D. 286    G. 371
B. 236    E. 316    H. 413
C. 265    F. 344    I. 455
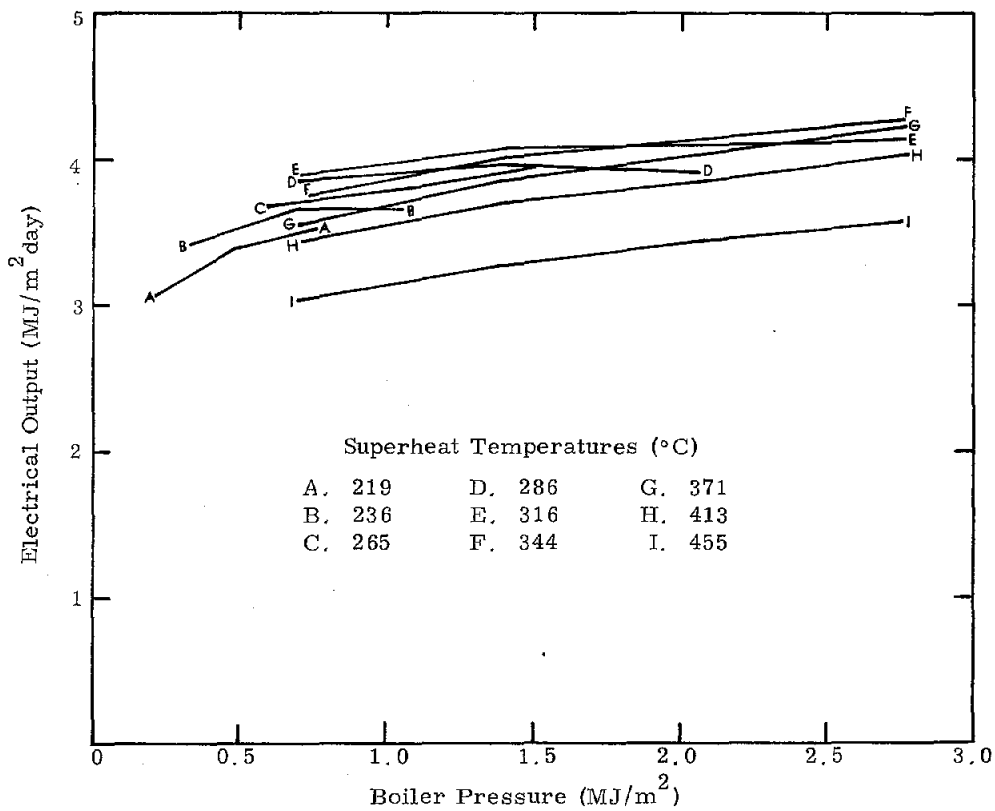
Figure 2-4. Combined Collector Output and Rankine Cycle Efficiency as a Function of Boiler Pressure for Various Superheat Temperatures

To determine the economically optimum temperature, collector area and storage capacity required for a typical 221 GJ/day (209 MBtu/day) electric load were computed. The storage unit was a stratified tank using Therminol 66, or Therminol 88 for temperatures above 316°C (600°F). Both fluids cost $1200/m$^3$ at their respective operating temperatures. Figures 2-5 and 2-6 show collector-plus-storage cost for $50/m$^2$ ($4.65/ft$^2$) and $100/m$^2$ ($9.30/ft$^2$) collectors. The superheat temperature which minimizes cost for both collector prices is 413°C (775°F), and the optimum boiler pressure is 2.76 MPa (400 psi).

The optimum temperature is somewhat higher than had been planned, and it will result in a 30% cost reduction for the collectors and storage.

It has been suggested that supercritical power generation cycles using other working fluids may be superior to the subcritical toluene cycle. These other cycles and fluids will be investigated.
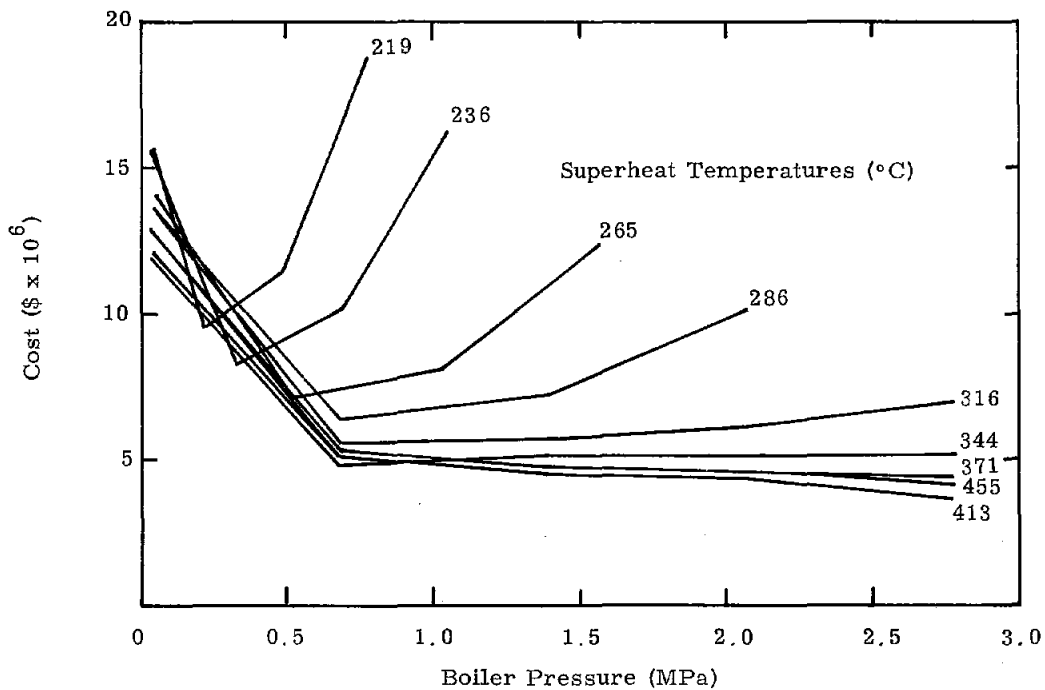


Figure 2-5. Collector - plus - Storage Cost for $50/m$^2$ Collectors
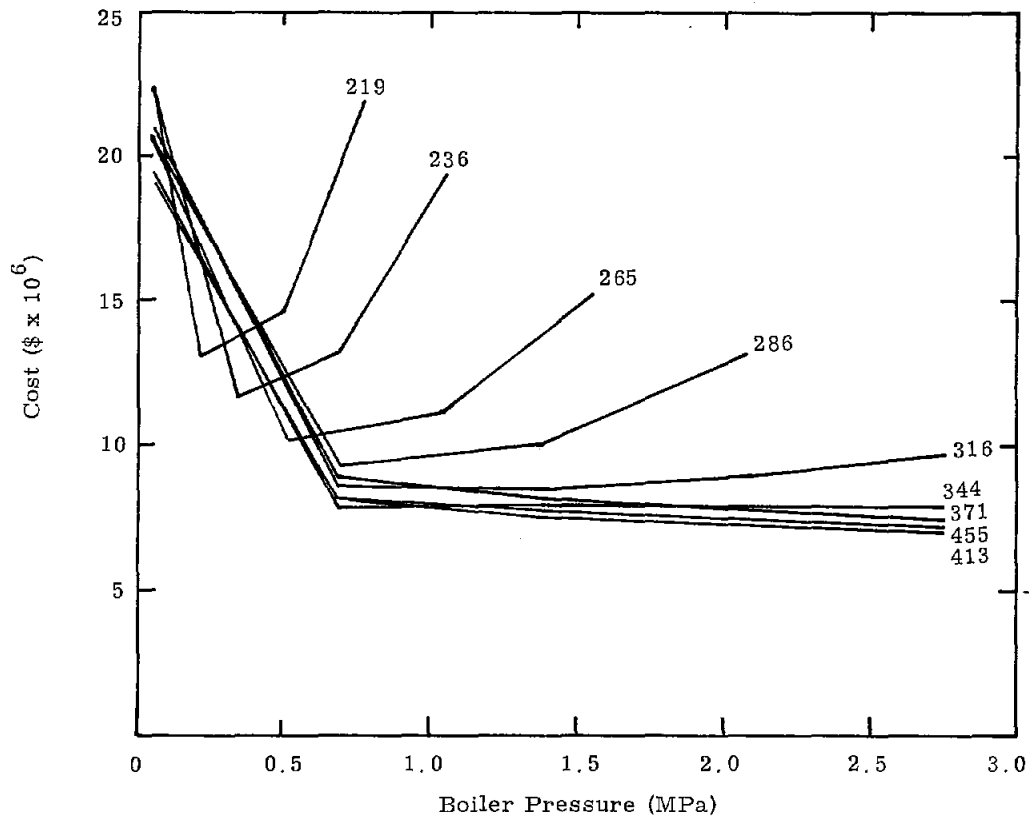
Figure 2-6. Collector - plus - Storage Cost for $100/m² Collectors

Collector Optimization -- A comparison of two collector designs based on a figure of merit has been completed. The collector configurations compared are shown in Figure 2-7. Figure 2-8 shows the results.

The figure of merit is defined as follows:

$$M = C/(E - B/N_c)$$

where

        M - Figure of merit, $/10³ kJ

        C - Total collector field construction costs on a mass-production basis

        E - Thermal energy output per day, kJ

        B - Electrical energy consumed by auxiliaries per day, kJ

        $N_c$ - Rankine cycle efficiency. A value of 16.2% was used in this study since all calculations were made for winter solstice.

For this study the collector field costs were as follows for the 2.74 m (9-ft) wide collectors:

        Collector: $183/m² ($17/ft²)

        Pump: $2.15/m² ($0.20/ft²) of collectors

Therminol 66: $1.71/m ($0.52/ft) of collector length

Plumbing: $5800/collector loop

For the 2 m (6.56-ft) wide collectors:

Collector· $162/m$^2$ ($15/ft$^2$)

Pump: $2.15/m$^2$ ($0.20/ft$^2$) of collectors

Therminol 66: $0.85/m ($0.26/ft) of collector length

Plumbing: $4200/collector loop

The collector designs assumed a reflectivity of 0.85 and no plugs in the receiver tubes.

The cost figures were selected to provide a realistic comparison between the two collector designs. They are subject to change as design changes are made.

The conclusions of the study are that the narrower collector has a significant advantage over the wider collector when costs are considered. Also when large collector fields are designed, collector lengths of the order of 150 m (492 ft) should be used.
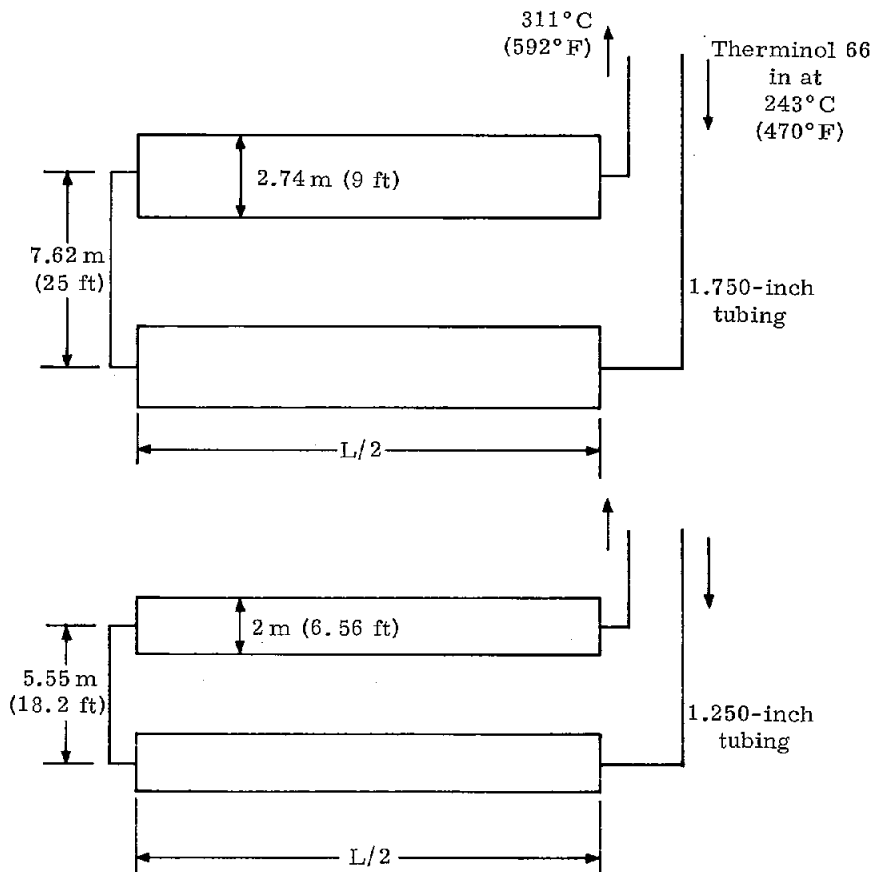


Figure 2-7. Collector Configuration
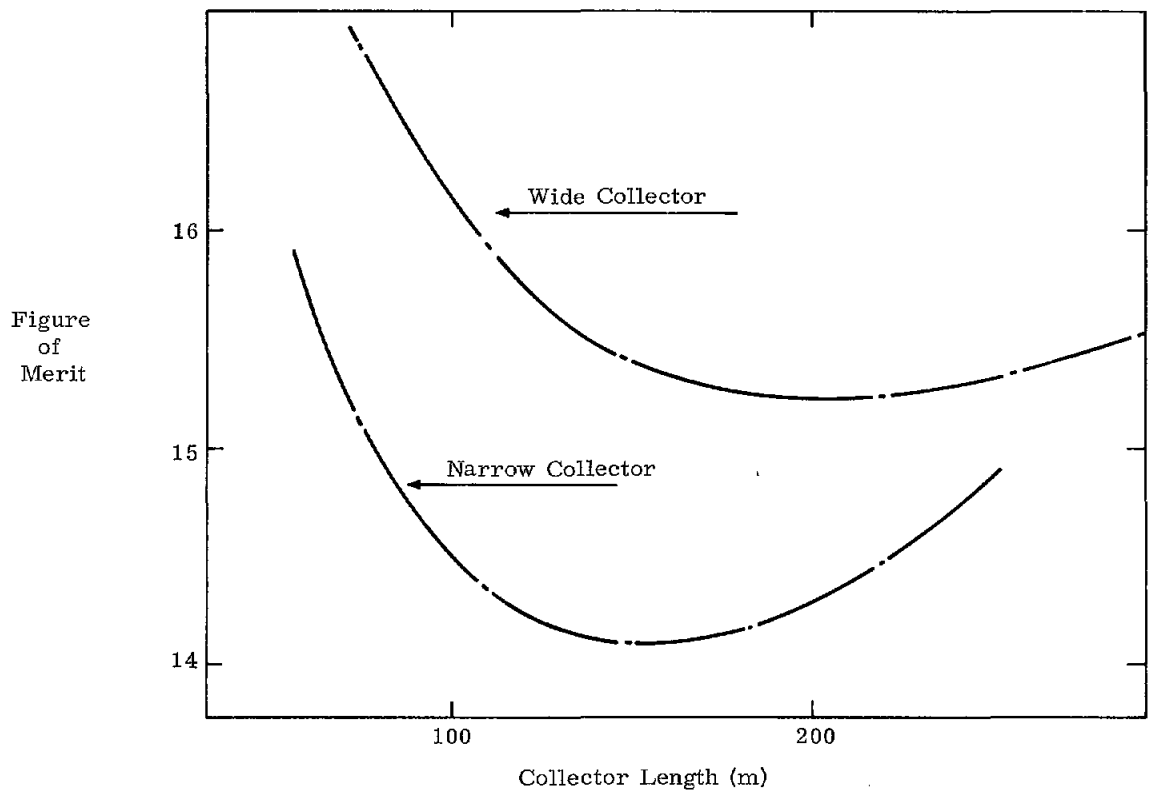
Figure 2-8. Figure of Merit

<u>Analyses of Several Thermodynamic Cycles for Energy Conversion from Sensible Heat</u>

<u>Sources</u> -- Several variations of moderate temperature water and toluene Rankine cycles were analyzed and compared with respect to their cycle efficiencies and the temperature drop (energy extracted) which might be realized from a sensible heat source. The cycle conditions assumed were chosen to be compatible with those required by the present solar total energy prototype system. Several other cycles and working fluids were also analyzed, including a supercritical cycle with regeneration and a near supercritical cycle without regeneration. The results from the analyses are summarized in Table 2-VIII. Though the analyses are only of a survey nature and far from exhaustive, they do indicate that supercritical Rankine cycles should be considered for any follow-on systems in the near term and that the "wet" cycles using saturated liquid at the prime mover inlet should be considered for advanced development.

Although this study was done specifically for the solar total energy program, the results are of course appropriate to other systems using sensible heat sources such as geothermal or recovered waste heat.

Cycles 1 and 2 in Table 2-VIII indicate that superheat cycles using water and toluene have roughly equivalent efficiencies and result in about the same temperature drop in the heating medium at a given efficiency level. Increasing the amount of superheat in both cycles decreases cycle efficiency while increasing the heat source temperature drop (and conversely for a decrease in the level of superheat).

Cycle 3 was an attempt to find a suitable fluid and cycle which would not require either a reheater or a regenerator (to minimize costs) and yet be supercritical or nearly so to get a large $\Delta T$ in the heating source. Fluorinol - 50$^{®}$ is a 50 mole % trifluoroethanol - 50 mole % water (85% - 15% by weight) mixture which yields a saturated vapor after an isentropic prime mover expansion under the conditions shown. Although this fluid gave rather poor efficiencies compared to the other fluids, there may be fluids of a similar nature which would yield more promising results.

Cycle 4 uses 100% trifluoroethanol with a critical temperature of 227°C (440°F). As can be seen in the table, this cycle yields a very attractive combination of good cycle efficiency and a large temperature drop. Trifluoroethanol has several other good points such as a moderate critical pressure (4.93 x 10$^{6}$ Pa or (4.93 Pa or 715 psia) and a low freezing point (-45°C or -49°F), and is nonflammable. Some of its disadvantages are a temperature stability limit of 330°C (625°F) and a relatively high cost of about $11/kg ($5/lb). This fluid and cycle combination, or other's like it, should be considered for any new generations of solar total energy systems.

TABLE 2-VIII

Summary of Cycle Impact on Conversion Efficiency and Sensible Heat Source $\Delta T$

| Cycle Number | Working Fluid | Cycle Temperatures High/Low ($^\circ$C) | ($^\circ$F) | Cycle Efficiency[a] Ideal/Nonideal (%) | Sensible Heating Source $\Delta T$ (Ideal) ($^\circ$C) | ($^\circ$F) | Comments |
|---|---|---|---|---|---|---|---|
| 1 | Water | 310/32 | 590/90 | 35/29 | 85 | 185 | Superheat Cycle With Two Reheats. Maximum Pressure is 5.15 MPa (600 psia). |
| 2 | Toluene | 316/38 | 600/100 | 37/30 | 88 | 190 | Superheat Cycle With Regeneration. Maximum Pressure is 1.38 MPa (200 psia). |
| 3 | Fluorinol-50[b] | 316/38 | 600/100 | 23/18 | 143 | 290 | Superheat Cycle Without Regeneration. Maximum Pressure is 6.2 MPa (900 psia). |
| 4 | Trifluoroethanol | 316/38 | 600/100 | 33/28 | 171 | 340 | Supercritical Cycle With Regeneration. Maximum Pressure is 5.5 MPa (800 psia). |
| 5 | Water | 302/32 | 575/90 | 30/25 | 227 | 440 | Saturated Liquid at Inlet to Prime Mover. Prime Mover Exhaust is Approximately 65% Liquid. |
| 6 | Toluene | 293/32 | 560/90 | 31/26 | 230 | 445 | Saturated Liquid at Inlet to Prime Mover. Prime Mover Exhaust is Saturated or Slightly Superheated Vapor. |

Notes:  a.  Nonideal cycle calculations assume the following component efficiencies which might be typical of a 300-MW$_e$ plant:

Generator efficiency - 0.98
Turbine and feed-pump efficiencies - 0.85
Regenerator efficiency (where used) - 0.90
Pressure-drop losses and parasitic power losses not considered.

b.  Registered trademark of the Halocarbon Products Corporation

Cycles 5 and 6 were speculative attempts at determining what might be the ultimate cycle as far as getting a large temperature drop and hence the maximum energy extraction from a sensible heat source. In both cases, the results are very attractive. Such cycles theoretically yield a good efficiency and by far the largest temperature drop of the six cycles studied. In addition, they are conceptually as simple as Cycle 3 with only two heat exchangers required. The biggest question as to the feasibility of these cycles would be the availability of a suitable prime mover. For water in Cycle 5, the expansion ratio is approximately 7000 to 1, and the prime mover exhaust would contain about 65% liquid. For comparison, an isentropic expansion of saturated steam from 316°C to 32°C (600°F to 90°F) yields an expansion ratio of approximately 1000 to 1, and the prime mover exhaust would contain about 35% liquid. The high liquid content is a major limitation for conventional steam turbines which require superheating or reheating to limit liquid content to 10% or less in the turbine exhaust.

Cycle 6 appears somewhat more favorable for a prime mover with a required expansion of approximately 2000 to 1, and the resultant prime mover exhaust would be saturated or slightly superheated vapor.

Since Cycles 5 and 6 appear to offer substantial advantages over conventional cycles, they are suggested for further study and possible development. It is recommended that the availability of a suitable prime mover be further explored as a parallel effort. As possible starting points, Lawrence Livermore Laboratory has done work in the area of nozzles and turbines for "wet" expansions which might be applicable, and certain classes of positive displacement expanders might be appropriate. The worm-and-gear type prime movers look particularly attractive because it is anticipated that these machines would operate quite well with wet vapors or even liquids since that would promote good sealing, and these machines also appear capable of large expansion ratios in a single stage.

Task 3. Collector Field

## 3.1 Reflectors and Structure

Fabrication and basic installation of the 200-m$^2$ (2160-ft$^2$) field of east-west collectors has been completed. The collector field consists of four continuous 18.3-m (60-ft) troughs in two rows aligned on east-west axes. See Figure 3-1 for an overall view (before installation of the last 60-ft section). Center-to-center spacing between rows is 7.6 m (25 ft). Each of the 18.3-m troughs consists of five of the 2.7 x 3.7 m (9 x 12 ft) trough units, mechanically connected at the ends to form a single structural trough.

Figure 3-1. Solar Total Energy Test Facility (collector field lower left)

Each 2.7 x 3.7 m unit consists of a thin plywood shell structure 19-mm (0.75-inch) thick, fabricated to the specified parabolic contour and mounted on a framework of five transverse wooden ribs joined at their outer ends by longitudinal members (see Figure 3-2). The plywood shell structure was produced in four shorter sections, 0.9-m (36-in.) long, which were assembled and bonded to form the full-size shell. The completed shell is bonded to the rib framework which in turn is attached to a simple tubular steel frame with flat steel end plates. The end plates are bolted to flanges on the ends of the trunions on the pylons. Stress analyses of wind loads have verified design adequacy in both 13.4-m/s (30-mph) operational and 40.3 m/s (90 mph) survival situations.

Each 2.7 x 3.7 m unit is supported at the ends by a narrow pylon of welded steel sheet. The pylon height places the rotational axis of the unit 1.5 m (5 ft) above the concrete bases to which the pylons are bolted. The concrete pedestals for the collectors have set-in threaded rods by which the pylons are attached and aligned. Figure 3-2 shows the underside of one of the troughs and the pylon structure.

Development plywood panels for the trough shells were fabricated to evaluate variations in such parameters as veneer material, veneer thickness, total assembly thickness, and facing materials. These 0.9 x 2.7 m (3 x 9 ft) panels were evaluated by (1) cutting test specimens to determine mechanical properties, (2) testing in environmental chambers to determine adequacy of protective finishes, and (3) inspection to determine contour accuracy of the parabolic contour.
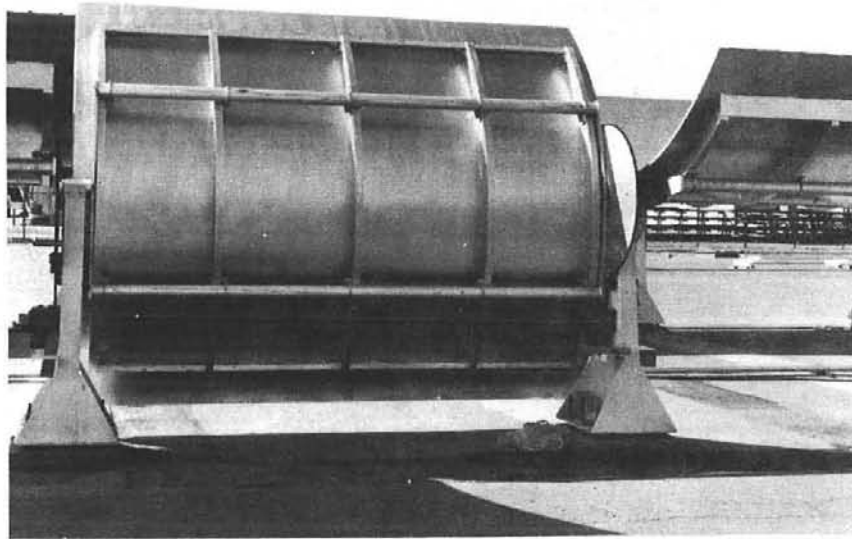
Figure 3-2. One 3.7-m Sector (1/5) of an 18.3-m Trough

Four of the plywood panels were used to assemble a prototype 2.7 x 3.7 m (9 x 12 ft) unit with which assembly techniques were developed. This completed unit was fitted with reflectors and mounted in a 45° fixed-tilt, north-south framework for further evaluation. The reflectors for this unit consisted of six sheets of silvered glass which had been sagged to parabolic contour and six sheets of Alcoa's lighting sheet with an Alzak finish. The glass mirrors cover one end of the unit and the mechanically clamped Alzak the other end.

Drive System -- Although each 18.3-m (60-ft) trough is connected to form a single structure, driving torque is applied to each of the five units from a single motor by means of a common shaft which runs the length of the trough. This drive shaft has a right angle worm gear reducer at each pylon to tap off power to a second worm gear reducer, which drives a chain-and-sprocket assembly connected to the trough structure. The motor-to-trough reduction ratio is 40,000:1.

The drive motor is a reversible 1/2-hp, 50-Vdc electric motor mounted on the pylon at the west end of the trough. The motor is larger than previously planned to provide sufficient torque in the event of unexpected friction loads, wind, etc. With an input of 1000 rpm, the 40,000:1 ratio will provide a maximum tracking rate of 9°/minute. Installation and checkout of the drive system has not been completed because of the late arrival of the small worm gear reducers.

Reflector Materials -- Development efforts aimed at making the reflective material an integral part of the trough shell structure met with limited success. Fabrication techniques attempted thus far have resulted in acceptable and functional reflector surfaces but without the desired accuracy. To date the troughs with integrally molded reflectors are not of the required optical quality; slope errors of up to 1.5° have occasionally occurred while errors of 0.5° are common. These errors are due to mold inaccuracy, the uneven shrinkage of adhesives, impregnating resins, or glues, the warpage of the sheet material after fabrication, and combinations of these.

Evaluation of integral reflectors on parabolic troughs indicated that a better means of applying reflector material was needed. On the basis of previous successful experiments with mechanical clamping of sheet reflector materials, it was determined that this approach would produce a more accurate, more acceptable reflector surface for the large troughs. The concept of mechanical clamping requires a separate thin sheet of material (such as a 0.64-mm (0.025-in.) aluminum sheet) which can be held or clamped so that it is forced to conform to the basic trough contour. The structural integrity of the sheet allows it to assume the basic trough contour smoothly as it is bent, thereby bridging the small irregularities of the trough surface. The primary method of clamping is to exert force on the edge of the sheet at the outer rims; the force direction is tangential to the parabolic slope at the rim. The separate reflector sheet must be slightly larger than the rim-to-rim arc length of the parabola; the extra length is a function of the clamping device design.

Using a clamped structural sheet with a highly reflective material applied to it allows important versatility in collector design. Installation of the reflector material can be delayed until late in the assembly sequence, thereby eliminating the extra precautions which would otherwise be required to protect the reflector throughout fabrication and assembly. Replacement of a damaged or degraded reflector section of a trough can be done easily. In a developmental solar collector field, this approach will permit easy substitution of new and better reflector materials as they become available.

Reflective films have been in development at the Sheldahl Company in Northfield, Minnesota, for some time. Three promising reflector materials were ordered for initial use on the 200-m$^2$ collector field; these films were to be laminated to 0.64-mm (0.025-in.) thick aluminum sheets, 0.9-m (36-in.) wide and of adequate length for mechanical clamping to the troughs. The three films were: (a) second-surface-aluminized FEP Teflon, (b) front-surface-aluminized Mylar with a protective acrylic polymer coating, and (c) front-surface-silvered Mylar with a protective acrylic polymer coating. (The metal coatings are applied by metal evaporation in a vacuum.) Specular reflectance values of 0.80 to 0.89 were achieved with 0.92 as a realistic goal.

Several problems arose with the two front-surface-reflector sheets. The single-layer, acrylic-polymer coating proved to give limited environmental protection.

A multilayer coating probably would have solved this problem but the time scales for obtaining and installing suitable equipment to apply multiple coats were unacceptably long for Sandia's requirements. For these reasons, the entire 200 $m^2$ of collectors will be covered with the second-surface-aluminized Teflon reflector sheets. Half of the required sheets have been delivered and the remainder are expected in November.

## 3.2 Receivers

The final design of the Phase IV-A receiver tube assembly was briefly described in the last semi-annual report. A cross sectional view of this design is shown in Figure 3-3. The receiver tube OD is 41 mm (1-5/8 in.) and the Code 7052 glass has an OD of 64 mm (2.5 in.). The annulus is an appropriate size to minimize conduction-convection losses should the vacuum be lost. Eight receiver tube assemblies have been completed and sufficient parts are on hand to complete five more. The remainder of the receiver tubes, to complete the requirement for twenty assemblies, are being recoated (black chrome) at the ERDA Bendix facility to increase the absorptance to at least 0.95. Figures 3-4 and 3-5 show views of the ends of completed assemblies. All of the parts have been commercially procured. The only "in-house" work has been the black-chrome-coating effort at Bendix and the glass joining and assembly efforts at Sandia. Each receiver tube assembly will include a turbulence generator to preclude liquid overheating due to asymmetric energy input.

Figure 3-6 shows a receiver tube assembly supported in the support assembly.

All receiver tube assemblies should be mounted in the field by February 1976.
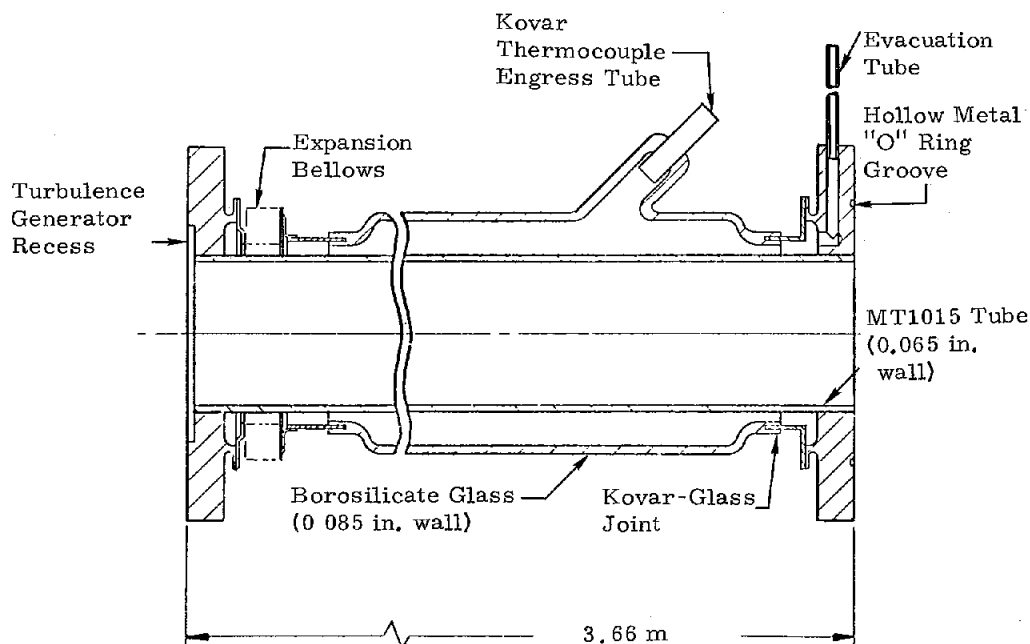


Figure 3-3. Collector Pipe Assembly (dwg. S15424)
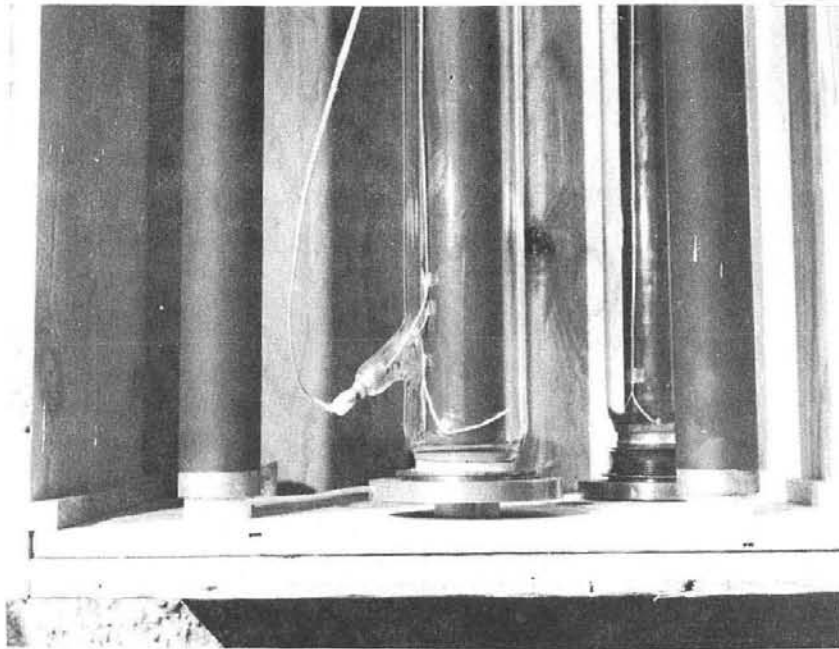
Figure 3-4. One End of Completed Receiver Tube Assemblies



Figure 3-5. Another View of Same Receiver Tube Assemblies
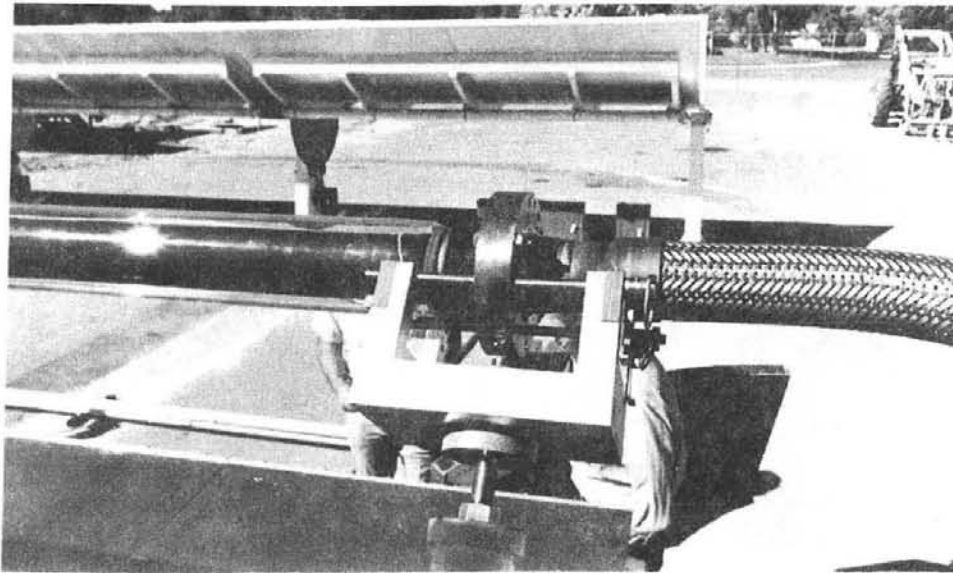
Figure 3-6. A Receiver Tube Assembly in its Support

## 3.3 Tracking and Control

Two types of tracking and control systems are being incorporated into the four collector troughs of Phase IV; one is an active sun sensor/servo control system (Figure 3-7), the other a digital shaft-encoder/computer-command system (Figure 3-8). Each system will be able to control the troughs to follow the sun's movement and maintain proper focus.
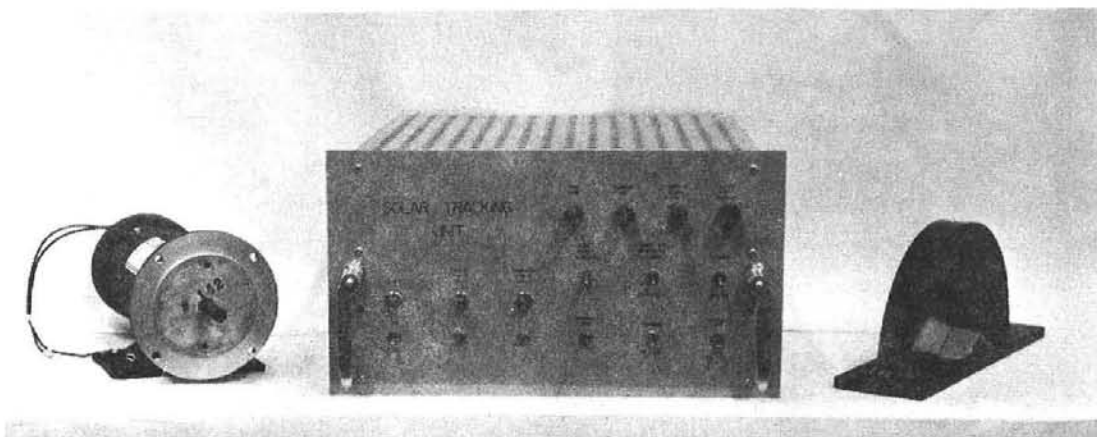


Figure 3-7. Components of Active Sun Sensor/Servo Control Tracking System
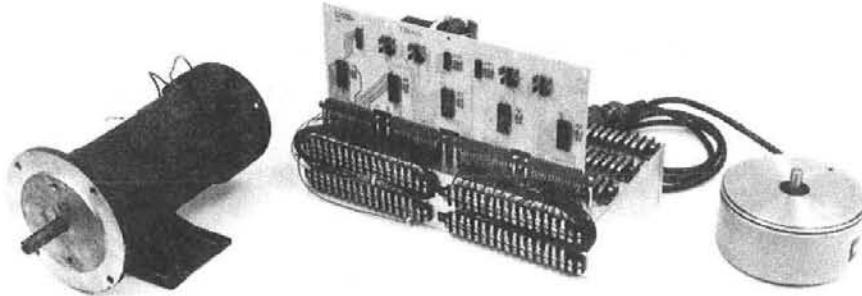
Figure 3-8. A Digital Shaft-Encoder/Computer-Command Tracking System

Active Sensor/Servo System -- This tracking and control system has been under development for several months with prototype systems mounted on two fixed-tilt, north-south reflectors. The sensor design is suitable for use with either north-south or east-west collectors. The basic requirements for this system were:

- Flexibility and versatility
- Capable of tracking in both rotational directions
- Acquisition angle of 180°
- Tracking error of less than 0.1 degree
- Automatic defocus on power loss
- Automatic (temporary) shutdown if sun is lost due to clouds
- Interface with computers.

The system consists of a sun sensor, control circuit, and drive motor. The sun sensor is located on, and aligned with, the focal plane of the reflector trough. The control circuit contains the logic circuitry which assesses the input from the sensor and produces signals to control the drive motor. The control circuit also contains a switch panel for selection and control of operational modes (manual or automatic), and circuitry for the emergency defocusing.

Sun Sensor -- Earlier a sensor which had both fine and coarse sensing circuits was investigated. The present version has been simplified and uses only a single sensing circuit. This sensor component, shown in Figure 3-9, consists of a semicircular shadow-board divider and four silicon photovoltaic cells. Each pair of cells is connected in series and mounted on one side of the

divider on opposing 30° slopes; this arrangement allows sun sensing throughout an entire 180° (dawn to dusk) passage of the sun. Each cell has a filter of evaporated aluminum on glass to attenuate the sun's intensity by 90 percent. The filters allow the cells to operate in an unsaturated mode, producing a linear current output with respect to the cell illumination. The semicircular divider has a radius of 150 mm with a 35-mm-wide sunshade around the circumference. The plane of the divider is aligned parallel to the focal plane of the reflector trough. When the trough is not pointing at the sun, two of the cells are illuminated and two are shadowed. The difference in illumination produces a larger current in the illuminated cells. The output from both pairs of cells is fed into a differential amplifier with a resultant error signal, which is used to drive the drive motor until the signals from both sets of cells are the same.
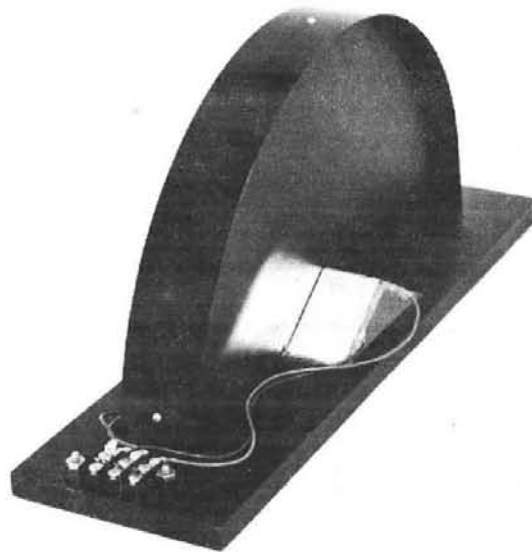


Figure 3-9. Sun Sensor Unit (semicircular divider has 150-mm radius, is 35-mm wide)

Control Circuit -- The electronic circuitry within the control panel has been changed only slightly during this reporting period to improve operational stability. The schematic of this circuit was published in the previous semiannual report.

Safety Features -- Some important safety features have been incorporated into this system to prevent damage to various components. In the event of power failure to the collector field during operation, tracking drive and fluid flow would be stopped with possible overheating damage to the receiver tube or the heat transfer fluid. A power failure drop-out relay has been incorporated

so that power failure automatically applies power from a standby battery to drive the collector out of focus and on to the limit of travel. Once the limit switch is activated, the battery circuit is opened so that manual resetting is required to put the system back into operation.

During normal field operation, there exists the possibility of overheating. To preclude damage, thermocouples have been mounted on each set of receiver tubes to supply temperature information to a commercial controller. Should the thermocouples indicate temperatures above an established level, the controller automatically commands the tracking and drive system controller to (1) defocus the collector and drive the trough to a limit switch, and (2) switch the fluid pump to maximum slow rate. Again, manual reset is required.

Collector Drive Motor -- The collector drive motor has been changed from a 1/6-hp, 10,000-rpm motor with an integral 10:1 gear reducer to a 1/2-hp dc motor. The torque requirement of 10 in.-lb at 1,000 rpm remains unchanged because the 1/2-hp motor is operated at a reduced voltage. (The change was made because of malfunctions encountered in the integral 10:1 reducer.) The larger motor will also provide a safety factor in the event torques required to drive the troughs are higher than expected.

Digital Shaft-Encoder/Computer-Command Control System -- This alternative tracking system is capable of several important functions in this developmental solar collector field. One function is to evaluate the performance of the analog sensor system discussed above. The digital shaft encoders can be used to measure the angular position of the collectors; by comparing data from both control systems in the minicomputer, it can monitor the function of the servo system and alert the operator if malfunctions occur. With the shaft encoders, the computer can generate the control outputs to command the drive motor circuits and steer the collectors independently of the analog solar sensors. Additional functions such as collector defocus, daily repositioning of the north-south collectors, and on-line monitoring of the collector drive system can be done expediently through computer software additions. The analog sensor approach is being evaluated and compared in cost, complexity, and performance to the digital shaft-encoder/computer method.

The shaft-encoder tracking system has been fabricated and the software required to check out the system has been completed. Preliminary operation has been satisfactory. Installation of the encoders is awaiting completion of the troughs and their drive trains.

One additional function of this tracking system will be to determine the amount of torsional deflection which occurs as the 18.3-m (60-ft) collector troughs are driven through their 170° of travel. Two encoders, one at each end of the trough, will be used in this evaluation of the trough and drive-train stiffness.

## 3.4  Fluid Transfer System

The fluid transfer system interconnects the collectors, the blending tank, the cooler, and the high-temperature storage tank, as shown schematically in Figure 3-10. The design of this fluid loop includes valves, pumps, piping, and instrumentation to operate in several modes.

The fluid loop is designed to operate from commercial valve controllers under normal conditions. Initially, the computer will be used to help establish flow rate under complex conditions. It is anticipated that the controllers will be capable of performing the control functions of the computer, and the goal is to arrive finally at a system which does not require computer control.

The collector portion of the loop provides the solar energy input into the fluid. The problem of controlling fluid flow rate through the field is discussed in detail under Task 6. Control is accomplished using thermocouples at the input and output of each string of collectors to provide information to the speed controller of the positive displacement pump so that a nominal collector field output temperature of 310°C (591°F) is maintained. The collector field may be operated as a single series loop or two shorter parallel loops, as controlled by valve V7. When operating in the parallel mode, the fluid temperatures at T1 and T2 are compared by a controller which adjusts V7 to keep them equal.
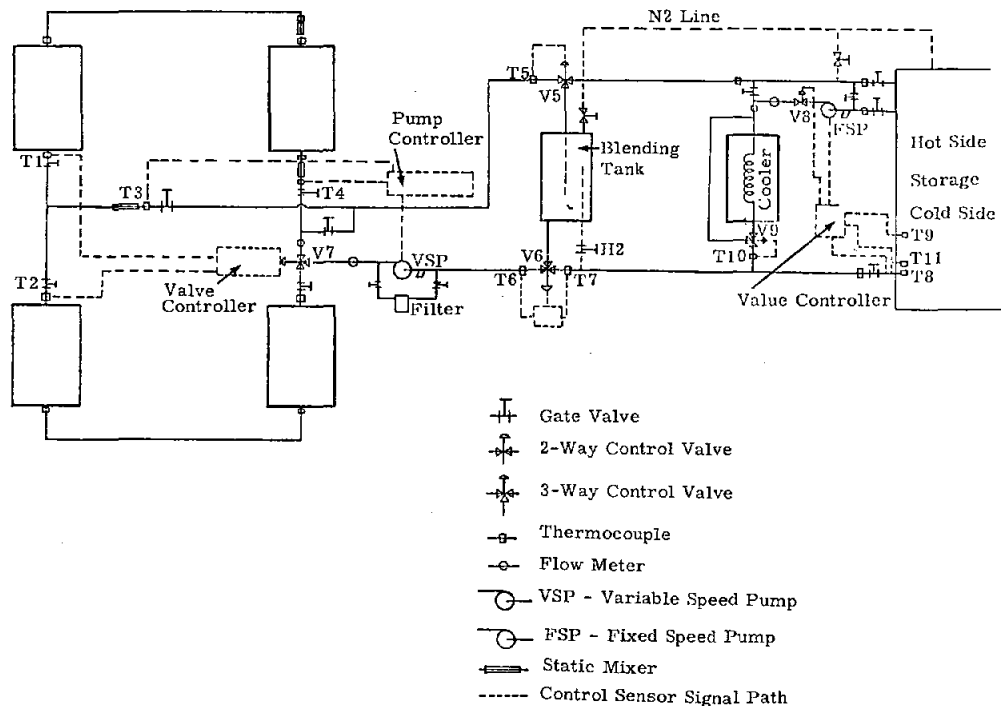


Figure 3-10.  Collector Field and Storage Control

During the period covered by this report, the design of the fluid transfer system has been completed, orders placed for the valves and insulation, and a construction contract placed for fabrication and installation of the system. Construction is underway with completion scheduled for December 1976. When complete, the system will be checked for leaks with pressurized nitrogen. Following a successful nitrogen pressure-leak check, the system will be filled with Therminol 66 and checked again. On successful completion of this check, the system will be insulated and readied for daily operation.

All components (insulation, valves, tubing, controller, etc.) are on site awaiting assembly with the exception of two pumps and the blending tank; these components are due in October and November.

The purpose of the blending tank is to provide a small temporary storage for fluid exiting the collector field at temperatures less than the desired temperature for entry into the storage tank. The blending tank is particularly useful during transient operating conditions such as morning start-up. There are two control strategies for using the blending tank during transient conditions: a mixing mode, and a buffer mode. The following brief descriptions of these two modes are based on early morning start-up; procedures for the passing of a large cloud would be similar.

In the mixing mode, valve V5 passes all fluid below storage temperature (311°C or 592°F) from the collectors directly into the blending tank. Valve H2 is open and valve V6 is fully open between the tank and the variable-speed pump (VSP), which circulates the under-temperature fluid around the collector-blending tank loop. As fluid exiting the collectors comes up to the required temperature, valve V5 shifts to pass all fluid straight into storage. At this time, fluid to feed the field comes from the bottom of the high-temperature storage tank, passes into the blending tank where it is mixed with that fluid and then passes through V6 to the VSP and the collector field. Steady-state operation is established in this manner.

In the buffer mode, the blending tank is empty as morning start-up begins. Valve H2 is closed. Fluid initially flows from the bottom of the high-temperature storage through V6, the VSP, and the collectors to V5, which sends all fluid less than 311°C (592°F) into the blending tank. Instrumentation within the tank senses minimum and maximum levels as well as temperature. Valve V6 is used to modulate exiting fluid flow from the blending tank so that it is mixed with the fluid coming from storage. Thermocouples T6 and T7 are compared and used to control valve V6 to mix the two incoming fluids (from the blending tank and from the high-temperature storage) so that the mixed fluid furnished to the VSP is no more than 5.5°C (10°F) different from the temperature of fluid coming from storage. In this fashion, steady-state operation is established and the blending tank is emptied.

The mixing mode has been selected as the primary strategy for start-up and transient conditions since it appears to be simpler and offers better temperature control. The buffer mode is

a backup option. Actual testing in the next few months will establish and refine these control strategies.

The other two portions of this fluid transfer system, the cooler and high-temperature storage, are discussed in following paragraphs.

3.5 Cooler

The cooler, shown on the right side of Figure 3-10, acts as a thermal load on the collector/ storage system in two primary modes. In one mode, the heated fluid returning from the collector field can be diverted directly to the cooler rather than going to the storage tank allowing the collector field to be independently operated. In the second mode, the cooler can be used to cool the fluid in the storage tank by activating the fixed-speed pump (FSP) and control valve V8 which will remove fluid from the upper portion of the storage tank, cool it, and return it to the bottom of the tank.

If the storage tank should be completely filled with the heated fluid from the collector field, continued circulation of the high-temperature fluid would result in overheating, causing damage to both the collectors and the fluid. To prevent overheating the cooler pump is activated and control valve V8 is opened fully when the hot fluid reaches thermocouple T8 in the storage tank. The cooler will continue to operate in this manner until the level of the hot fluid rises above thermocouple T9.

The temperature of the fluid leaving the cooler is regulated by the three-way control valve V9. The valve blends hot fluid from the bypass line into the fluid coming from the cooler to maintain the desired outlet temperature as sensed by thermocouple T10.

Before the cooler is started, the fluid in it and the bypass line are at ambient temperature. To prevent this mass of cold fluid from being introduced into the collector field abruptly when the cooler is started, a cooler preheat cycle has been added. As the level of the hot fluid moves lower in the storage tank and before it reaches thermocouple T8, thermocouple T11 activates the preheat cycle which starts the cooler pump and sets the control valve V8 for a low flow rate through the bypass line. The low flow rate allows the cool fluid of the bypass to be slowly introduced into the collector field flow line. Control valve V9 will automatically block flow from the cooler until the fluid coming from the bypass line exceeds the set-point temperature of the valve. At this point, the bypass line is preheated and normal operation may begin.

The cooler, delivered in September 1975, is a McQuay Company unit with a capacity of $1.06 \times 10^6$ KJ/hr ($1 \times 10^6$ Btu/hr). The pump is a centrifugal type (Dean Brothers) which was delivered in September 1975. Installation of these units is planned for November 1975.

# Task 4. High-Temperature Storage

## 4.1 Storage Unit

The high-temperature storage tank has been installed at the Solar Total Energy Test Facility site in Albuquerque. The tank is sketched in Figures 4-1 and 4-2, showing internal piping and thermocouple probes as well as insulation. The tank, initially designed for high-pressure (10.3 Mpa or 1500 psi) water storage, will be used at low pressure ($\sim$ 172 kPa or 25 psi) with Therminol 66. The thermocline concept will be exploited and initial testing with Therminol 66 is planned to evaluate the storage concept.

Preliminary tests with water up to $\sim$ 204°C (400°F) indicated that the thermocline is stable once formed. In particular, test results indicated that initial thermocline width was very dependent on tank inlet flow rate. As a result the diffuser shown in Figure 4-3 has been constructed for use in the tank. The thermocline concept has not been tested with Therminol 66.
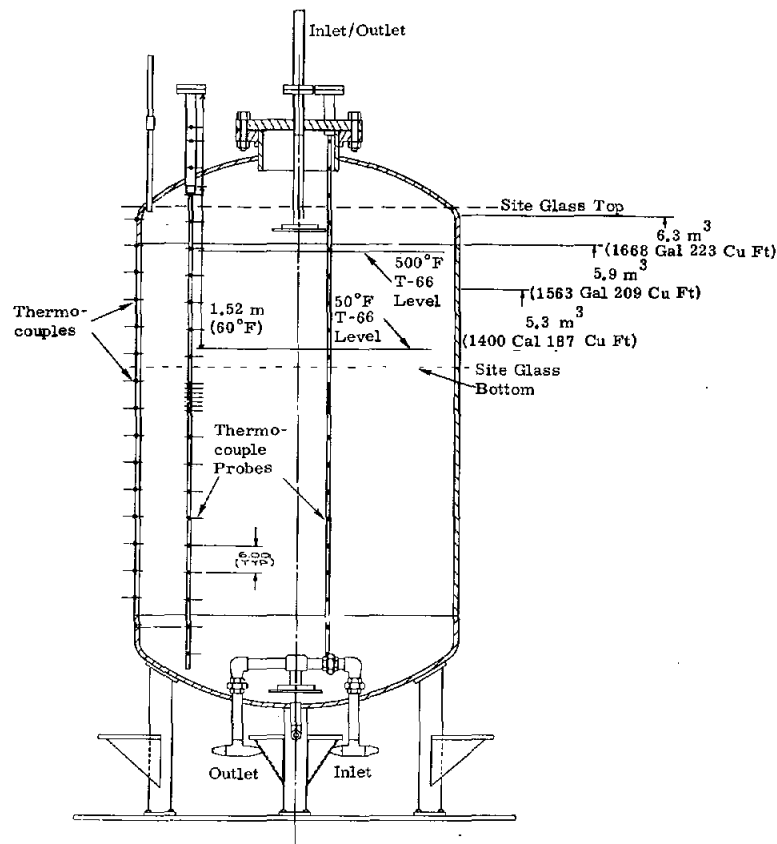


Figure 4-1. High-Temperature Therminol 66 Storage Tank Without Insulating Jacket
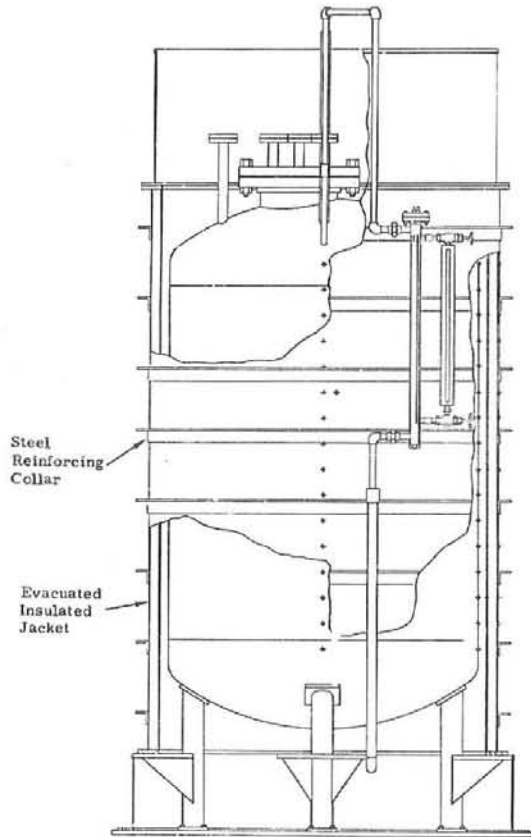
Figure 4-2. Vacuum-Insulated Jacket in Place on High-Temperature Storage Tank.

Steel
Reinforcing
Collar

Evacuated
Insulated
Jacket
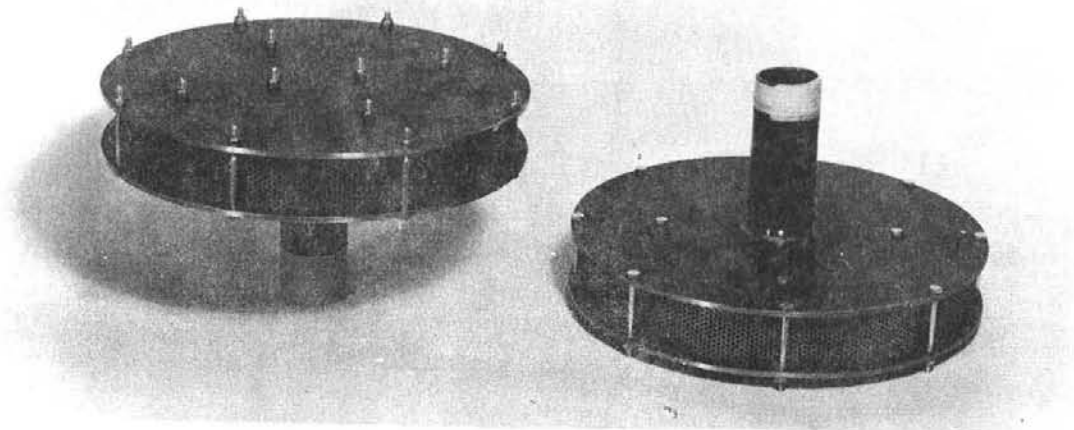


Figure 4-3. Storage Tank Fluid Diffuser (15-in. diameter, 2 in. thick)

## 4.2 Storage Fluid Transfer System

The storage fluid transfer system is shown in Figure 4-4. The major components are the toluene boiler, the Rankine loop heater, and the storage tank.

The purpose of the storage fluid transfer system is to move heated Therminol 66 through the toluene boiler in a controlled manner. If high-temperature storage is at normal operating temperature, the fluid is pumped directly from the high-temperature side of the storage tank, through the boiler, and back to storage. If storage is below operating temperature, the fluid is circulated through valves V4, V3, the VSP, V2, the heater, V1, and the boiler.

The variable speed pump is a Viking pump, Model No. KK-4124-R, with a John Crane Type 15 WT metal bellows seal. This pump is scheduled to arrive in October 1975.

During the last six months the design of the pipelines and control valves of the storage fluid loop has been completed. Control valves have been ordered from Honeywell and construction contracts placed for installation of this loop.
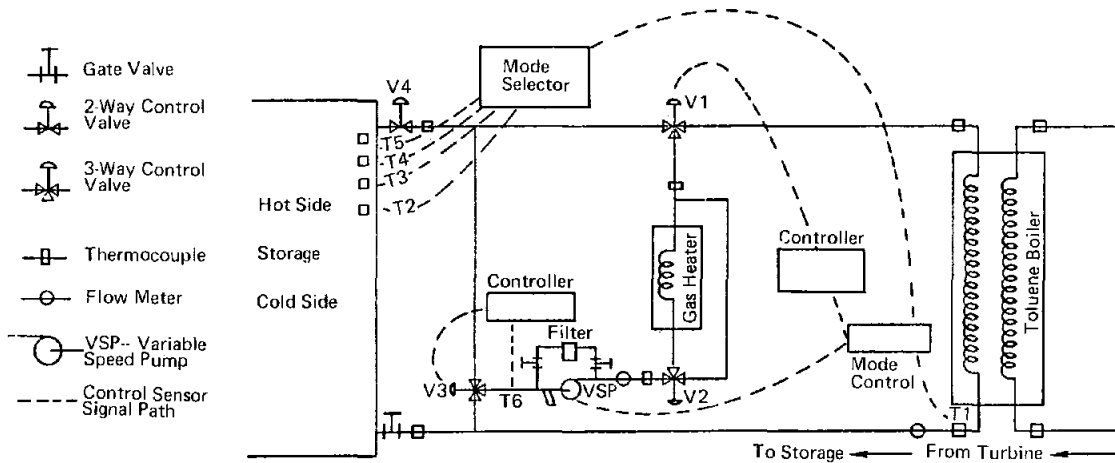


Figure 4-4. Storage Fluid Loop

## Task 5. Turbine/Generator System

### 5.1 Toluene Boiler (Heat Exchanger)

The heat exchanger to transfer the heat from the Therminol 66 (T-66) fluid to the toluene working fluid for the turbine/generator was delivered and installed during the summer. The heat exchanger consists of four separate elements--one for preheating, two for boiling, and one for

superheating (see Figure 5-1). Each element is cylindrical and is part of a continuous vertical stack mounted on four threaded rods attached to an overhead support in the turbine room of the control building. This arrangement was chosen to minimize conductive heat loss paths. With insulation by a 10.2-cm (4-in.) thick ceramic fiber blanket, heat loss from the exchanger will be less than 1/2% of the heat transferred.
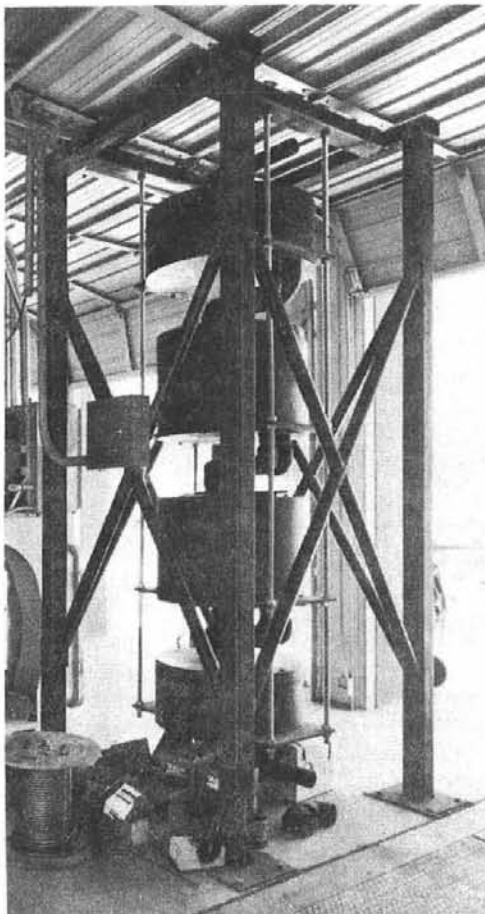


Figure 5-1. Toluene Boiler (heat exchanger)

5.2 Turbine/Generator

The turbine/generator and associated hardware from Sundstrand Energy Systems arrived at Sandia and was set in place at the test facility in August 1975. The unit is shown in Figure 5-2. Completion of the installation of the unit was expected in September, but it has been delayed because of the unavailability of several plant items such as junction boxes and valves. Following completion of the installation, the system will be operated in the direct gas-fired mode to debug the test facility plumbing, wiring, and instrumentation. If the results are satisfactory, the system

will be replumbed to operate in the indirect heating mode as a part of the collector-storage subsystem.

Before being shipped to Sandia, the Sundstrand unit was operated about 200 hours at the supplier's plant following its first sustained run on June 23, 1975. Preliminary efficiency measurements by Sundstrand at the end of July indicate that the unit is 2 to 3 points low from Sundstrand's initial projections, e.g., 10.6% vs 13.4% at 93°C (200°F) summer condenser conditions at full load. Sundstrand's measurements will be verified during our shakedown tests. Sundstrand is presently studying their test data to determine where possible problems lie.

The lower than expected efficiency of the Sundstrand unit affects several other major components in the test facility such as the collector field, the high-temperature thermal storage, the boiler system, and the cooling loop. However, preliminary analyses indicate that the facility is flexible enough to accommodate the decreased turbine system efficiency with the only marginal item being the boiler system under full-load summer conditions.
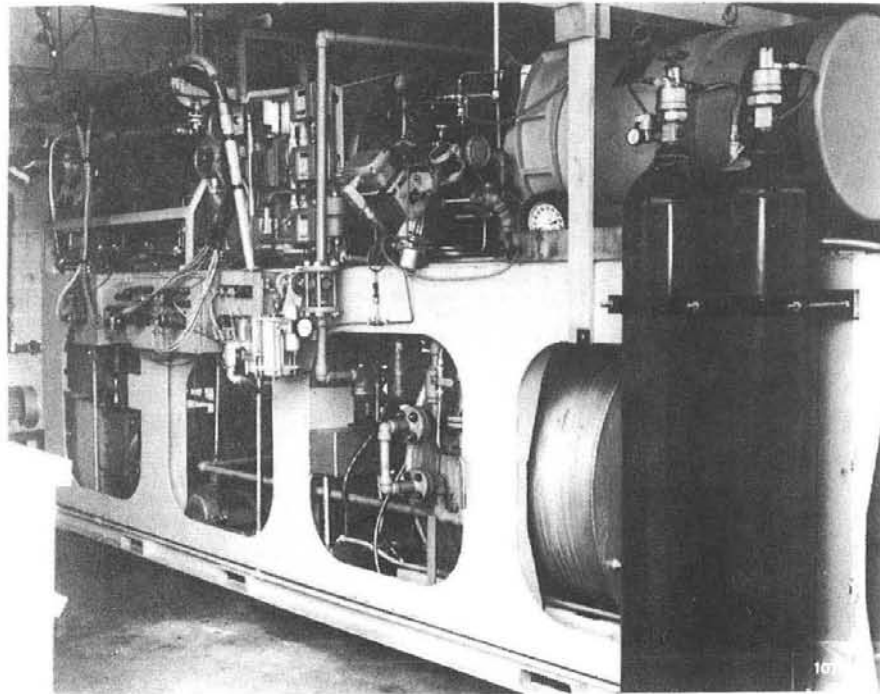


Figure 5-2. Sundstrand Turbine/Generator

## 5.3 Rankine Loop Heater

The Rankine loop heater is used to heat the T-66 when sufficient thermal energy is not being collected and is not in storage. This unit is the natural-gas-fired heater used by Sundstrand to vaporize toluene in their total energy turbine package. The design application was for vaporizing toluene to the super-critical state at a rate from 317 to 3170 MJ/hr (300,000 to 3,000,000 Btu/hr). The current application is to heat Therminol at heat rates of 106 to 950 MJ/hr (100,000 to 900,000 Btu/hr). Consequently, careful attention is being given to the use and control of this heater because of the difference in applications. One particular aspect of concern is the avoidance of hot spots that could conceivably exceed the decomposition temperature of the T-66. During start-up, the maximum flow rate of T-66 is low and laminar flow will persist in the heater. Heat transfer during laminar flow is poor, potentially causing undesired hot spots. It is therefore necessary to provide recirculation to increase the temperature and Reynolds number enough to insure turbulent heat transfer.

Another item of concern is that the minimum flame setting of the heater is higher than the minimum desired in the solar application. None of these problems preclude the use of the heater but they do complicate the methods of use and control. A study contract was placed with Sundstrand to determine heater performance which indicated that the heater would be adequate for solar applications if the minimum flame setting is reduced from 317 to 106 MJ/hr. This modification was accomplished with minimum difficulty.

## 5.4 Turbine Heat Exchanger

The turbine load heat exchanger is the interface between the condenser cooling loop and the cooling tower loop. This exchanger is to keep the cooling tower water, which becomes contaminated by the evaporation process, out of the condenser and low-temperature storage. A "Graham Heli-Flow" counterflow heat exchanger capable of transferring 632,000 kJ/hr (600,000 Btu/hr) was installed in August.

## 5.5 Cooling Tower

The cooling tower used to dissipate the reject heat from the organic Rankine cycle (ORC) turbine and the absorptive air conditioner (simultaneously as necessary) is an induction-type cooler supplied by Baltimore Air Coil, Inc. The unit is shown in Figure 5-3. The tower is capable of cooling 0.022 m$^3$/s (350 gpm) of water from 309° to 303°K (96.5° to 85°F) with a summer cay ambient temperature of 36°C (96°F) and a wet bulb temperature of 21°C (70°F). This cooling capability is equivalent to 2.1 x 10$^6$ kJ/hr (2 x 10$^6$ Btu/hr). The tower uses an induction spray for evaporative cooling and consequently does not require fans with their attendant noise. The basic cooling tower, pumps, and connecting plumbing from the remote tower to the turbine building were installed and functional in September.
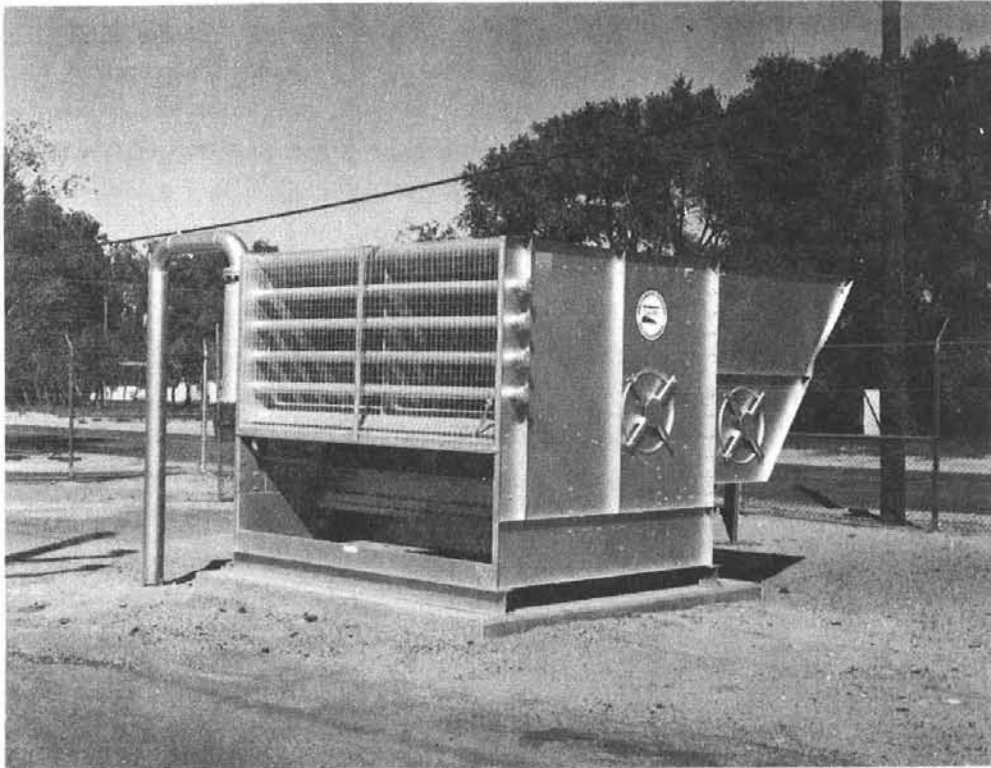
Figure 5-3. Induction-Type Cooling Tower

## 5.6 Load Bank

The load bank for the generator is a stepped-resistor type with a capacity of 49 kW, 3-phase, balanced-load, 60-Hz, 480 volts with forced-air cooling. The steps are as follows:

| Step Number | 1 | 2 | 3 | 4 | 5 | 6 | 7 | 8 | 9 | 10 | 11 |
|---|---|---|---|---|---|---|---|---|---|---|---|
| Capacity (kW) | 10 | 10 | 5 | 5 | 5 | 5 | 5 | 1 | 1 | 1 | 1 |
| Total (kW) | 10 | 20 | 25 | 30 | 35 | 40 | 45 | 46 | 47 | 48 | 49 |

Any combination of these steps may be used. The load bank, which was installed in August, has provisions for remote operation from the motor control center and a thermal cutoff in the event of overheating.

## 5.7 Condenser Fluid Transfer System

The condenser fluid loop is the fluid system that interconnects the turbine condenser with the turbine load heat exchanger of 5.4. In Phase IV-B, the loop will also interconnect the low-temperature storage, the low-temperature storage heater, the solar energy project building, and

the project building thermal load simulator. The fluid used in this loop is a 30% ethylene glycol/water solution. The requirements for the system have been established as follows:

1. Maintain constant cooling water output temperature from the ORC system condenser regardless of system load. Have the capability of changing system control to maintain instead constant ORC fluid output temperature from condenser.

2. Use the turbine load heat exchanger to cool low-temperature storage, by-passing condenser when so doing.

3. Sense when storage is full and automatically divert flow to the turbine load heat exchangers.

4. Have the capability of blending flow from cold side of low-temperature storage with flow direct from condenser to maintain any desired condenser supply temperature (needed when temperature of low-temperature storage is lower than desired condenser supply temperature).

The parts of this system necessary for Phase IV-A, i.e., requirement No. 1 above, have been completed and initial fluid-flow testing has been successfully conducted. Provisions have been made so that those parts of the system required for Phase IV-B, i.e., requirements Nos. 2, 3, and 4, can be easily added.

## 5.8  Cooling Tower Fluid Transfer System

The cooling tower fluid transfer system presently connects the cooling tower described in 5.5 with the turbine load heat exchanger of 5.4 This fluid transfer system was constructed as part of the test facility control building and became operational in September. In Phase IV-B, the cooling tower loop will also connect to the absorptive air conditioner and to the project building thermal load simulator.

Task 6.  Instrumentation and Control System

## 6.1  Control and Equipment Center

A 140-m$^2$ (1500-ft$^2$) building has been constructed to house system components and control equipment. This building houses all major system equipment except the collector field, high- and low-temperature storage, and cooling tower. The building was completed in July; various components and control equipment are being moved into the building daily. The control room of the building is shown in Figure 6-1.
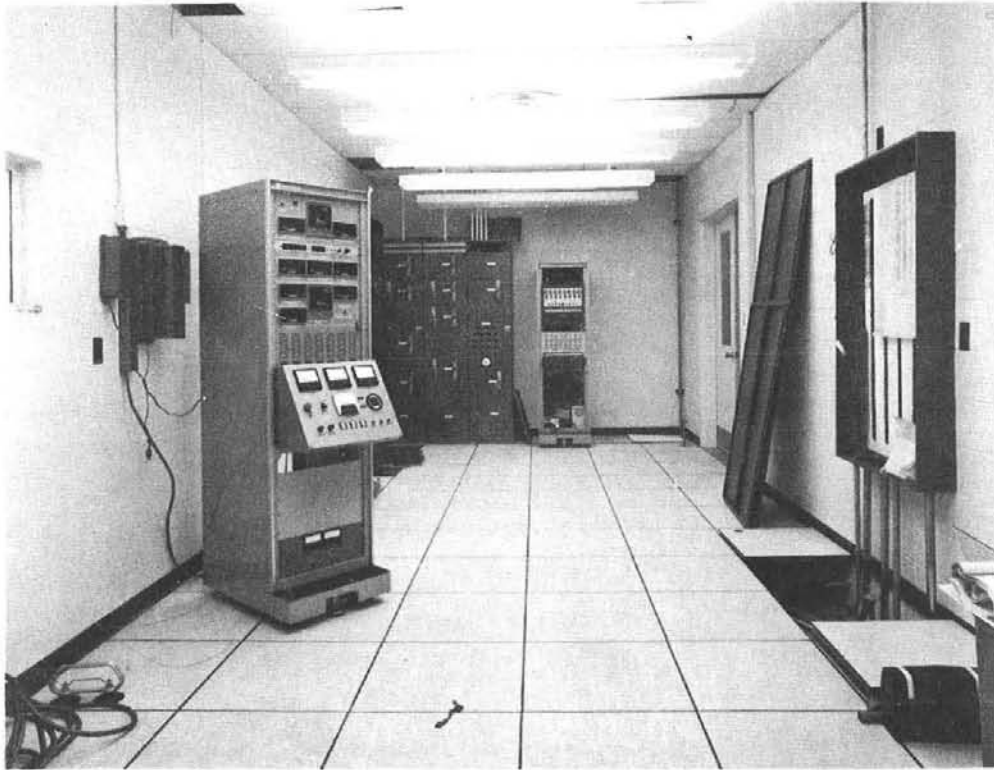
Figure 6-1. View of Control Room in Equipment Building

## 6.2 Control and Instrumentation

Overall control of the system is maintained by control of the fluid transfer systems. The fluid transfer systems will be controlled at three levels.

1.  Commercial controllers represent the lowest level of control capability. Pump speed and flow-control valve settings are varied by single-channel commercial or industrial controllers. These controllers vary the settings to achieve a constant temperature and most of them have proportional, integral (reset), and rate features.

2.  Delta® Honeywell control-monitor equipment is the middle level of control. The Delta® system can:

    Change set points on the controllers

    Monitor process temperatures and flow rates

    Send alarms if any process variable is out of safe tolerance or a motor is not running, etc.

    Present slides of circuits which are in alarm mode.

3.  The minicomputer, at the highest level of control, has the capability to change set points of the controllers through the Delta® system, or it can bypass both the Delta® and the

controllers and directly control selected motors or valves through simple digital-to-analog converters. The minicomputer can then control by algorithms. Thus, optimum control strategies or characteristics can be developed through minicomputer programs, eliminating the need for hardware modification or adjustment.

4. An additional capability of the minicomputer which may be used in controlling output temperatures of the collector field is the ability to temporarily defocus selected groups of collectors. This option may be especially useful when a long series string of collectors is used on partly cloudy days.

It will be the goal to control the system with the first two levels; the third level will be used for performance calculations by holding all settings constant until temperatures stabilize.

At the end of this reporting period about one-half of the instrumentation and control wiring installation had been completed. In the instrumentation system, the minicomputer has been interfaced with (1) the Delta® Honeywell control monitor system--control level No. 2 above (2) the digital shaft-encoder multiplexer (Figure 3-8), and (3) the line printer. The printer has been added since the previous report to provide high-speed printout of data and program listings.

Other progress has included:
- Procurement and delivery of all instruments and control components needed for system operation
- Writing of the minicomputer operating system executive software
- Near completion (99%) of the "watchdog timer," which is a safety device to detect "inattention" by the minicomputer. If the timer is allowed to run a full cycle without being reset by input from the minicomputer, the timer will put the collector field into a safe mode by defocusing the collectors and increasing pump speed to maximum.

Turbine Controls -- The organic Rankine cycle (ORC) turbine must be modified to accommodate operation with solar heated T-66. As delivered from Sundstrand, the ORC system consisted of a natural-gas-fired toluene heater and a toluene-charged turbine. Modifications planned for solar operation include functionally separating the heater from the turbine and providing independent electronic monitors and controls for the turbine and heater. System safety features, such as the overtemperature sensors and toluene vapor sniffer, will continue to function if either the heater or turbine is in use. Also, if an unsafe condition is detected, the turbine is shut down and the natural-gas flame extinguished. A complete test of all system safety devices is planned which will include the detection of overtemperatures and activation of the $CO_2$ fire extinguishers.

Sundstrand has, under contract, completed computer simulation models of the T-66-to-toluene heat exchanger made by Graham and of the ORC operating components, such as the regenerator, condenser, feed pump, bandvalve, and turbine. These models have been reviewed and verified through performance comparison with actual ORC test results.

These turbine system component models have been programmed onto Sandia's CDC 6600 computer system. A series of computer simulations is planned to explore the system's performance under different control strategies and to optimize the energy input/output efficiency.

Collector Field Control -- Several control strategies for the collector field start-up were examined using the analytical model contained in the computer program CONTRL, as previously reported. The basic philosophy of the control strategies is best described by the flow diagram shown in Figure 6-2. The control input to the field is the flow rate, i.e., the output temperature of the field is controlled by adjusting the flow rate. The controller examines parameters in the field (such as field output temperature, solar insolation, or midfield temperature) and uses these parameters in conjunction with the output temperature set point to determine proper flow adjustments.

The first control strategy which was tried used proportional control based on output field temperature only. This strategy did not produce the desired stability. Next, both the output temperature and the solar insolation were used in the control algorithms. Improved stability during start-up resulted from this additional control information.
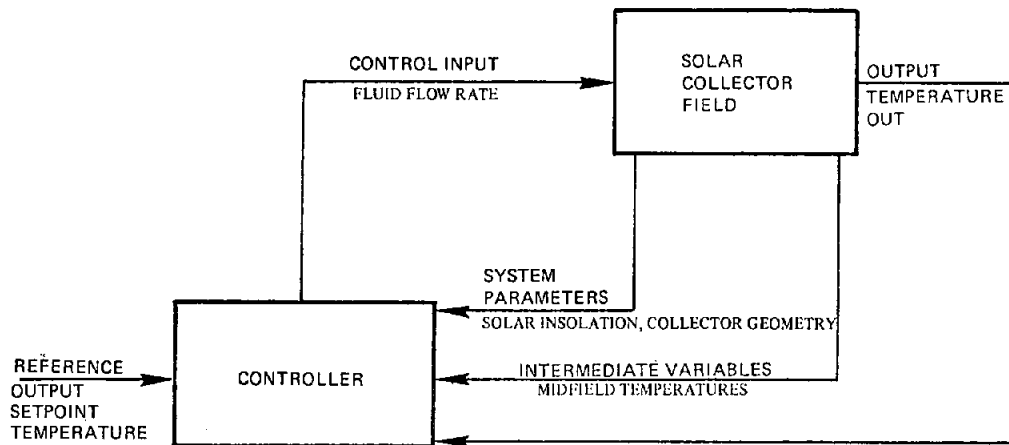


Figure 6-2. Basic Closed Loop Solar Control System

This strategy was further expanded to include a feed-forward temperature from the middle of the collector field. Increased anticipation was the primary reason for using a midfield temperature. For systems which have long transport delays (such as the solar collector field), increased anticipation usually increases controllability. Compared to the results of the previous strategies, the feed-forward/feedback control strategy considerably increased controllability. This computer simulation of collector field fluid transfer system control has been completed. No more such computer runs will be made unless actual test experience indicates that control

problems exist.

A movie has been made to illustrate the effects of various control strategies on the dynamic temperature response of the solar collector tubes and the associated piping. The 8-minute movie is titled "Fluid Temperature Control for Solar Collector Fields." It was made through the use of computer graphics to present in easily comprehended fashion the instantaneous temperature conditions of the entire collector fluid loop as variations in solar input and flow rate occur. The cause and effect relationships and trends are illustrated dynamically.

Instrumentation of many types has been provided throughout the entire solar total energy system to obtain data in sufficient detail for successful system operation, system safety, and the subsequent analysis of a large number of parameters. This acquisition system will operate as follows:

- All instrument outputs will be recorded on magnetic disc or computer-compatible magnetic tape.

- Instrument outputs required for operation will be presented on digital meters.

- Instrument outputs required for analysis of rapidly changing transient conditions will be presented on continuous chart recordings.

- Any outputs desired may be printed out on the minicomputer control terminal or the line printer.

- Any plots desired may be made on the minicomputer control terminal.

- Further analysis may be made at a later time by playing back the magnetic tape to either this system or the larger scientific computers.

Task 7. Collector Test Facility

Testing of receiver tube assemblies in the collector test facility has been substantially completed. The results are shown in Figure 7-1 and Table 7-I. The black-chrome/sulfamate-nickel combination is clearly superior to the others evaluated. Tables 7-II and 7-III show that reasonable correlation has been achieved between test results and the numerical and analytical computer models which have been constructed.

The equipment is now available to evaluate different turbulence generators (in addition to cylindrical plugs) for asymmetrically heated receiver tubes. Testing should begin in November 1975. The purpose of the testing is to determine which turbulence generator design will cause the highest average liquid heat transfer coefficient and the lowest viscous drag increase. The present turbulence generator (a cylindrical plug) will be replaced should a better one be identified.
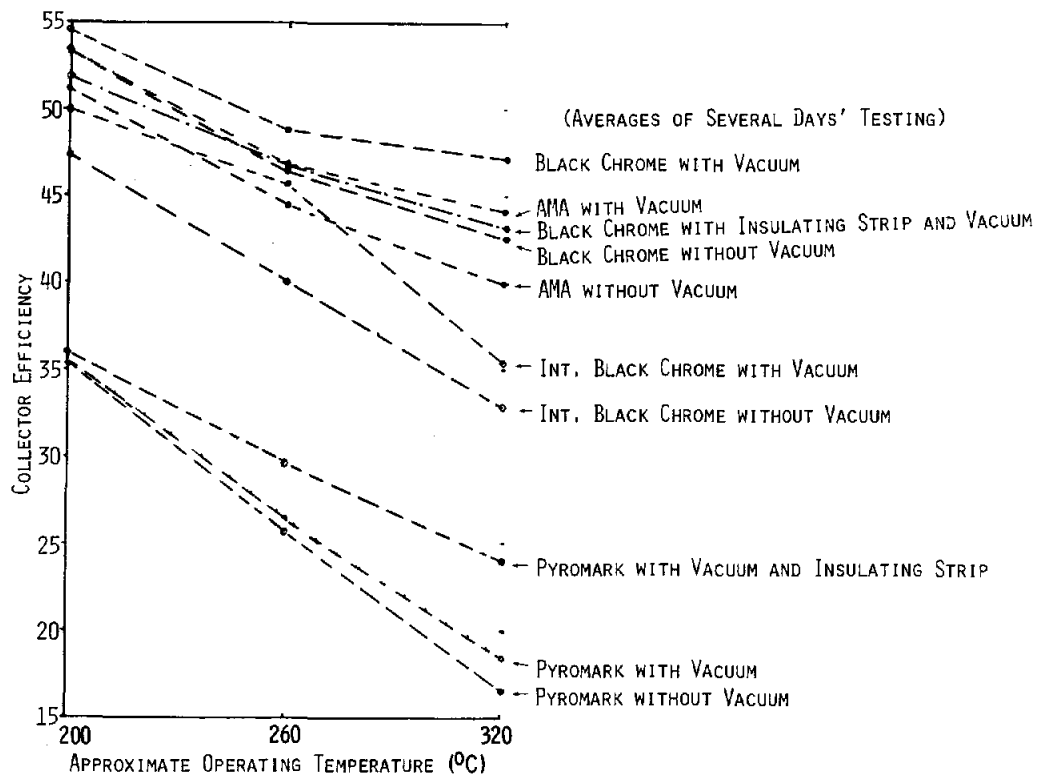
Figure 7-1. Test Results from 90° Rim Angle Alzak Reflector

TABLE 7-I

Average Collector Efficiency Percentage at 316°C (600°F)

| Receiver Tube Coating | No Vacuum | Vacuum | Vacuum w/Insulator | Vacuum w/Plug | No Vacuum w/Plug | Remarks |
|---|---|---|---|---|---|---|
| Pyromark (Tempil) ($\alpha = 0.98$, $\epsilon = 1.0$) | 16.2 | 18.32 | 23.9 | X | X | Average of 10 days' data for Vacuum/No Vacuum. Average of 4 days' data for Vacuum w/Insulator. |
| Intermediate Black Chrome on Bright Nickel ($\alpha = 0.88$, $\epsilon = 0.24$) | 32.1 | 34.6 | | | | Average of 8 days' data |
| AMA (Honeywell) ($\alpha = 0.97$, $\epsilon = 0.38$) | 39.0 | 43.1 | 42.2 | | | Average of 5 days' data for Vacuum/No Vacuum. Vacuum w/Insulator, 1-day average. |
| Black Chrome on Sulfamate Nickel ($\alpha = 0.97$, $\epsilon = 0.28$) | 41.6 | 46.2 | 43.1 | | X | Average of 9 days' data for Vacuum/No Vacuum. Average of 6 days' data for Vacuum w/Insulator. |

NOTES:  1.  Volume flow rate approximately 5.7 ℓ/min (1.5 gpm) (Re > 12,000)

2.  Test temperature varied between 302° and 311°C (575° and 591°F)

3.  Collector Efficiency Percentage =

$$\frac{\dot{m} \, C_p \, (T_{OUT} - T_{IN})}{(\text{Aperture Area}) \, (\text{Direct Insolation})}$$

4.  Direct Insolation Range: 861-990 W/m$^2$ (273-314 Btu/ft$^2$hr)

5.  Wind Velocity Range: 0.24-3.46 m/sec (0.73-11.4 ft/sec)

6.  Internal cylindrical plug of 1.59-cm (5/8-in.) diam

7.  X = To be tested

8.  Alzak reflector ($\rho \cong 0.7$)

TABLE 7-II

Comparison of Analytical to Experimental Results

| | Normal Isolation (W/m²) | (Btu/ft²hr) | Ambient Wind Velocity (m/s) | (ft/s) | Ambient Temperature (°C) | (°F) | Initial Fluid Temperature (°C) | (°F) | Efficiency (%) Experimental | Analytical |
|---|---|---|---|---|---|---|---|---|---|---|
| **For Fluid Temperature 316°C (600°F)** | | | | | | | | | | |
| Pyromark | 915 | 290 | .87 | 2.84 | 8 | 46 | 307 | 585 | 16.2 | 16.2 |
| Pyromark, Vacuum | 918 | 291 | .73 | 2.41 | 8 | 46 | 308 | 586 | 18.3 | 19.7 |
| Pyromark, Vacuum and Insulation | 930 | 295 | .77 | 2.52 | 4 | 40 | 307 | 585 | 23.9 | 26.9 |
| IBC | 934 | 296 | .65 | 2.12 | 8 | 47 | 308 | 587 | 32.1 | 34.5 |
| IBC, Vacuum | 934 | 296 | .66 | 2.18 | 8 | 47 | 308 | 586 | 34.6 | 39.5 |
| AMA | 949 | 301 | .65 | 2.13 | 9 | 49 | 305 | 581 | 39.0 | 35.4 |
| AMA, Vacuum | 949 | 301 | .67 | 2.19 | 10 | 50 | 305 | 581 | 43.1 | 39.7 |
| **For Fluid Temperature 260°C (500°F)** | | | | | | | | | | |
| Pyromark | 911 | 289 | .68 | 2.22 | 8 | 47 | 264 | 508 | 25.2 | 26.9 |
| Pyromark, Vacuum | 915 | 290 | .77 | 2.54 | 8 | 47 | 264 | 507 | 25.8 | 29.6 |
| Pyromark, Vacuum and Insulation | 880 | 279 | 1.03 | 3.38 | 8 | 47 | 261 | 502 | 29.7 | 33.4 |
| IBC | 962 | 305 | .79 | 2.60 | 8 | 46 | 259 | 499 | 39.1 | 39.5 |
| IBC, Vacuum | 959 | 304 | .77 | 2.54 | 8 | 47 | 259 | 498 | 44.6 | 43.5 |
| AMA | 984 | 312 | .78 | 2.55 | 12 | 53 | 255 | 491 | 43.5 | 41.9 |
| AMA, Vacuum | 981 | 311 | .92 | 3.02 | 11 | 52 | 256 | 493 | 45.7 | 45.0 |
| **For Fluid Temperature 204°C (400°F)** | | | | | | | | | | |
| Pyromark | 858 | 272 | 1.15 | 3.76 | 8 | 47 | 208 | 407 | 34.7 | 36.5 |
| Pyromark, Vacuum | 867 | 275 | 1.12 | 3.67 | 8 | 46 | 208 | 407 | 35.2 | 39.3 |
| Pyromark, Vacuum and Insulation | 817 | 259 | 2.94 | 9.63 | 14 | 57 | 206 | 403 | 35.6 | 40.4 |
| IBC | 959 | 304 | .72 | 2.37 | 10 | 50 | 204 | 400 | 46.3 | 50.8 |
| IBC, Vacuum | 959 | 304 | .69 | 2.25 | 10 | 50 | 204 | 399 | 48.8 | 54.0 |
| AMA | 968 | 307 | .73 | 2.38 | 13 | 56 | 202 | 395 | 50.0 | 48.4 |
| AMA, Vacuum | 968 | 307 | .73 | 2.38 | 13 | 56 | 202 | 395 | 52.1 | 51.3 |

TABLE 7-III

Measured and Calculated Efficiencies for a Cylindrical Parabolic
Focusing Collector with a Black Chrome Plated Receiver Tube
(nonevacuated annulus)

| | Fluid Inlet Temperature (°C) | Direct Solar Intensity (W/m$^2$) | Ambient Temperature (°C) | Wind Speed (m/s) | Efficiency (%) | |
|---|---|---|---|---|---|---|
| | | | | | Measured | Calculated |
| 1 | 305 | 941 | 16 | .6 | 46 | 46 |
| 2 | 304 | 926 | 28 | 1.9 | 44 | 46 |
| 3 | 304 | 900 | 25 | 1.3 | 46 | 45 |
| 4 | 305 | 866 | 21 | 2.5 | 35 | 44 |
| 5 | 307 | 904 | 21 | 1.1 | 39 | 46 |
| 6 | 305 | 935 | 23 | 3.4 | 39 | 46 |
| 7 | 306 | 935 | 16 | .7 | 45 | 46 |
| 8 | 258 | 922 | 32 | 3.3 | 49 | 49 |
| 9 | 262 | 957 | 20 | .5 | 45 | 49 |
| 10 | 259 | 922 | 30 | 1.0 | 49 | 49 |
| 11 | 249 | 922 | 26 | 1.4 | 50 | 49 |
| 12 | 254 | 891 | 22 | 1.8 | 43 | 49 |
| 13 | 257 | 932 | 23 | 1.7 | 42 | 49 |
| 14 | 253 | 929 | 24 | 2.8 | 46 | 49 |
| 15 | 256 | 935 | 17 | .6 | 49 | 50 |
| 16 | 204 | 853 | 29 | 1.0 | 59 | 52 |
| 17 | 206 | 954 | 23 | .5 | 56 | 53 |
| 18 | 207 | 926 | 30 | 1.7 | 54 | 52 |
| 19 | 205 | 922 | 27 | 2.8 | 52 | 52 |
| 20 | 208 | 894 | 24 | 1.0 | 50 | 52 |
| 21 | 204 | 941 | 24 | 1.0 | 52 | 52 |
| 22 | 202 | 929 | 25 | 2.2 | 51 | 52 |
| 23 | 209 | 938 | 21 | .6 | 54 | 52 |

Task 8. Improved Data Base Compilation

## 8.1 System Load Profiles

Electric Load Data for Solar System Simulation -- The Public Service Company of New Mexico
has made available to Sandia Laboratories additional data on residential electric load profiles.
These data represent the average electric power consumption profiles for groups of customers
three residential rate classes, including a total of 127 individually monitored residential customers

within the City of Albuquerque. Each of these groups of customers were selected at random within each of the three residential rate classes. The data cover an 8-month period from November 1973 through June 1974. Residential electric power consumption profiles representing weekday and weekend usage for winter, spring, and summer seasons have been developed for the Residential General rate class from these data (Figure 8-1).
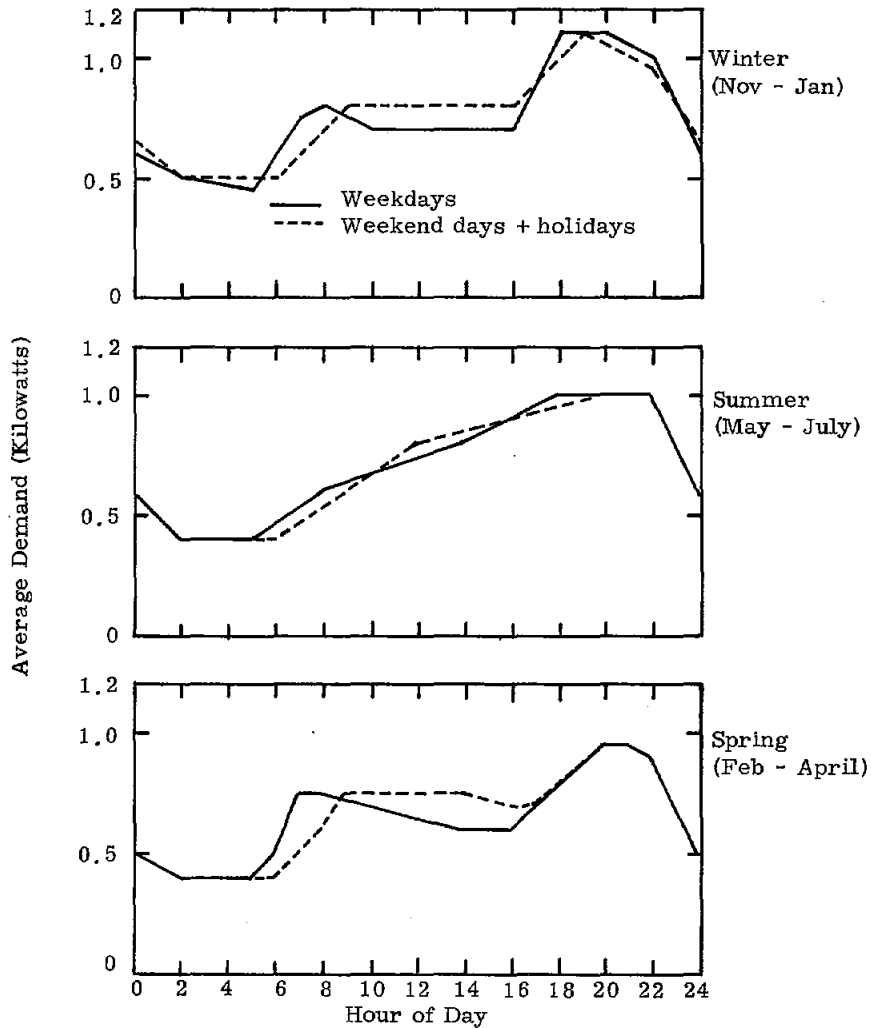


Figure 8-1. Profiles of Daily Residential
Electric Power Consumption
by Season

Thermal Loads -- No change in the definition of the 2000-dwelling-unit, mixed-load community has been made during this reporting period. A description of the methodology used in selecting the community design as well as a detailed description of HLOAD (the thermal analysis computer program) is contained in a recent report.[1] Tables 8-I and 8-II report the building characteristics and results of the thermal analysis of this community.

---

[1] R. W. Harrigan, "Application of Solar Total Energy to a Mixed-Load Community," Sand75-0542, Sandia Laboratories, TBP.

TABLE 8-I

Thermal Characteristics of Building Types

| | Heat-Transfer Coefficients $(J/m^2\text{-}C\text{-}s)$ | | Building Heat Capacity(c) $(J/m^2\text{-}C)$ | Infiltration (room changes per hour) | Average Peak Occupancy per Unit | Interior Design Temp $(^\circ C)$ | |
|---|---|---|---|---|---|---|---|
| | Wall (a) | Roof (b) | | | | Heating | Cooling |
| Single Family Detached | .454 | .227 | $5.1 \times 10^4$ | 1.0 | 4 | $19 (66^\circ F)$ | $25 (77^\circ F)$ |
| Single Family Attached | .454 | .227 | $10.2 \times 10^4$ | 1.0 | 4 | 19 | 25 |
| Low-Rise Apartments | .454 | .227 | $10.2 \times 10^4$ | 1.0 | 4 | 19 | 25 |
| High Rise Apartments | .454 | .227 | $68.9 \times 10^4$ | 1.5 | 4 | 19 | 25 |
| Schools | .454 | .227 | $5.1 \times 10^4$ | 1.5 | 1520 | 19 | 25 |
| Commerical | .454 | .227 | $5.1 \times 10^4$ | 1.5 | 400 | 19 | 25 |

a. Corresponds to R13 wall

b. Corresponds to R22 roof

c. Heat capacity is based on roof area.

## TABLE 8-II

### Average Daily Community Thermal Loads[*]
(all values in GJ)

| | SFD (139 m$^2$) | | | SFA (116 m$^2$) | | | LR (850 m$^2$) | | | HR (113 m$^2$) | | | 3 Schools (7587 m$^2$) | | | Commerical (7432 m$^2$) | | |
|---|---|---|---|---|---|---|---|---|---|---|---|---|---|---|---|---|---|---|
| | Heat | A/C | HW | Heat | A/C | HW | Heat | A/C | HW | Heat | A/C | HW | Heat | A/C | HW | Heat | A/C | HW |
| Spring | 78.6 | 0 | 32.9 | 67.1 | 0 | 52.9 | 27.1 | 0 | 31.4 | 22.9 | 0 | 14.3 | 4.3 | 0 | 1.1 | 2.9 | 0 | 0 |
| Summer | 0 | 112.9 | 27.1 | 0 | 11.4 | 42.9 | 0 | 54.3 | 25.7 | 0 | 28.6 | 11.4 | 0 | 0 | 0 | 0 | 15.7 | 0 |
| Fall | 2.9 | 1.1 | 25.7 | 0 | 1.3 | 40.0 | 0 | 0.6 | 24.3 | 0 | 0.1 | 11.4 | 0 | 1.0 | 0.9 | 0 | 1.0 | 0 |
| Winter | 129.2 | 0 | 32.9 | 104.3 | 0 | 52.9 | 47.1 | 0 | 31.4 | 37.1 | 0 | 14.3 | 8.6 | 0 | 1.1 | 4.3 | 0 | 0 |
| Year | 52.7 | 28.5 | 29.7 | 42.9 | 28.2 | 47.2 | 18.6 | 13.7 | 28.2 | 15.0 | 7.2 | 12.9 | 0.2 | 8.3 | 0.8 | 1.8 | 4.2 | 0 |

[*] SFD = 504 Single Family Detached Dwelling Units

SFA = 800 Single Family Attached Dwelling Units

LR  = 480 Low-Rise Dwelling Units

HR  = 216 High-Rise Dwelling Units

Figure 8-2 shows the basic physical sizes of the different building types comprising the community while Figure 8-3 portrays a possible community layout representing about one-fourth the total community.

In addition to the general community description above, incorporation of parabolic collectors into the overall community architecture has been investigated by the University of New Mexico Architectural Department. A first design effort is shown in Figure 8-4.



**RESIDENTIAL**

WALK-UP APTS — 10 UNITS/BUILDING, 480 FAMILIES, 24%

ELEVATOR APTS — 54 UNITS PER BUILDING, 216 FAMILIES, 13.5 STORIES HIGH, 11%

SINGLE FAMILY DET. — 504 FAMILIES, 25%

SINGLE FAMILY ATT. — 5 UNITS/BUILDING, 800 FAMILIES, 40%

**EDUCATIONAL**

ELEMENTARY SCHOOLS 1&2

Jr. HIGH SCHOOL 3

**COMMERCIAL 4**
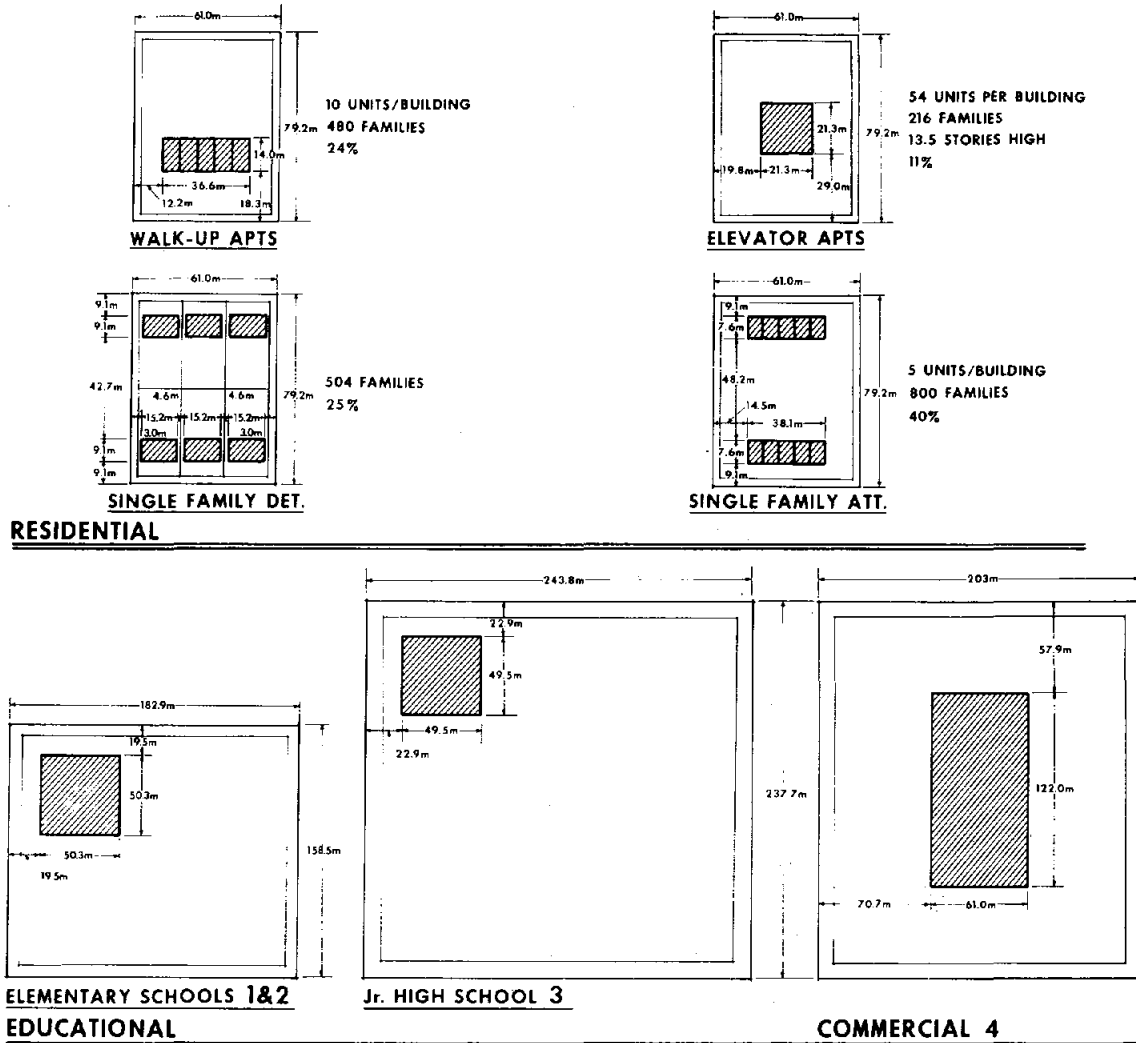
Figure 8-2. Mixed-Load Community Components

SINGLE FAMILY DETACHED     SINGLE FAMILY ATTACHED
LOW-RISE/HIGH DENSITY      HIGH-RISE/HIGH DENSITY
SCHOOL          COMMERCIAL        30.0m (100 FT.) SCALE
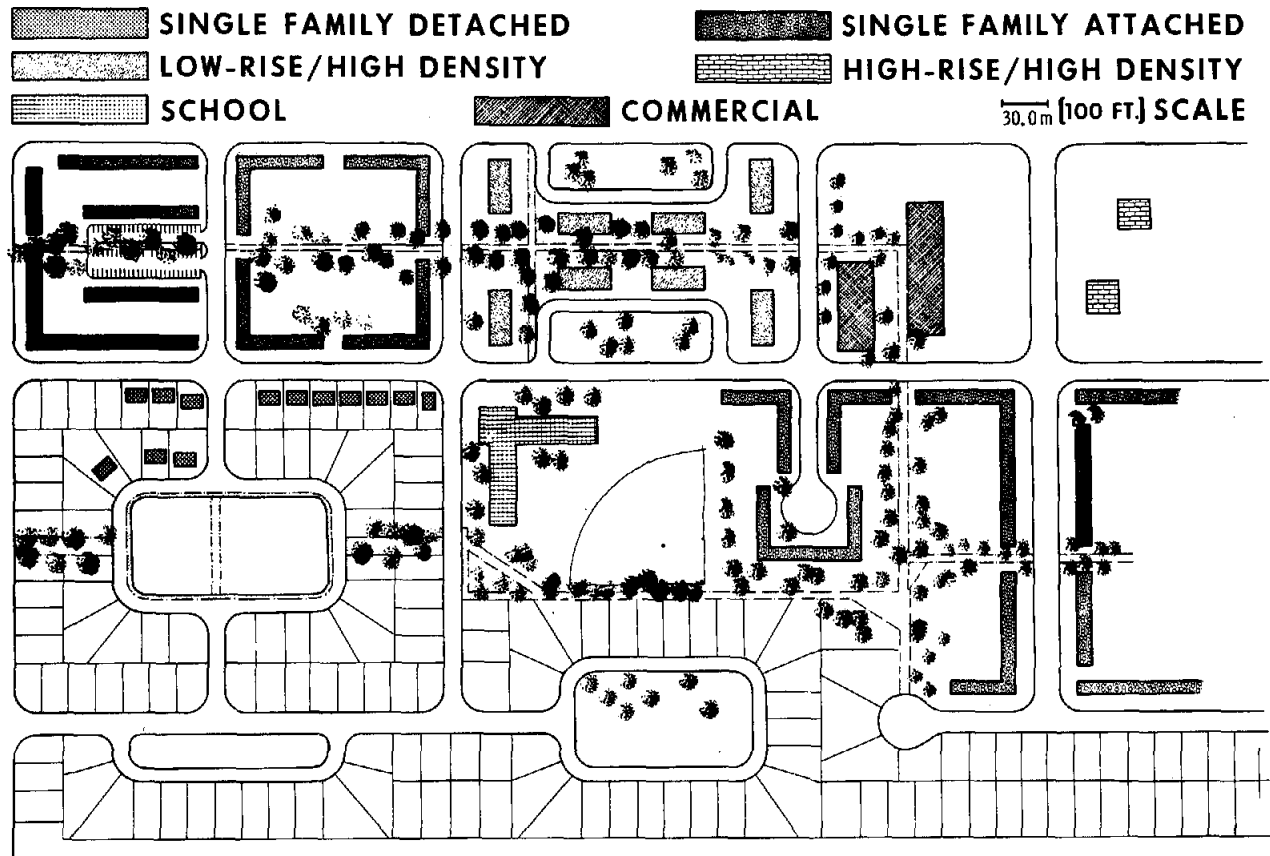
Figure 8-3. Mixed-Load Community Layout
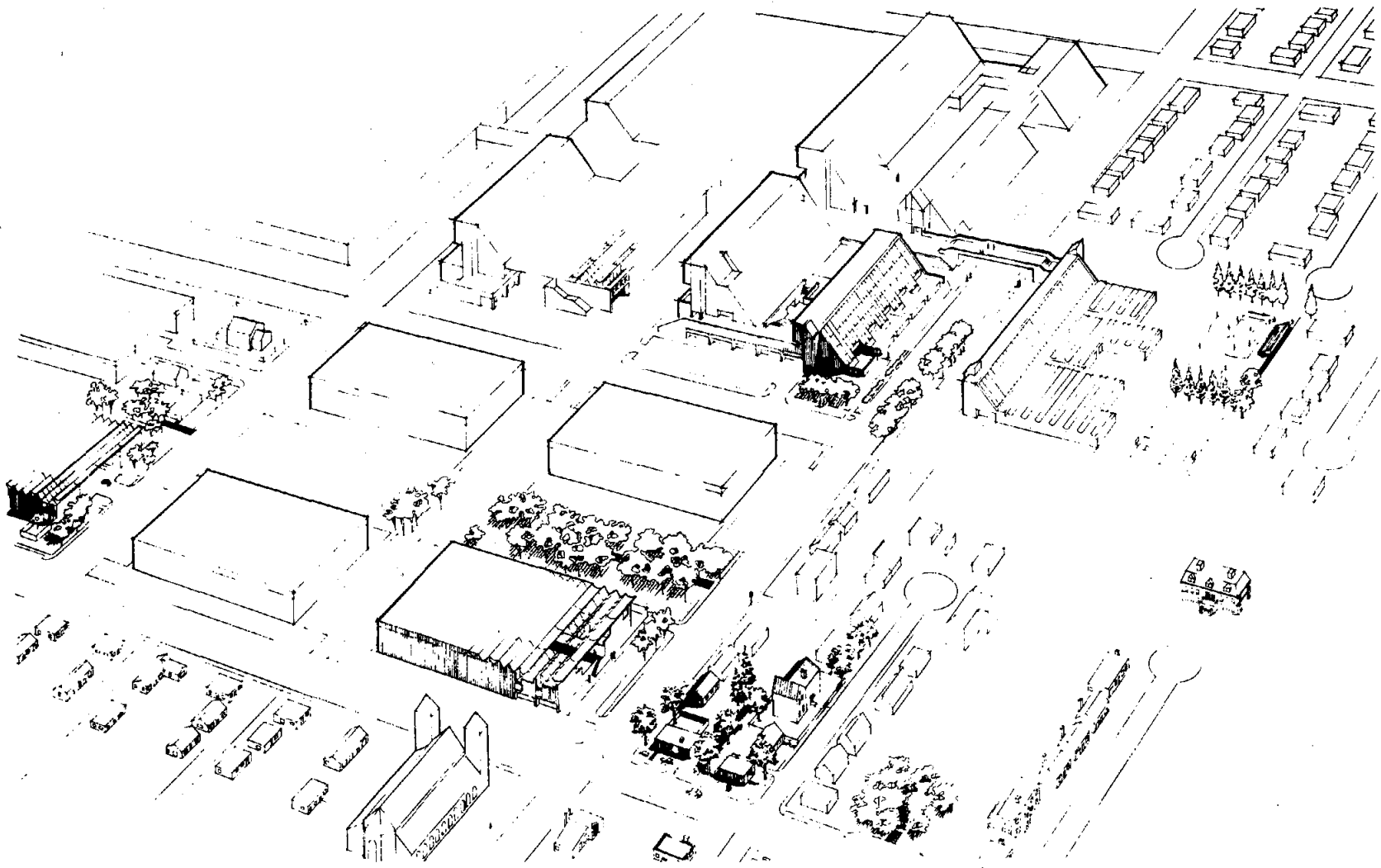
Figure 8-4.  Solar Total Energy System
Preliminary Architectural Sketch (University
of New Mexico Department of Architecture)

## 8.2 Solar and Weather Data

Solar Data -- The general lack of direct-normal solar radiation data along with the need for such data as input for solar total energy systems analysis led to a thorough search for a method of estimating direct-normal radiation from measurements of total-horizontal radiation. The results of this search are a collection of estimation formulas for different seasons and locations.[1]

The process of using this technique to generate direct-normal data samples for a selection of U.S. locations is underway and will be completed in a few months. Specifically, a computer tape of the 1962 and 1963 hourly readings of total-horizontal solar radiation for eight U.S. cities has been obtained from the National Climatic Center. Estimates of the corresponding hourly direct-normal readings are being generated. Finally, these hourly total-horizontal and direct-normal solar radiation data are being merged with hourly readings of those surface parameters which are relevant to solar energy systems studies. The result will be a single computer tape containing solar and weather data for 24 hours per day for two years and eight cities; the cities are Albuquerque, Blue Hill, Mass., Fort Worth, Miami, Nashville, Omaha, Seattle, and Los Angeles.

In connection with the efforts to improve the knowledge of direct-normal radiation, two other solar data sources have been prepared. The first of these consists of readings of total-horizontal and direct-normal radiation intensities at 10-minute intervals for Albuquerque in 1962. The readings were taken from copies of total and direct strip chart records obtained from the National Climatic Center. These solar data were carefully checked for anomalies and then merged with hourly values of temperatures, wind speed and direction, sky cover, and visibility. The data tape is available from the Argonne Data Center under the code name DATABQ62.

Another data source which was prepared for deriving correlations between direct and total radiation consists of four representative sample weeks of total and direct data at 10-minute intervals for Albuquerque, Blue Hill, and Omaha. These samples are representative of those locations and the four seasons since the total-horizontal radiation for a sample week equals the long-term weekly average total radiation for the corresponding season and location. This data source, which will also be available through the Argonne Data Center, has not yet been combined with weather data.

A Portable Solar Monitoring Station -- To assist in data acquisition for solar energy experiments in various and sometimes remote locations, a contract to assemble a versatile, high-quality, portable solar and weather monitoring unit was let to EG&G. The unit directly measures total-horizontal, direct-normal, and diffuse radiation as well as temperature, pressure, wind speed and

---

[1] E. C. Boes, "Estimating the Direct Component of Solar Radiation." SAND75-0565, Sandia Laboratories, Nov., 1975.

direction, and humidity. The data is automatically recorded on cassette tape at optional sample rates.

Tentative plans call for operating the unit at various locations around Albuquerque to allow comparison with the data recorded by the National Weather Service at the city's airport. A prime candidate location is on Sandia Crest, a peak about 1 vertical and 12 lateral miles from the NWS station.

Another experiment under consideration is operating the unit for several months at Santa Fe, New Mexico, which would allow a comparison of current direct-normal radiation readings with the numerous direct-normal readings made at Santa Fe between 1912 and 1922 by the U. S. Weather Bureau. Such a comparison is potentially very interesting, especially to individuals curious about long-term climatic change.

## Task 9. Phase IV-B Supportive Energy Research

### 9.1 Collector Fabrication Development

A pair of precision metal parabolic molds have been in use throughout this reporting period in the fabrication of small parabolic test sections. The molds are 0.6 x 1.2 m (2 x 4 ft) with a 76.2-cm (30-in.) focal length. The 1.2-m dimension is from rim to rim. A variety of test sections have been fabricated for evaluation of their contour accuracy before and after subjection to environmental testing.

These recent fabrication techniques have included:
- Plywood units for evaluation of process parameters
- Plywood skin/honeycomb core
- Aluminum skin with both paper and aluminum honeycomb cores
- Fiberglass/polyester skins with paper honeycomb core
- Fiberglass/polyester skins with fiberglass/polyester core
- Melamine skins with paper honeycomb core.

These units have been placed in outdoor exposure racks as well as in environmental chambers for accelerated aging.

Inspection of parabolic reflectors has required development of new techniques to avoid laborious mechanical measurements. Optical inspection techniques using a laser on an optical bench have been investigated and appear very promising. One technique consists of mounting the laser so that it can be moved across the trough from rim to rim, thereby providing an incoming light beam which is always parallel to the focal plane. Figure 9-1 illustrates the equipment setup. The reflected beam is detected by an area detector centered at the focus. Deviation of the reflected beam

from the theoretical focus can be detected and plotted as a function of the rim-to-rim dimension. Translation of the laser position along the trough's longitudinal axis allows multiple traverses rim to rim, so that a "map" of the reflector contour can be made. One such plot made early in this development effort is shown in Figure 9-2. The individual traces of this plot represent slope error measured by a single rim-to-rim traverse; because of special circumstances for this particular setup longitudinal slope errors were not plotted, but both can be measured with appropriate area detectors. Rim angle also has an important bearing on this inspection technique. These 0.6 x 1.2-m (2 x 4-ft) units had a 45° rim angle, allowing a planar line or area detector to be used. For higher rim angles, other types of detectors (perhaps cylindrical) will be required.

Another variation of this inspection technique, using a computer to reduce the raw data, could eliminate the laser movements. The laser would be positioned in the trough focal plane and would then swivel in azimuth and elevation to scan the trough reflector surface in a series of sweeps from that single position. The detector would have to be moved along the focal line in coordination with the laser sweep. The incoming light beams would not be parallel, but the computer could solve the ray trace problems and provide slope error plots for the trough surface.

The laser optical inspection technique is still in early development but it appears to offer significant promise as a tool for evaluating development units, for initial fabrication process control, and perhaps for production inspection.
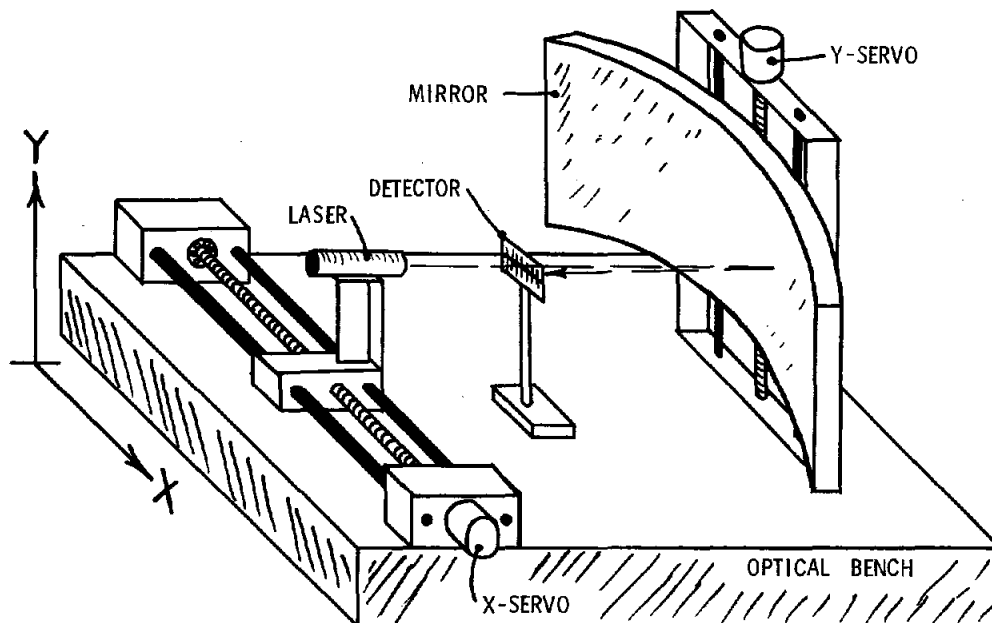


Figure 9-1. Laser Ray Trace Setup
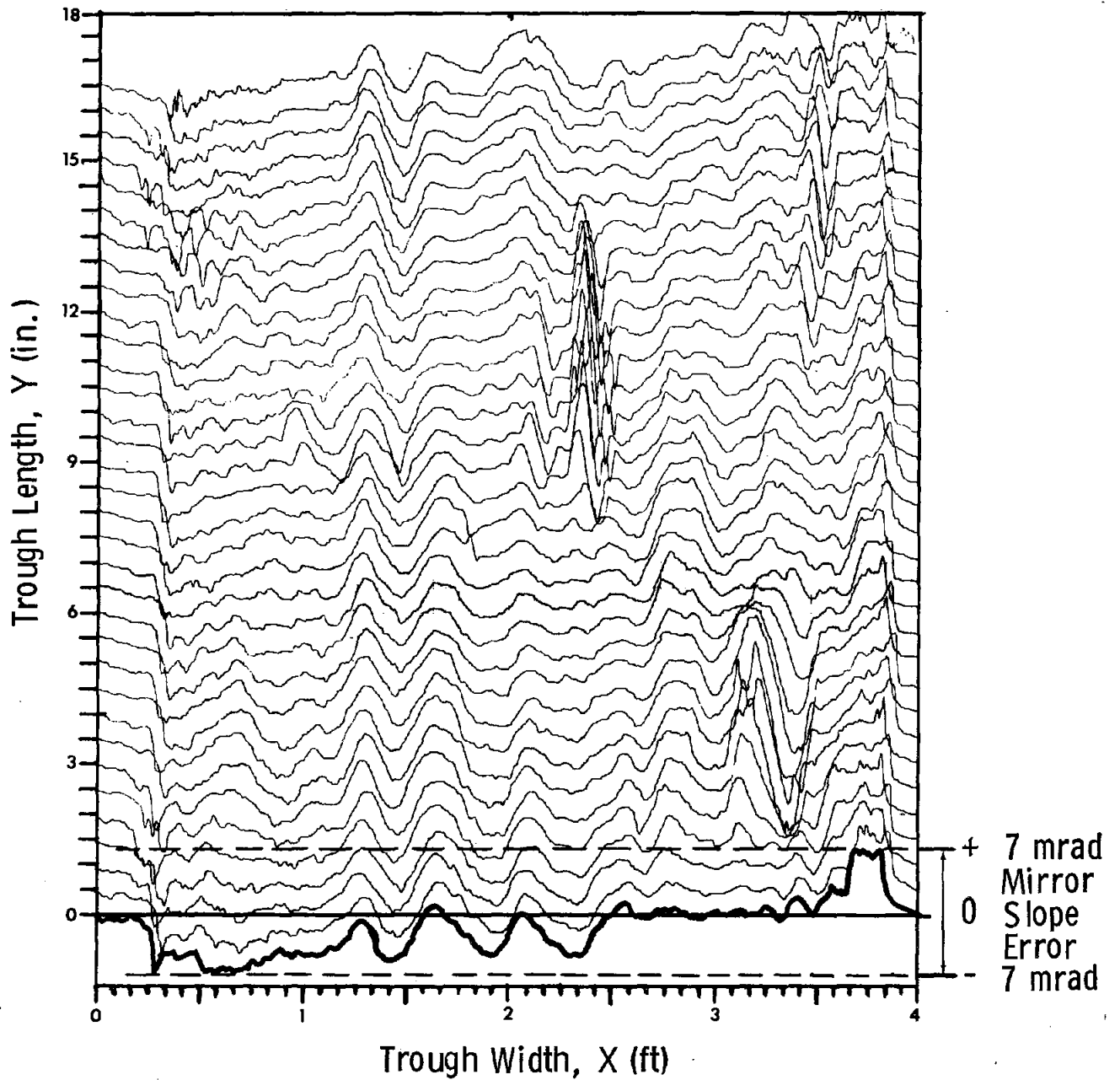
Figure 9-2. Transverse Slope Error of Parabolic
Mirror Test Section

## 9.2 Storage Technology

Although the Phase IV-A storage component is designed to store thermal energy in the form of high-temperature heat transfer oil (Therminol 66), alternative technologies are being investigated. While the thermocline concept, if functional, minimizes the number of storage tanks, a large amount of heat transfer oil is required. The high cost of Therminol 66 ($1200/m$^3$ or $5.50/gal) has prompted the search for new storage technologies.

Perhaps one of the most promising techniques compatible with the Sandia total energy system is mixed rock/hot-oil storage. The oil storage tank would be filled with small rocks (pea gravel and sand) and the thermal energy would be stored in both the hot oil and the rocks. Thermal stratification would be maintained as in the present Sandia system. The great advantage of this concept (proposed by Rocketdyne Corporation) is that the rock would displace up to 65% of the oil volume (the heat-storage capacity of rocks is very close to that of the oil). This concept might possibly reduce storage costs 65%.

An additional storage concept explored during this reporting period was a commercial unit employing heat of fusion as a storage medium. The storage unit uses the heat of fusion of sodium hydroxide doped with selective impurities and the resultant storage medium is called Thermkeep. A numerical heat-transfer analysis showed Thermkeep to be incompatible with the Sandia Solar Energy concept because the temperature in the storage unit tends to decrease uniformly from the high-temperature to the low-temperature end, while a uniform high-temperature region separated from a uniform low-temperature region by a narrow heat exchange area is necessary to maintain the high toluene outlet temperature required by the ORC.

Study has shown that a heat-of-fusion storage unit would perform properly in the Sandia system if the storage medium and the heating fluid have a phase change at the desired toluene outlet temperature. A heating fluid phase change in the storage unit would require boiling the fluid in the collector field, which would required a new absorber tube design, or using a heat exchanger between the collector fluid and the storage unit heating fluid.

A study which considers storing energy in a flywheel is summarized in section 2.2.

## 9.3 Theoretical Studies

Sizing of Reflector and Receiver Tube Assembly for Phase IV-B -- A composite computer program has been written which calculates the energy deposited upon a receiver tube (described in the previous semiannual report), the fluid flow characteristics and heat-transfer coefficient of the liquid within the receiver tube, and the thermal losses from the receiver tube assembly. Through the use of this computer program, attempts are being made to determine the sizes of reflectors and receivers for Phase IV-B.

The Phase IV-A collector rim angle of 90° was selected because it resulted in the shortest maximum rim-to-receiver distance. The receiver tube diameter was based upon an assumed reflected energy distribution, an assumed tracking accuracy, and the receiver tube coating photon reflection angle. The receiver tube subtended angle from the rim is 1-3/4°.

The new code permits trade-offs between energy intercepted (as a function of energy distribution and receiver-tube diameter) and energy lost (as a function of receiver-tube diameter) for different rim angles. Some of the results are portrayed on Figure 9.3. For the given conditions and a given energy distribution (caused by mirror slope errors and tracking errors and assumed to be a normal distribution), the optimum receiver-tube diameter can be determined. The figure suggests that a linear relationship (the apex connecting line) can be used to determine the receiver-tube diameter once the energy distribution is known. The energy distribution standard deviation of 0.00772 radians corresponds to a $-2\sigma$ (containing 95.46% of the energy) angle of 1.77°. The resulting optimum receiver tube diameter subtends a 1.4° angle from the rim.

Recent information described in Task 3.1 suggests than an energy distribution standard deviation of 0.0072 radians is attainable. With this distribution, the information portrayed in Figure 9-4 was generated. The figure shows that a reflector rim angle of between 105 and 110° results in the maximum efficiency which is approximately 1/2% higher than for a 90° rim angle.

Although the maximum efficiency normally means the greatest energy collection in a day, other considerations influence which rim angle should be chosen. For example, for the same liquid flow rate a smaller receiver diameter means more pump work because of increased pipe friction. The optimum receiver diameter for a 105° rim angle is smaller than that for a 90° rim angle and it is the net energy (collected energy less pump work expenditures) which must be considered. Another consideration is the arc length of the reflector material. For a given aperture, the arc length determines the amount and cost of reflector material and structure necessary to intercept a given quantity of energy. Table 9-I illustrate the influence of arc length and also shows optimum receiver-tube diameter. The 105° rim angle requires 8% more surface area than the 90° rim angle. The net-energy/construction-cost ratio will determine the rim angle to be chosen.

Both 70° and 80° rim-angle data are included in the table. The first two listed are equivalent to a 90°-rim-angle collector with 20 and 10° removed from the edges. The aperture for a 90° design is decreased by 16% when trimmed to an 80° rim angle while the arc length is decreased by 19%. The length of a trimmed 80° must increase to intercept the same energy and so must the number of support pylons, but cost savings may be realized since the support pylons are smaller and surface area is less.

These data illustrate that the selection of a rim angle and receiver-tube diameter will be influenced significantly by construction cost and energy collected.
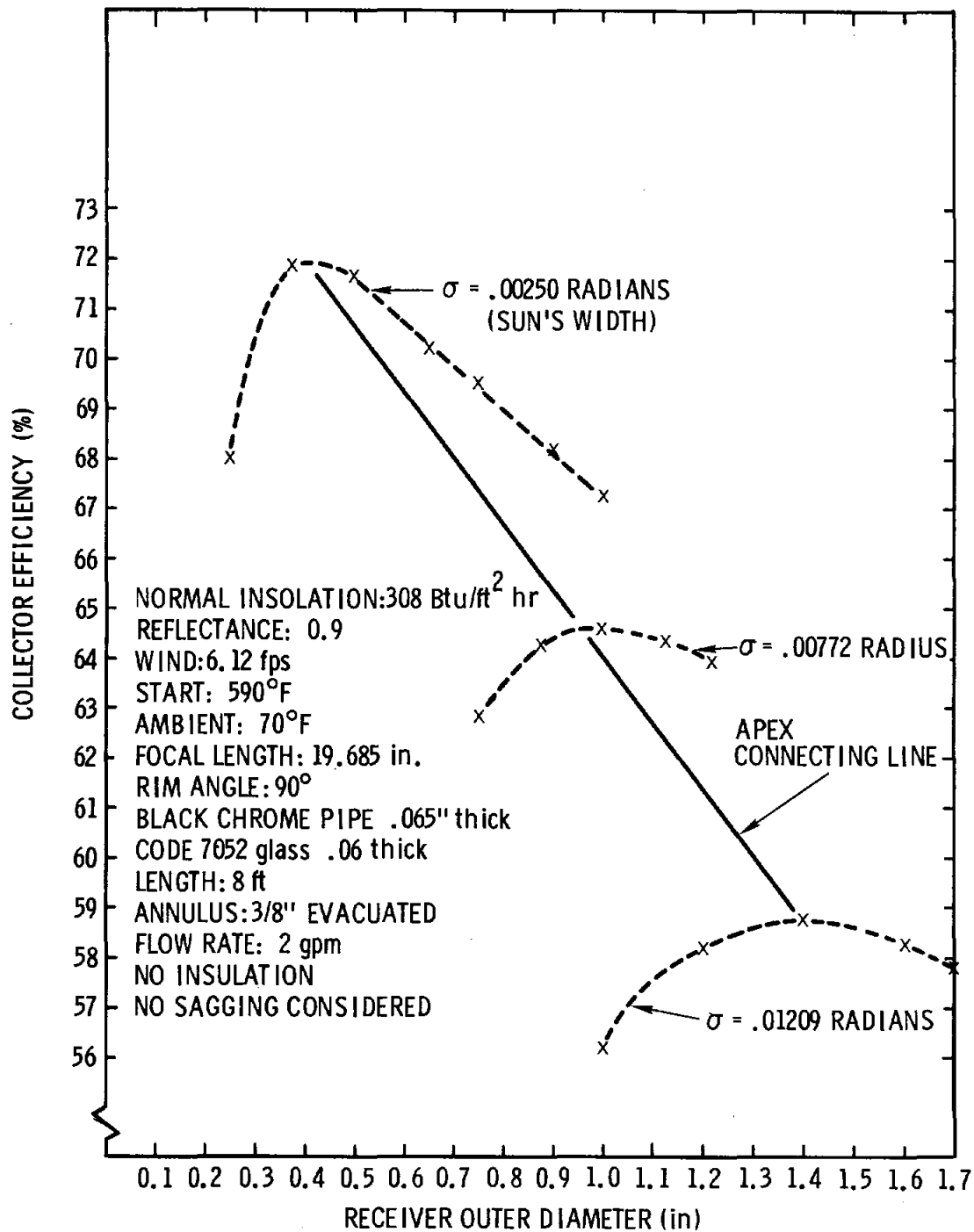
Figure 9.3. Energy Distribution vs Collector Efficiency

NORMAL INSOLATION = 308 Btu/ft$^2$ hr
REFLECTANCE = 0.9
WIND VELOCITY = 6.12 fps
START TEMP = 590°F
AMBIENT TEMP = 70°F
BLACK CHROME PIPE W/0.065 m WALL
CODE 7052 GLASS W/0.06 in. WALL
ANNULUS = 0.375 in. EVACUATED (0.5 Torr)
LENGTH = 8 ft
FLOW RATE = 2 gpm
NO SAGGING CONSIDERED
NO INSULATION
ENERGY DISTRIBUTION $\sigma$ = 0.00772 RADIANS
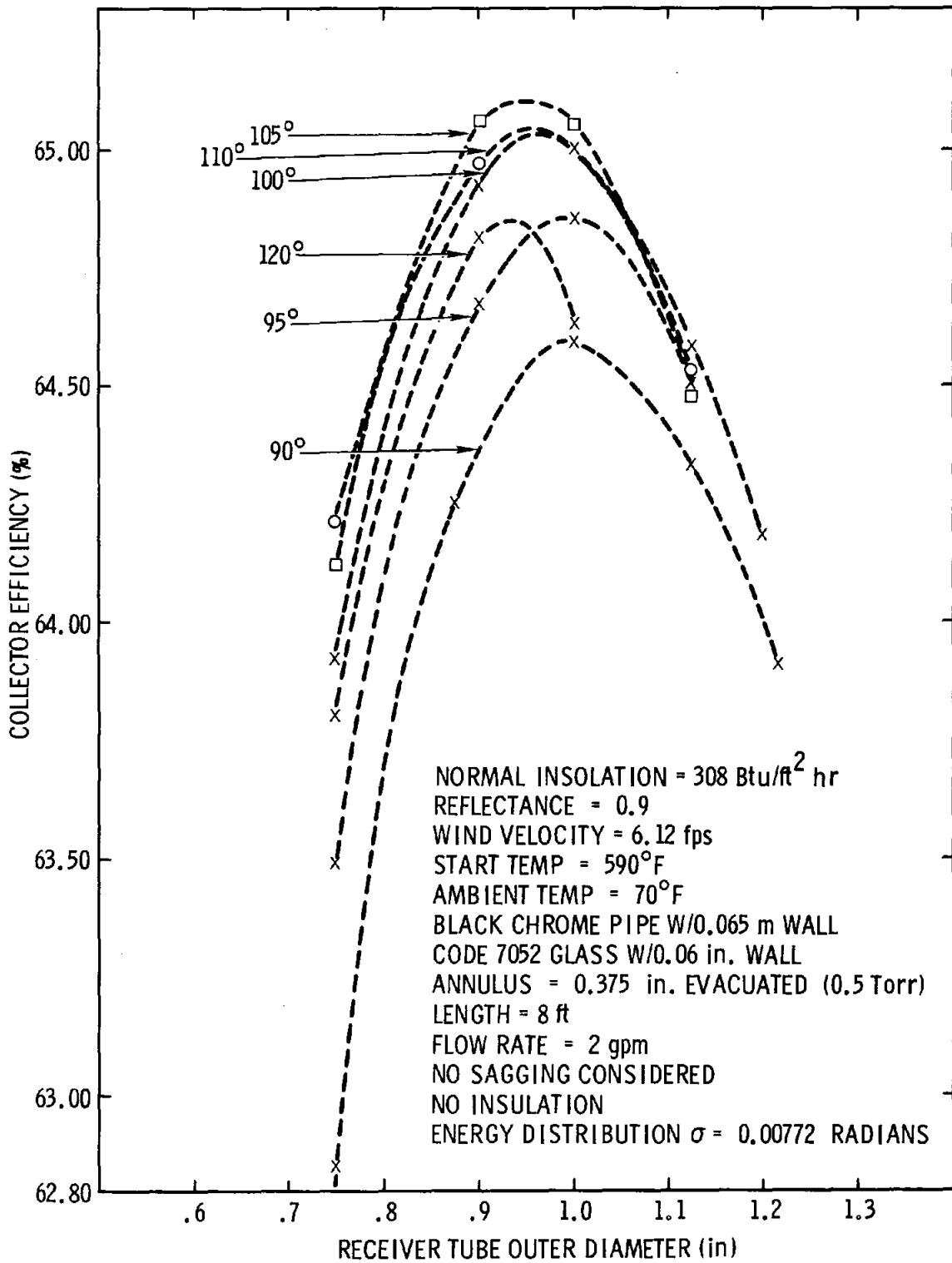
Figure 9-4. Rim Angle vs Collector Efficiency

79

## 9.4 Solar Energy Availability

Solar Radiation Availabilities to Various Collector Schemes: Frequent simultaneous readings of direct-normal and total-horizontal solar radiation are required to calculate the daily amounts of solar energy available to various types of collectors. The general lack of such radiation data is the reason that collector performance comparisons are usually based upon theoretical energy availability rather than actual data.

The 4-week solar data sample which contains simultaneous direct-normal and total-horizontal readings at 10-minute intervals for the four seasons at Albuquerque, Blue Hill, and Omaha offered an opportunity for comparison based upon actual data. Calculations of both the direct and total intensities incident upon various tracking and fixed, tilted surfaces were made assuming sky brightness to be twice that of ground brightness.

A few of the more interesting results are given here; complete details will be published in a separate report.

Figure 9-5 shows a comparison of the average daily total radiation available to a fixed surface tilted upward 40° toward the South and the average daily total radiation available to a surface which partially tracks the sun by rotating daily about an axis parallel to the earth's axis. The curves are based upon only the points shown. Each point is the average of the seven daily totals for the sample week. Because the 40° tilted surface has nearly the same slope as the axis of the tracking surface (Albuquerque's latitude is 35°), the difference in the curves is an approximation of the energy gain available to tracking as opposed to nontracking flat-plate collectors. Figure 9.5 also shows the average daily direct radiation available to a surface rotating about a polar axis.

Figure 9-6 shows daily total radiation available to a surface tilted 60° from horizontal and daily total radiation available to a south-facing, vertical surface. Notice that in the winter the south-facing vertical receives only 10 to 20% less than the surface tilted up 60°.

Finally, Figure 9-7 shows a comparison of the average daily diffuse-horizontal radiation available at the three locations. The accuracy of these curves is somewhat questionable because the diffuse-horizontal intensity is computed by subtracting the direct from the total radiation. Nonetheless, it is interesting to observe that none of the three locations seems to have significantly more diffuse radiation than the others.
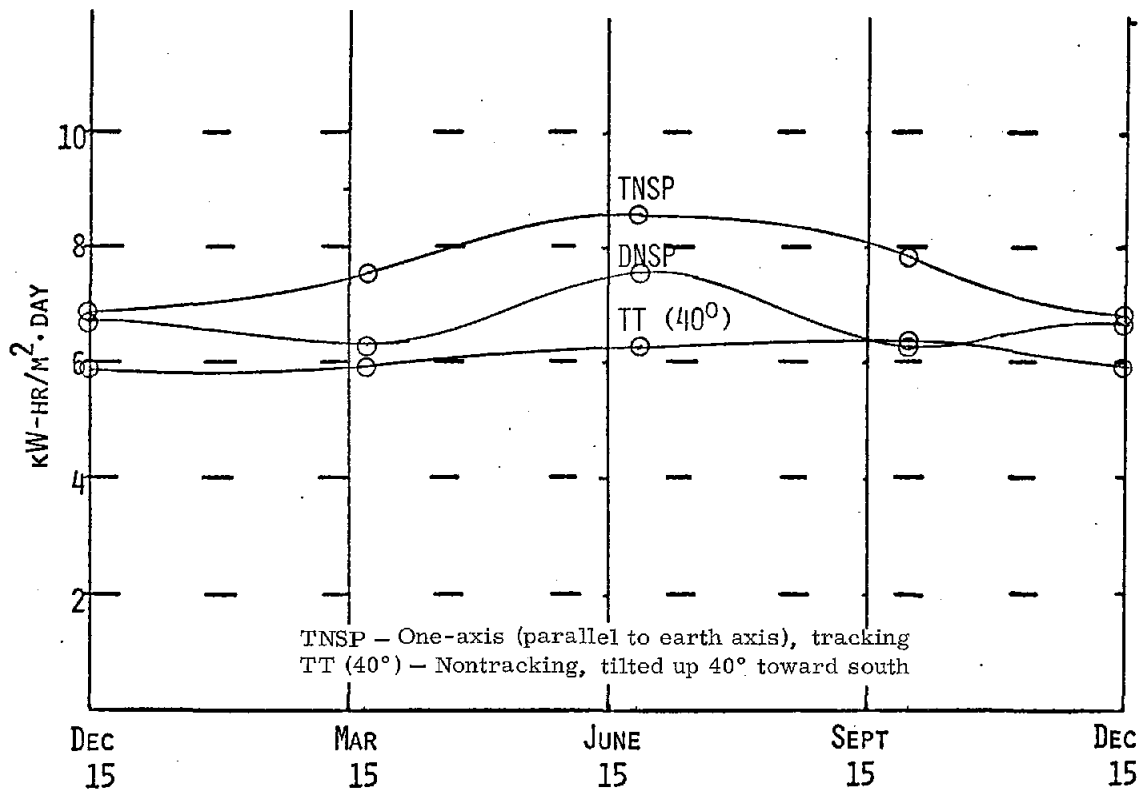
Figure 9-5. Average Daily Incident Radiation on a Surface in Albuquerque

TNSP — One-axis (parallel to earth axis), tracking
TT (40°) — Nontracking, tilted up 40° toward south
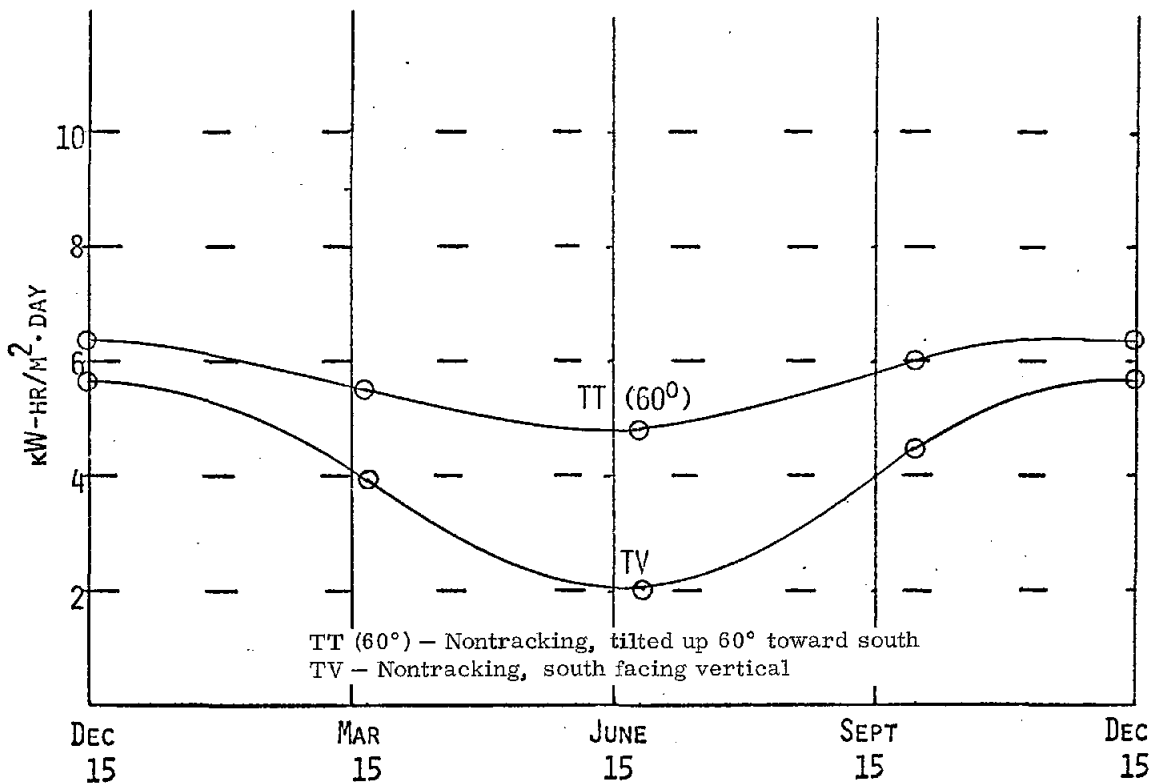


Figure 9-6. Average Daily Incident Radiation on a Surface in Albuquerque

TT (60°) — Nontracking, tilted up 60° toward south
TV — Nontracking, south facing vertical

TABLE 9-I

Rim-Angle/Efficiency Trade-Offs

| Rim Angle (Degrees) | Approx. Optimum Collector Efficiency (%) | Approx. Optimum Receiver OD (mm) | (in.) | Arc Length (m) | (in.) | Remarks |
|---|---|---|---|---|---|---|
| 70 (trimmed 90°) | 63.7 | 23 | 0.9 | 1.51 | 59.36 | 90° rim angle focal length 1.4-meter aperture |
| 80 (trimmed 90°) | 64.3 | 23 | 0.9 | 1.86 | 73.16 | 90° rim angle focal length 1.678-meter aperture |
| 70 | 62.4 | 29 | 1.13 | 2.16 | 84.77 | 2-meter aperture |
| 80 | 63.8 | 27 | 1.05 | 2.22 | 87.19 | 2-meter aperture |
| 90 | 64.6 | 25 | 1.00 | 2.30 | 90.38 | 2-meter aperature |
| 95 | 64.9 | 25 | 1.00 | 2.35 | 92.35 | 2-meter aperture |
| 100 | 65.0 | 24 | 0.95 | 2.40 | 94.64 | 2-meter aperature |
| 105 | 65.1 | 24 | 0.95 | 2.47 | 97.31 | 2-meter aperature |
| 110 | 65.0 | 24 | 0.95 | 2.55 | 100.46 | 2-meter aperature |
| 120 | 64.8 | 24 | 0.95 | 2.76 | 108.67 | 2-meter aperature |

Normal Insolation = 971 $W/m^2$ (308 $Btu/ft^2hr$)
Reflectance = 0.9
Wind Velocity = 1.86 m/sec (6.12 fps)
Start Temp - 310°C (590°F)
Ambient Temp = 21°C (70°F)
Black Chrome Pipe W/O 65 mm wall
Code 7052 Glass W/O 2 mm wall
Annulus = 10 mm (0.375 in) Evacuated (0.5 Torr)
Length = 2.44 m (8 ft)
Flow Rate = 7.57 lit/min (2 gpm)
No Sagging Considered
No Insulation
Energy Distribution $\sigma$ = 0.00772 Radians
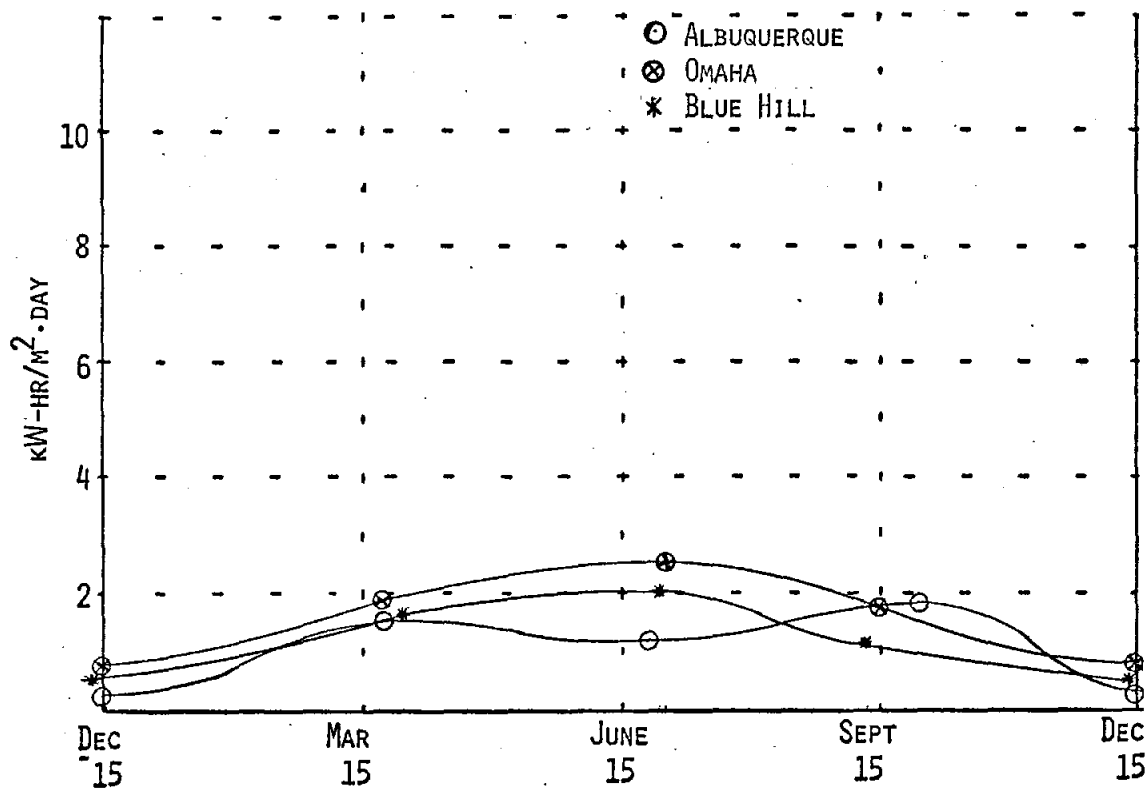
Figure 9-7. Diffuse, Horizontal Radiation

Task 10. Coating Evaluation

Electrodeposited black chrome on sulfamate nickel has been chosen as the solar selective coating for the Phase IV-A collector field. This coating was chosen because it has excellent solar selective properties ($\alpha_s \geq$ 095 and $\epsilon_{t,H}$ (300°C) $\leq$ 0.30), it is stable under ultraviolet radiation and also in air at 350°C, and it can be easily applied to the 3.66-m (12-ft) long by 41-mm (1-58/-in.) diameter collector pipes.

Electroplating conditions established for the collector pipes are a treatment time of 2-3/4 $\pm$ 1/4 minutes at a direct current density of 165 $\pm$ 10 A/ft$^2$. For a fresh bath or after the bath has remained idle for more than 48 hours, a run-in of 45 minutes on a clean, dummy cathode is required to stabilize the bath. Without the run-in procedure, high emittance coatings are obtained. The 3.66-m pipes have been coated in 2.44-m (8-ft) long tanks and were coated one end at a time with masking to prevent overlap. The pipes were lightly buffed prior to optical measurements.

Two additional optical measurement instruments were obtained in August to supplement our measuring equipment. The new instruments are (1) a portable infrared reflectometer for normal total emittance measurements (Gier-Dunkle Model DB-100), and (2) a portable solar reflectometer for normal solar absorptance measurements (Gier-Dunkle Model MS-251). The solar reflectometer

uses a Xenon lamp as a solar simulator and thus measures the absorptance relative to an approxi-
mation of the extraterrestrial solar spectrum. The infrared reflectometer measurement normally
corresponds to an 100°C black body spectrum (peak at 7.8 $\mu$m). However, by using a sapphire
filter, the measurement spectrum can be shifted to peak at 5.8 $\mu$m (with a width of 2.8 $\mu$m).
With this filter, the measured infrared emittance for black chrome on sulfamate nickel corresponds
very closely to total hemispherical emittance at 300°C (see Figure 10-1). In this way, both instru-
ments are used to measure the solar selective properties of selected areas of the collector pipes.

Twenty-five collector pipes with black-chrome coating have been received from Bendix,
Kansas City. Measured solar absorptance and normal total emittance values are listed in Table
10-I. As shown in the table, the pipes were plated in three groups. The average solar absorp-
tance, $\overline{\alpha}_s$, for the first group is 0.96, while the average emittance, $\overline{\epsilon}$, is 0.26. For group II,
$\overline{\alpha}_s$ = 0.95 and $\overline{\epsilon}$ = 0.22; for group III, $\overline{\alpha}_s$ = 0.92 and $\overline{\epsilon}$ = 0.16. It should be noted that within
each group the coatings on each pipe do not vary by more than $\pm$0.01 absorptance units. However,
because of the low solar-absorptance values obtained for the group III pipes, this group will be
replated in order to obtain $\alpha_s$ values of 0.95 or higher. For the replating, both portable Gier-
Dunkle instruments will be shipped to Bendix for in-line process monitoring to ensure that the
proper solar selective properties are obtained.

The evaluation of alterative coatings is continuing. A proprietary vacuum-deposited, mutli-
layer solar coating from Optical Coating Laboratory, Inc., has been tested. The total hemispher-
ical emittance ranged from 0.13 $\pm$0.02 at 120°C to 0.16 $\pm$0.02 at 305°C, while the solar absorp-
tance averaged 0.95. High-temperature-stability tests in air are planned.

In addition, preliminary results have been obtained for an alternate black-chrome coating
produced by Udylite Corp., Warren, Michigan. Initial samples have good solar absorptance (0.98)
and low emittance values ($\epsilon_{t,H}$(300°) ~ 0.30). However, some coatings have changed significantly
after heating to 300°C in vacuum. Tests of this coating at 300°C in an air environment are planned.
At the present time, we are assisting Udylite in setting up their own coating evaluation capability.

TABLE 10-I

Solar Absorptance - Normal Total Emittance
Measurements of Phase IV-A Receiver Tubes

| | Date | Pipe | $\alpha_s(m=1)$ Beckman | $\alpha_s(m=0)$ Gier-Dunkle | $\epsilon$ Gier-Dunkle Sapphire Filter |
|---|---|---|---|---|---|
| Group I | 6-02-75 | 12-10 | 0.97 | --- | --- |
| | 6-03-75 | 12-11 | 0.96 | --- | --- |
| | 6-03-75 | 12-12 | 0.97 | 0.94 | 0.28 |
| | 6-04-75 | 12-9 | 0.96 | --- | --- |
| | 6-05-75 | 12-8 | 0.93 | --- | --- |
| | 6-06-75 | 12-7 | 0.95 | 0.94 | 0.23 |
| | 6-09-75 | 12-6 | 0.96 | --- | --- |
| | 6-09-75 | 12-4 | 0.94 | --- | --- |
| | 6-10-75 | 12-3 | 0.96 | --- | --- |
| | 6-11-75 | 12-5 | 0.96 | --- | --- |
| Group II | 7-30-75 | 12-27 | 0.96 | --- | 0.23 |
| | 7-31-75 | 12-26 | 0.95 | 0.94 | 0.24 |
| | 7-31-75 | 12-28 | 0.96 | --- | 0.24 |
| | 8-01-75 | 12-19 | 0.95 | --- | 0.24 |
| | 8-04-75 | 12-23 | 0.94 | 0.93 | 0.20 |
| | 8-05-75 | 12-20 | 0.95 | --- | 0.24 |
| | 8-05-74 | 12-21 | 0.94 | --- | 0.20 |
| | 8-06-75 | 12-24 | 0.94 | 0.93 | 0.20 |
| | 8-06-75 | 12-22 | 0.94 | --- | 0.20 |
| Group III | 9-19-75 | 12-13 | 0.92 | 0.92 | 0.16 |
| | 9-19-75 | 12-15 | 0.91 | 0.90 | 0.16 |
| | 9-22-75 | 12.18 | 0.92 | 0.91 | 0.15 |
| | 9-22-75 | 12-14 | 0.92 | 0.91 | 0.16 |
| | 9-23-75 | 12-17 | 0.92 | 0.91 | 0.16 |
| | 9-23-75 | 12-16 | 0.92 | 0.91 | 0.16 |
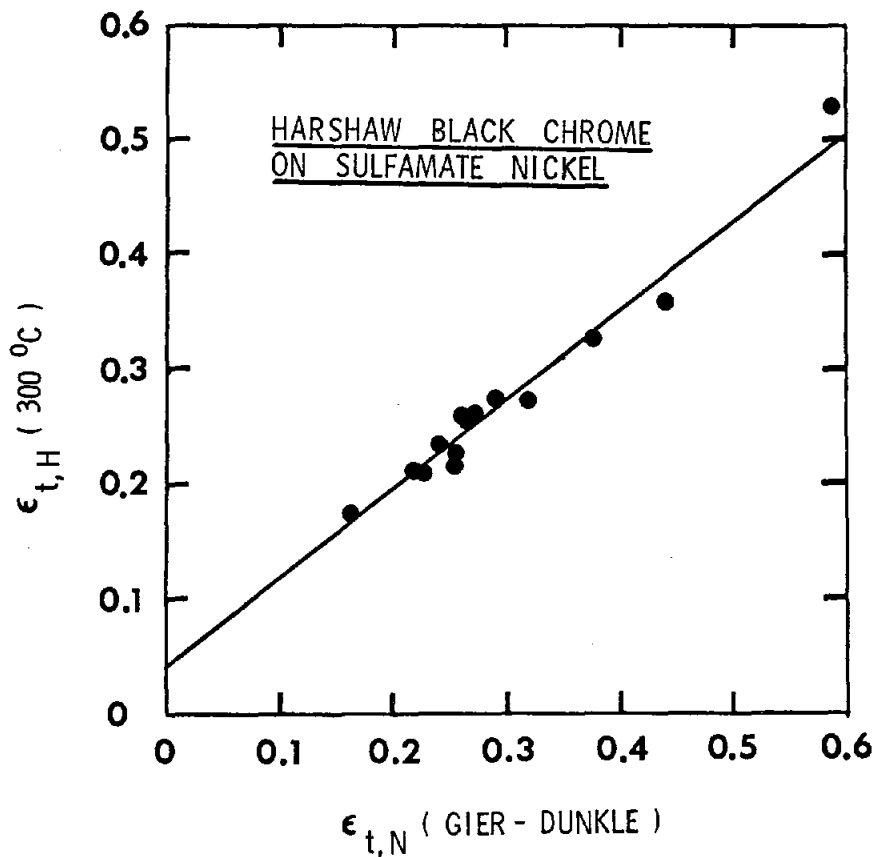
Figure 10-1. Measured Infrared Emittance of Harshaw
Black Chrome on Sulfamate Nickel

## Task 11. Technology Utilization

Sandia Laboratories Advanced Energy Project Department and Aerospace Corporation hosted a Solar Total Energy Technology Symposium on July 10 and 11, 1975, at Sandia Laboratories. The symposium was attended by about 200 representatives of industry, technical associations, universities, research institutes, and governmental agencies from across the nation. The two days of sessions included keynote addresses by ERDA officials, 18 papers covering a broad spectrum of solar systems, and tours of local solar facilities.

A log book for recording briefings and associated tours of the solar total energy site was begun on July 1, 1975. During the first 3-month period, more than 60 entries include the names of 125 persons plus the attendees at three symposia. The visitors included individual citizens, several TV news organizations, and a wide variety of government, industrial, and university faculty re- , presentatives. All of the SCORE (Student Competition on Relevant Engineering) participants toured the site, which was adjacent to the SCORE demonstration area. Foreign visitors came from industry, but primarily from universities and governmental agencies of New Zealand, Australia,

India, Brazil, Great Britain, Egypt, Sweden, Germany, Switzerland, and Canada, as well as NATO and the UN.

The publications, conference papers, presentations, and patent disclosures of this reporting period are tabulated in Section II. In summary, there were 10 published Sandia documents, 14 papers presented at technical engineering conferences, 25 presentations and one patent disclosure by the personnel involved with the Solar Total Energy Project.

# SECTION IV. APPENDICES


A.   A Method to Estimate Costs of Rankine Cycle Hardware
for Solar Thermal-Electrical Energy Conversion Systems


At present, no significant solar electric systems exist. Thus, no solar electric experience is available to use as a basis for estimating costs. A reasonable approach is to extract data on existing fossil fueled systems and develop relative cost information for each significant element of those systems. This information is included in Appendix B. However, solar electric systems may differ significantly from conventional systems in several areas, particularly efficiency, which must be considered before conventional cost information can be used in cost estimating.

In Appendix B there are 13 factors which are considered; these will be discussed individually in more detail. The reader is encouraged to read and understand the original work in Appendix B before continuing.

1.  Land - A solar system will not require a significant amount of land, neither more nor less than a fossil fueled system. The collectors will require extra land, but the land for them is not included here. Therefore, it is judged that there is no difference in the land requirement between solar and fossil systems. The factor remains 0.11.

2.  Powerhouse - The powerhouse will be essentially the same for both solar and conventional systems. Therefore, the factor remains 0.88.

3.  Structures - Structural costs for solar and conventional systems will probably not be very different. Therefore, the factor remains 0.29.

4.  Items Associated with Fossil Fuel - (Handling Facilities, Burners, Ash and Exhaust System, etc.) There are no analogous parts for a solar system unless a fossil fuel backup is used, in which case all or part of this factor must be included. The factor remains at 1.57.

5.  High Temperature Heat Exchangers - Because solar systems have lower cycle efficiencies than fossil systems, more heat must be transferred and consequently larger heat exchangers are required. The adjustment can be made as follows:

$$\text{Solar Factor} = \text{Fossil Factor} \times \frac{E_{ff}}{E_s}$$

$$= 1.2 \times \frac{E_{ff}}{E_s}$$

where $E_{ff}$ and $E_s$ are the Rankine cycle conversion efficiencies for the fossil fuel system and the solar system, respectively.

6. <u>Feed Water Equipment</u> - Less efficient solar systems, in general, require more volumetric flow which is proportional to the cycle efficiency ratio. Therefore, the

$$\text{Solar Factor} = \text{Fossil Factor} \times \frac{E_{ff}}{E_s}$$

$$= 0.17 \times \frac{E_{ff}}{E_s}$$

7. <u>Water Supply and Treatment</u> - A less efficient system will require treatment of more water, but the cost of treatment equipment will probably not change. Therefore, the factor remains 0.06.

8. <u>Plant Controls and Instrumentation</u> - Only minor differences will exist between solar and fossil fuel systems. Therefore, the factor remains 0.17.

9. <u>High Temperature and/or Pressure Piping</u> - As in Item 6 above, less efficient solar systems will require higher flow rates and bigger pipes to transfer the energy. Therefore, the

$$\text{Solar Factor} = \text{Fossil Factor} \times \frac{E_{ff}}{E_s}$$

$$= 0.24 \times \frac{E_{ff}}{E_s}$$

10. <u>Turbo-Generator</u> - The generator will be the same for both systems. The turbine for the solar system will probably require fewer stages than the turbine for a fossil plant, but a lower efficiency solar system will require higher flow rates and a larger turbine, and there will probably not be a significant difference in cost. Therefore, the factor remains 1.00.

11. <u>Condenser and Auxiliaries</u> - This needs to be adjusted according to the amount of reject energy.

$$\text{Reject Heat (R)} = \text{Heat Added (Q)} \times (1 - E)$$

$$\text{Power (P)} = Q \times E$$

$$Q = P/E$$

$$\frac{R_{solar}}{R_{fossil\ fuel}} = \frac{Q_s\ (1 - E_s)}{Q_{ff}\ (1 - E_{ff})} = \frac{\dfrac{P}{E_s}}{\dfrac{P}{E_{ff}}} \times \frac{1 - E_s}{1 - E_{ff}}$$

$$= \frac{E_{ff}}{E_s} \times \frac{(1 - E_s)}{(1 - E_{ff})}$$

Therefore, the solar factor becomes

$$.08 \times \frac{E_{ff}}{E_s} \times \frac{(1 - E_s)}{(1 - E_{ff})}$$

12. <u>Cooling Water Circulating System</u> - Same as Item 11.

$$.19 \times \frac{E_{ff}}{E_s} \times \frac{(1 - E_s)}{(1 - E_{ff})}$$

13. <u>Miscellaneous</u> - No change.

Let's now consider an example in which we assume that $E_s = 25\%$ and that $E_{ff} = 38\%$ which is the average for the plants that Table B-I in Appendix B is based on. For this case, Table B-I would be replaced by the following:

| Item | Factor |
|---|---|
| 1. Land | .11 |
| 2. Powerhouse | .88 |
| 3. Structural | .29 |
| 4. Fossil Fuel | 1.57 |
| 5. High Temperature Heat Exchangers | $1.2 \times \dfrac{.38}{.25} = 1.82$ |
| 6. Feed Water Equipment | $.17 \times \dfrac{.38}{.25} = .26$ |
| 7. Water Supply and Treatment | .06 |
| 8. Plant Controls | .17 |

| Item | Factor |
|------|--------|
| 9. High Temperature/Pressure Piping | $.24 \times \dfrac{.38}{.25} = .36$ |
| 10. Turbo-Generator | 1.00 |
| 11. Condenser and Auxiliaries | $.08 \times \dfrac{.38}{.25} \times \dfrac{1 - .25}{1 - .38} = .15$ |
| 12. Cooling Water Circulating System | $.19 \times 1.75 \times \dfrac{1 - .25}{1 - .38} = .35$ |
| 13. Miscellaneous | .64 |
| Total | 7.66 |
| Total (Less Item 4) | 6.09 |
| Total (Less Items 1, 2 and 4) | 5.10 |

Thus, if we compare the total (less Items 1, 2, and 4) above with the corresponding value from Table B-I we find that the solar powered Rankine cycle hardware is (5.10 - 4.04)/4.04 or 26% more expensive and we would multiply Equations 1 and 2 in the appendix by the factor $\dfrac{5.10}{4.04}$ or 1.26 for this example.

B. Initial Cost vs Peak Capacity Estimate for a Solar Total
Energy Rankine Cycle Power Conversion System

The purpose of this memo is to provide a preliminary cost estimate for the Rankine cycle part of the solar total energy conversion system. The cost estimated in this memo is the initial "as-installed" cost. Costs associated with power distribution and transmission, financing of the system, normal operation, maintenance, recurring tax and insurance costs, etc. are not included.

The estimated initial cost of a solar input Rankine cycle energy conversion system less land, powerhouse and fossil fuel backup system is given by the following equations:

$$\$ = 18.0 + .278P \qquad \text{(for values of P between 1 and 1,000)} \qquad (1)$$

$$\$ = .992P^{.825} \qquad \text{(for values of P between 1,000 and 1,000,000)} \qquad (2)$$

where
   P = peak electrical generating capacity in kilowatts
   $ = initial cost in 1973 kilodollars

The cost of the land and powerhouse are not included in the basic equations, since in the Solar total energy concept the power conversion system may be integrated with other subsystems in a common structure or site. The cost of a fossil fuel backup system is likewise not included, since the backup system may not be part of the solar plant. The estimated cost of these items or of a system composed of any combination of items can be found by multiplying the right hand side of the equations by the appropriate factors. These factors will consist of a numerator and a denominator found by combining relative cost fractions from Table B-I. In all cases, the denominator of the factor will be 4.04 since this is the total relative cost for the baseline system described by Equations 1 and 2. The numerator will be the sum of the relative costs for all items which make up the system for which a cost estimate is desired. For example, if it is desired to include the cost of the land and powerhouse, Equations 1 and 2 should be multiplied by the factor (5.03/4.04). If only the cost of the turbogenerator set is required, the equations should be multiplied by (1.00/4.04), etc.

Equations 1 and 2 also assume that the total system design and components exist i.e., that no engineering or development is required. The equations also assume that costs associated with the time required for construction or installation on-site are negligible. These assumptions can be valid for smaller "packaged" systems but would be unrealistic for systems requiring substantial engineering or on-site construction time. For large systems where system engineering and on-site

engineering or on-site construction time. For large systems where system engineering and on-site construction time cannot be neglected, these items can be estimated as follows (from reference cited in Table B-II):

Engineering Cost - .09 x Direct Construction Cost (Given by Equation 2)

Indirect and Administrative Cost - .084 x Direct Construction Cost x Construction Time in Years

Interest Cost - Current or Projected Rate x Direct Construction Cost x Construction Time in Years

Equation 1 was derived in the following manner. First, the costs of various Rankine cycle components, relative to the turbogenerator cost for a typical large coal-fired generating plant, were compiled and are given in Table B-I. Relative cost data for two other similar but smaller plants were also analyzed and found to be in general agreement with the data given in Table B-I. The rationale implicit in the use of Table B-I is that the relative costs of the various Rankine cycle components are independent of system size (peak capacity). The second step in the derivation of Equation 1 was the compilation of costs for turbogenerator sets of from 2 kW to 1000 kW peak capacities. These data are given in Table B-II. The data are based on actual sales data and quotes received in 1973 from various suppliers contacted by Sandia. The cost data were then fit using a least mean square error routine and the resulting equation multiplied by the constant 4.04 from Table B-I to get an estimate for total system cost (less land, powerhouse and fossil fuel backup costs).

Equation 2 was derived by curve fitting data for installed power plant cost from Table 5.1 of "The Electric Power Business" by Edwin Vennard, McGraw-Hill, 1970. Mr. Vennard is president of Commonwealth Management Consultants who are Edison Power Company's prime consultants. The resulting equation was adjusted from 1968 dollars to 1973 dollars using "The Handy-Whitman Index of Public Utility Construction Costs," Whitman, Requardt and Associates, 1974 and adjusted for a non-fossil fuel system less powerhouse and land using the appropriate factors from Table B-I.

Unfortunately, there are very few readily available checkpoints for Equations 1 and 2, but reasonable agreement between estimated and actual supplier's quotes or projections has been obtained where comparison has been made. For example, substitution of 2 kW for P in Equation 1 yields a cost estimate of 18.5 k$ as compared to the 14.3 k$ (plus shipping, sales taxes and installation) quoted by Ormat Turbines, Ltd. of Israel for an oil-fired 2 kW Rankine cycle system. Substituting 100 kW into equation 1 yields 45.8 k$ which compares favorably with the 35 k$ - 45 k$ (plus shipping, sales taxes, cooling tower and installation) projected by Sundstrand Aviation for their 100 kW gas-fired Rankine cycle system. Both the Ormat and Sundstrand systems include oil or gas firing equipment but no fuel storage or handling items.

To check Equation 2, the actual cost of six coal-fired power plants of 235 MW to 1,012 MW capacity was derived from "The Eighteenth Steam Station Cost Survey," Electrical World Magazine, November 1, 1973 issue. Each plant was built in 1970 or later and the total cost adjusted to 1973 dollars using the Handy-Whitman Index as described previously. The total cost data were then further adjusted to remove the cost of land, powerhouse, and fossil fuel equipment by using a factor of (4.04/6.60) from Table B-I. The resulting adjusted costs were then compared with the costs predicted by Equation 2. The error ranged from -4.6% to -34.7% and averaged -14.6%. Next, it was assumed that the plant construction time was two years and that the prevailing interest rate was 8%. The predictions yielded by Equation 2 were then revised to include engineering, indirect, administrative and interest costs as discussed in the summary. The error in the revised costs now ranged from +20.2% to -17.9% and averaged +7.5%. Thus, it appears that Equation 2 could be expected to predict actual costs within ±30% and possibly better if actual construction time, etc. are known or can be accurately estimated.

It should be recognized that there is a substantial spread in power plant costs (particularly large power plant costs) even for plants of approximately the same capacity due to widely varying local construction costs, geographic and climatic conditions, cycle operating conditions (temperatures and pressures), type of heat rejection used (dry towers, rivers, etc.) and other factors which do not lend themselves to simplified analysis. However, Equations 1 and 2 combined with Table B-I appear to give reasonable estimates of total Rankine system or component costs for initial systems studies.

TABLE B-I

Cost of Bull Run Central Power Plant Components Relative to Turbogenerator Cost.
Derived from "The U.S. Energy Problem," Volume II Appendices - Part A,
Intertechnology Corporation Document PB-207518, November 1971.

| Item | Fraction of Turbogenerator Cost |
|---|---|
| 1. Land | .11 |
| 2. Powerhouse | .88 |
| 3. Structures | .29 |
| 4. Items Associated with Fossil Fuel (handling facilities, fuel burning equipment, ash handling equipment, exhaust system, etc.) | 1.57 |
| 5. High Temperature Heat Exchangers (boiler, superheater, rehater, etc.) | 1.20 |
| 6. Feed Water Equipment (preheater, pumps, motors, tanks, etc.) | .17 |
| 7. Water Supply and Treating System | .06 |
| 8. Plant Controls and Instrumentation | .17 |
| 9. High Temperature and/or High Pressure Piping | .24 |

TABLE B-I
(Continued)    •

| Item | Fraction of Turbogenerator Cost |
|---|---|
| 10.  Turbogenerator | 1.00 |
| 11.  Condenser and Auxiliaries | .08 |
| 12.  Cooling Water Circulating System (pumps, . motors, piping, etc.) | .19 |
| 13.  Miscellaneous Equipment | .64 |
| Total | 6.60 |
| Total Less Item 4 | 5.03 |
| Total Less Items 1, 2 and 4 | 4.04 |


TABLE B-II

Costs of Ten Different Sized Systems

| Capacity (kW) | Cost (k$) | Source |
|---|---|---|
| 2 | 2.0 | 5 |
|   | 4.5 | 2 |
| 3 | 3.7 | 1 |
| 5 | 3.0 | 1 |
| 10 | 4.1 | 1 |
|   | 3.8 | 5 |
|   | 2.5 | 5 |
| 20 | 6.0 | 1 |
| 100 | 18.0 | 4 |
|   | 11.3 | 1 |
|   | 10.0 | 5 |
|   | 9.6 | 6 |
|   | 9.0 | 2 |
| 250 | 50.0 | 3 |
| 400 | 17.5 | 1 |
| 500 | 30.0 | 4 |
| 1000 | 100.00 | 2 |
|   | 70.00 | 3 |
|   | 45.00 | 4 |

Source Legend:

1 — Coppus Engineering Corporation

2 — The Terry Steam Turbine Co.

3 — The Trane Company, Murray Division

4 — Turbodyne Corporation, Worthington Turbine Division

5 — The O'Brien Machinery Co.

6 — Carling Turbine Blower Co.

## C. Solar Transmittance of Various Materials

Attached are solar transmittance and reflectance values for various glasses, plastics and greenhouse materials. Because two measurement techniques were used, the data have been divided into two tables. The hemispherical solar transmittance, $\tau_{S,H}$, was determined using near-normal incident radiation with hemispherical detection of the transmitted beam. Because all transmitted radiation is measured, these data are useful for flat plate collector applications. The normal solar transmittance, $\tau_{S,N}$, was determined using normal incident radiation with approximately normal detection of the transmitted beam. In this case, only the radiation transmitted around the straight-through beam is measured; all scattered radiation is lost. Therefore, these data are useful for focusing collector systems, although each design may place different requirements on the acceptance angle (or cone) of the transmitted beam. For the measurements reported here, the acceptance angle is approximately ± 1°. More detailed transmittance data as a function of the acceptance angle can be obtained for selected materials if the need arises.

The data reported here were obtained by solar averaging spectral transmittance values over the wavelength range 0.25 $\mu$m to 2.5 $\mu$m. Technically, the transmittance measured here is termed external transmittance (as opposed to internal transmittance) since it is determined by both the absorbing and reflecting properties of the material. As previously mentioned, the data reported here are for normal incident radiation. However, I have performed hemispherical transmittance measurements as a function of incident angle up to ~75° for both S- and P- polarizations. Because of the large quantity of data involved, this information will be published in a separate report.

The solar reflectance values listed in the tables represent average solar hemispherical reflectance, $\rho_{S,H}$, for near-normal incident radiation. For non-absorbing materials, this reflectance is approximately equal to twice the single surface reflectance, R. (Actually, $\rho_{S,H}$ is equal to 2R/(1-R). From energy conservation, the amount of absorbed solar radiation, $\alpha_s$, is then given by

$$\alpha_s = 1.0 - \tau_{S,H} - \rho_{S,H} \; .$$

For some materials, such as Mylar A, the low solar transmittance is due in part to the high solar reflectance, not to large absorptance losses.

The cutoff wavelength is defined as the wavelength in the ultraviolet where the transmittance is equal to one-half the solar transmittance. This information will given one an idea as to whether a material is UV transmitting or absorbing.

Within each table, materials are generally listed in order of decreasing solar transmittance. However, for comparison purposes, similar materials have been grouped together (e.g., Teflons, Acrylics, etc.).

The Swedlow coated acrylic has a new Dow Corning abrasion-resistant coating applied to both surfaces. Because of the lower reflectance values, this coating acts like an anti-reflection coating and thus will increase the solar transmittance of acrylics. (In this case it did not, but only because it was applied to a relatively thick (0.273") piece of acrylic.) The Lucite 147 is an injection or extrusion molded material that has potential application as a Fresnel lens material. Teflon A is heat-sealable to itself or to metals and high-temperature fabrics. Teflon C is cementable on one side. Kalwall Sunlite and Filon Tedlar coated A748 are both commercial greenhouse glazings.

The measurement error is ± 0.01 transmittance units, while the error in the reflectance values is ± 0.005 reflectance units. Some samples, notably the greenhouse materials, show variations in transmittance from area to area of 1% for a 1 cm x 1 beam.

TABLE C-I

Normal Solar Transmittance

| Material | Thickness (in.) | Supplier | Cutoff Wavelength (μm) | Hemis. Reflectance | Normal Solar Transmittance | | | | |
|---|---|---|---|---|---|---|---|---|---|
| | | | | | m* = 0 | m = 1 | m = 2 | m = 3 | m = 4 |
| Quartz | 0.125 | Sandia Glass Shop | 0.25< | 0.064 | 0.94 | 0.94 | 0.94 | 0.95 | 0.95 |
| Teflon 100 C | 0.001 | Dupont | 0.25< | 0.031 | 0.93 | 0.93 | 0.93 | 0.93 | 0.93 |
| Teflon 100 A | 0.001 | Dupont | 0.25< | 0.035 | 0.91 | 0.91 | 0.91 | 0.92 | 0.92 |
| Pyrex (Corning 7740) | 0.134 | Sandia Glass Shop | 0.33 | 0.067 | 0.91 | 0.91 | 0.91 | 0.91 | 0.91 |
| Kovar Sealing Glass (Corning 7052) | 0.093 | Sandia Glass Shop | 0.34 | 0.072 | 0.88 | 0.90 | 0.90 | 0.91 | 0.91 |
| ASG Lustra Crystal | | Petterson | 0.33 | 0.080 | 0.89 | 0.90 | 0.90 | 0.90 | 0.90 |
| Acrylite | 0.0625 0.125 | Petterson | 0.35 | NM† | 0.86 0.83 | 0.89 0.87 | 0.89 0.88 | 0.89 0.88 | 0.89 0.87 |
| Plexiglas "G" | 0.0625 0.219 | Petterson | 0.35 | NM | 0.86 0.82 | 0.88 0.86 | 0.88 0.87 | 0.88 0.87 | 0.88 0.86 |
| Tedlar, Polished | 0.004 | Dupont | 0.31 | 0.080 | 0.86 | 0.88 | 0.88 | 0.89 | 0.89 |
| Tedlar, Unpolished | 0.004 | Dupont | 0.29 | 0.065 | 0.64 | 0.64 | 0.65 | 0.66 | 0.66 |
| Swedlow Continuous Cast Acrylic | 0.076 0.103 | Swedlow | 0.33 | 0.070 | 0.82 | 0.86 | 0.87 | 0.87 | 0.87 |
| Swedlow Coated Acrylic, Cell Cast | 0.273 | Swedlow | 0.39 | 0.058 | 0.79 | 0.85 | 0.86 | 0.87 | 0.88 |
| Acrylic Safety Glazing ANSIZ 97.1-1966.100 U | 0.224 | Sandia Stores | 0.35 | 0.068 | 0.80 | 0.84 | 0.85 | 0.86 | 0.86 |
| Israeli Collector Glazing | 0.092 | Peterson | 0.34 | NM | 0.84 | 0.86 | 0.86 | 0.86 | 0.86 |
| Glass for Mirror | 0.125 | Champion | 0.33 | 0.070 | 0.84 | 0.85 | 0.86 | 0.86 | 0.85 |

*m = Effective air mass for the solar spectral irradiance.

†NM = Not measured.
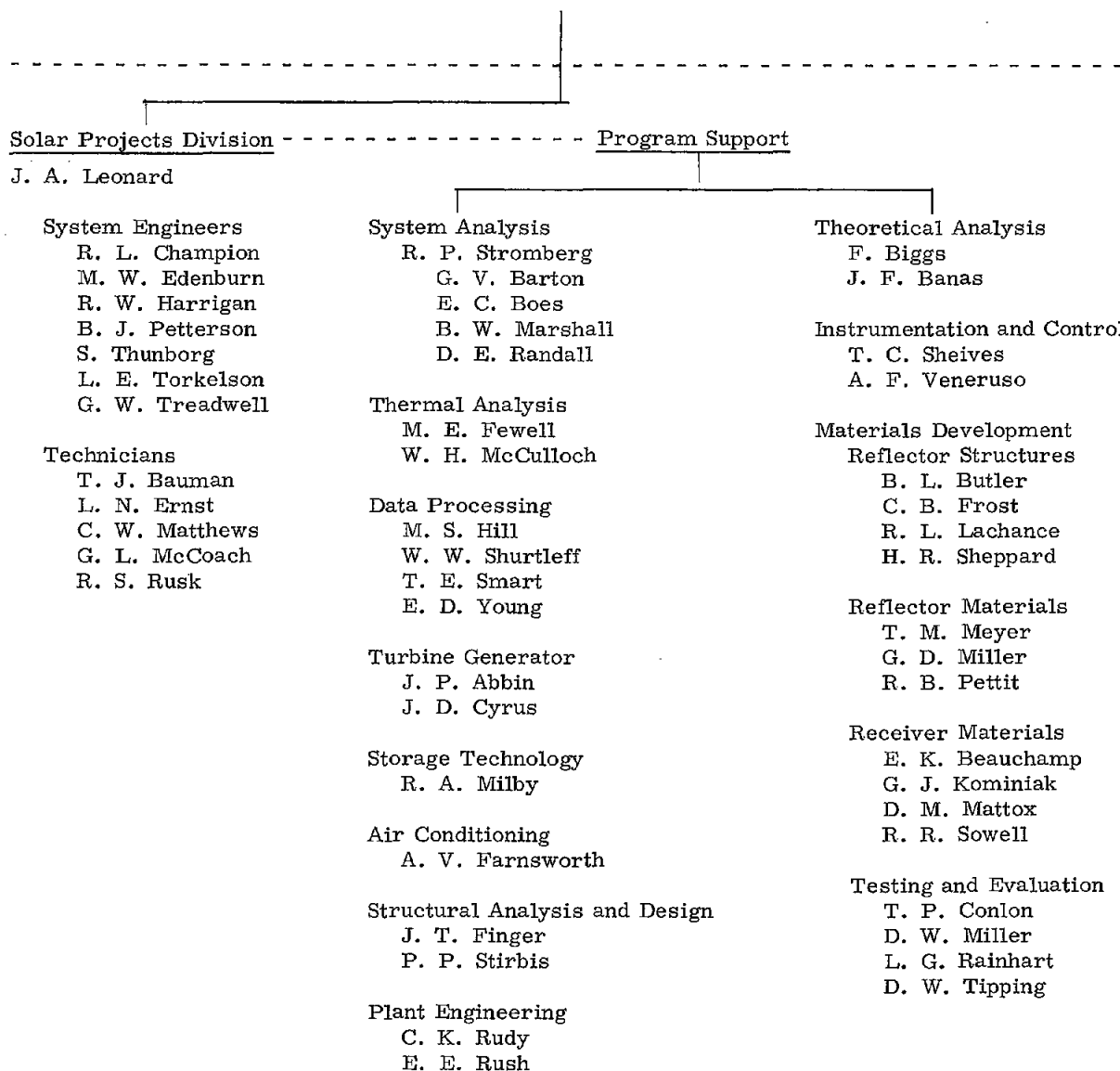
## TABLE C-II

### Hemispherical Solar Transmittance

| Material | Thickness (in.) | Supplier | Cutoff Wavelength (μm) | Hemis. Reflectance | Hemis. Solar Transmittance m* = 0 | m = 1 | m = 2 | m = 3 | m = 4 |
|---|---|---|---|---|---|---|---|---|---|
| Teflon 100 C | 0.001 | Dupont | 0.25< | 0.031 | 0.96 | 0.96 | 0.96 | 0.96 | 0.96 |
| Teflon 200 C / 300 C | 0.002 / 0.003 | Dupont | 0.25< | NM[†] | 0.95 | 0.95 | 0.95 | 0.95 | 0.95 |
| Teflon 500 C | 0.005 | Dupont | 0.25< | NM[†] | 0.94 | 0.94 | 0.94 | 0.94 | 0.94 |
| Teflon 100 A | 0.001 | Dupont | 0.25< | 0.035 | 0.95 | 0.95 | 0.95 | 0.95 | 0.95 |
| Teflon 1000 A | 0.010 | Dupont | 0.25< | NM | 0.94 | 0.94 | 0.94 | 0.94 | 0.94 |
| Aclar ‡22A | 0.002 | Rainhart; Allied Chem. | 0.25< | 0.060 | 0.94 | 0.94 | 0.94 | 0.94 | 0.94 |
| Corning Ultramicrosheet | 0.0045 | Butler; Corning | 0.30 | 0.071 | 0.91 | 0.92 | 0.92 | 0.92 | 0.92 |
| Tedlar, Polished | 0.004 | Dupont | 0.30 | 0.080 | 0.91 | 0.91 | 0.92 | 0.92 | 0.92 |
| Tedlar, Unpolished | 0.004 | Dupont | 0.30 | 0.065 | 0.89 | 0.90 | 0.91 | 0.91 | 0.91 |
| Rhom-Haas Korad C | 0.003 | Brumleve | 0.38 | 0.070 | 0.86 | 0.89 | 0.90 | 0.90 | 0.91 |
| Rhom-Haas Korad A, Std. Clear | 0.003 | Brumleve | 0.38 | 0.082 | 0.85 | 0.87 | 0.89 | 0.89 | 0.90 |
| Rhom-Haas Korad A, Std. Clear | 0.006 | Brumleve | 0.38 | 0.088 | 0.84 | 0.86 | 0.88 | 0.89 | 0.89 |
| Rhom-Haas Exp 55D-62A | 0.002 | Brumleve | 0.38 | 0.075 | 0.87 | 0.90 | 0.91 | 0.91 | 0.92 |
| Rhom-Haas Exp 55D-62A | 0.010 | Brumleve | 0.30 | 0.070 | 0.90 | 0.91 | 0.91 | 0.91 | 0.91 |
| Filon A748 Tedlar Coated | 0.028 | Filon Corp. | 0.38 | 0.082 | 0.82 | 0.84 | 0.85 | 0.86 | 0.86 |
| Kalwall Sunlite Regular | 0.025 | Kalwall Corp. | 0.38 | 0.079 | 0.83 | 0.85 | 0.86 | 0.86 | 0.87 |
| Kalwall Sunlite Regular | 0.040 | Kalwall Corp. | 0.38 | 0.079 | 0.81 | 0.83 | 0.84 | 0.84 | 0.85 |
| Kalwall Sunlite Premium | 0.025 | Kalwall Corp. | 0.38 | 0.078 | 0.83 | 0.85 | 0.86 | 0.87 | 0.87 |
| Kalwall Sunlite Premium | 0.040 | Kalwall Corp. | 0.38 | 0.087 | 0.77 | 0.79 | 0.80 | 0.80 | 0.80 |
| Swedlow Continuous Cast Acrylic | 0.076 | Swedlow Corp. | 0.38 | 0.070 | 0.83 | 0.86 | 0.87 | 0.88 | 0.88 |
| Swedlow Continuous Cast Acrylic | 0.103 | Swedlow Corp. | 0.38 | 0.070 | 0.84 | 0.87 | 0.88 | 0.88 | 0.88 |
| Swedlow Coated Acrylic (Cell Cast) | 0.273 | Swedlow Corp. | 0.38 | 0.058 | 0.80 | 0.85 | 0.86 | 0.87 | 0.87 |
| Acrylic Safety Glazing ANSIZ 97.1-1966.100 U | 0.224 | Sandia Stores | 0.38 | 0.068 | 0.83 | 0.86 | 0.86 | 0.87 | 0.86 |
| Lucite 147 | 0.120 | Dupont | 0.38 | NM[†] | 0.81 | 0.86 | 0.87 | 0.87 | 0.87 |
| Mylar D | 0.010 | Dupont | 0.38 | 0.112 | 0.84 | 0.86 | 0.86 | 0.86 | 0.86 |
| Mylar A | 0.002 | Dupont | 0.32 | 0.13 | 0.82 | 0.83 | 0.84 | 0.84 | 0.89 |
| Mylar A | 0.005 | Dupont | 0.38 | 0.19 | 0.74 | 0.76 | 0.77 | 0.77 | 0.78 |

*m = Effective air mass for the solar spectral irradiance.

†NM = Not measured.

D.   Program Technical Contributors[*]

Advanced Energy Project Department
G. E. Brandvold

Solar Projects Division - - - - - - - - - - - - - - - Program Support
J. A. Leonard

System Engineers
   R. L. Champion
   M. W. Edenburn
   R. W. Harrigan
   B. J. Petterson
   S. Thunborg
   L. E. Torkelson
   G. W. Treadwell

Technicians
   T. J. Bauman
   L. N. Ernst
   C. W. Matthews
   G. L. McCoach
   R. S. Rusk

System Analysis
   R. P. Stromberg
   G. V. Barton
   E. C. Boes
   B. W. Marshall
   D. E. Randall

Thermal Analysis
   M. E. Fewell
   W. H. McCulloch

Data Processing
   M. S. Hill
   W. W. Shurtleff
   T. E. Smart
   E. D. Young

Turbine Generator
   J. P. Abbin
   J. D. Cyrus

Storage Technology
   R. A. Milby

Air Conditioning
   A. V. Farnsworth

Structural Analysis and Design
   J. T. Finger
   P. P. Stirbis

Plant Engineering
   C. K. Rudy
   E. E. Rush

Theoretical Analysis
   F. Biggs
   J. F. Banas

Instrumentation and Control
   T. C. Sheives
   A. F. Veneruso

Materials Development
   Reflector Structures
      B. L. Butler
      C. B. Frost
      R. L. Lachance
      H. R. Sheppard

   Reflector Materials
      T. M. Meyer
      G. D. Miller
      R. B. Pettit

   Receiver Materials
      E. K. Beauchamp
      G. J. Kominiak
      D. M. Mattox
      R. R. Sowell

   Testing and Evaluation
      T. P. Conlon
      D. W. Miller
      L. G. Rainhart
      D. W. Tipping

[*]This list includes part-time contributors.

DISTRIBUTION:
TID-4500-R64, UC-62 (274)

American Gas Association
1515 Wilson Boulevard
Arlington, VA 22209
    Attn: Peter Susey

Argonne National Laboratory (2)
9700 South Cass Ave.
Argonne, IL 60439
    Attn: Martin L. Kyle
          Office of the Director
    Attn: Solomon Zwerdling
          Director of Solar Energy Programs

Barber-Nichols Engineering
6325 West 55th Ave.
Arvada, CO 80002

Battele Memorial Institute
Pacific Northwest Laboratory
P. O. Box 999
Richland, WA 99352
    Attn: Kirk Drumheller

Bell Laboratories
555 Union Blvd.
Allentown, PA 18103
    Attn: F. M. Smits

Associated Universities, Inc.
Brookhaven National Laboratory
Upton, NY 11973
    Attn: John Blewett

Institute of Energy Conversion
University of Delaware
Newark, DE 19711
    Attn: Karl W. Boer

Edison Electric Institute
90 Park Avenue
New York, NY 10016
    Attn: Louis O. Elsaesser
          Director of Research

Energy Research and Development   (13)
Solar Energy Division
20 Massachusetts Ave.
Washington, DC 20545
    Attn: H. Marvin
          R. Blieden
          George Kaplan (10)
          Sigmund Gronich

Energy Research and Development Adm.   (5)
Albuquerque Operations Office
Albuquerque, NM 87115
    Attn: D. L. Krenz   (3)
          R. R. Malone, SAO
          D. K. Nowlin

Envirodynamics, Inc.
3700 McKinney Ave.
Dallas, TX 75204
    Attn: J. E. Guthrie

Environmental Factors and Public Utilities Div.
Department of Housing and Urban Development
Washington, DC 20410
    Attn: Alan R. Siegel, Director

University of Idaho
Moscow, ID 83843
    Attn: H. Silha

Deputy to the Science Advisor
U. S. Department of Interior
Room 5204
Washington, DC 20204
    Attn: Martin Prochnik

Intertechnology Corporation
Box 340
Warrenton, VA 22186
    Attn: G. C. Szego, President

Lawrence Berkeley Laboratory   (2)
University of California
Berkeley, CA 94720
    Attn: Melvin Simmons
          Michael Wahlig

Lone Star Gas Company
901 S. Harwood St.
Dallas, TX 75201
    Attn: L. Hunt Sutherland

University of California
Lawrence Livermore Laboratory
P. O. Box 808
Livermore, CA 94550
    Attn: W. C. Dickinson

Congressional Research Service
Library of Congress
Washington, DC, 20540
    Attn: Harold Bullis
          Science Policy Division

Midwest Research Institute
425 Volker Blvd.
Kansas City, MO 64110
    Attn: Jerry O. Bradley

Advance Research Programs Laboratory
Central Research Laboratory
3M Center
St. Paul, MN 55101
    Attn: O. N. Salmon

DISTRIBUTION: (Cont.)

New Mexico State University
Las Cruces, NM 88001
    Attn: R. L. San Martin

University of New Mexico
Department of Mechanical Engineering
Albuquerque, NM 87113
    Attn: W. A. Cross
    For: M. W. Wilden

Northern Natural Gas Co.
2223 Dodge St.
Omaha, NB 68102
    Attn: John. M. De La Castro

Oak Ridge National Laboratory (2)
P. O. Box Y
Oak Ridge, TN 37830
    Attn: J. Johnson
          R. Pearlstein

Office of Science and Technology
Executive Office of the President
Washington, DC 20506
    Attn: Richard Balzhizer

Office of Technology Assessment
Old Immigration Building, Rm 722
119 D. Street, NE
Washington, DC 20002
    Attn: Ronal Larsen

Institute for Applied Technology
National Bureau of Standards
Room B-112 Tech (400.00)
Washington, DC 20234
    Attn: Karl Willenbrock, Director

Jet Propulsion Laboratory
Bldg 277 Rm 201
4800 Oak Grove Dr.
Pasadena, CA 91103
    Attn: V. C. Truscello

Omaha Public Power District
1623 Harney
Omaha, NB 68102
    Attn: A. R. Spangler

Public Service Co. of New Mexico (2)
P. O. Box 2267
Albuquerque, NM 87103
    Attn: Edward Kist
          G. Schreiber

The Pentagon
Room 3E114, Mail Stop 103
Washington, DC 20540
    Attn: Gus Dorough
          Deputy Director for Research and
          Advanced Technology

Solar International
300 Wyoming, N. E.
Albuquerque, NM 87112
    Attn: Roland Kurth

Southern California Gas Co.
P. O. Box 3249
Terminal Annex
Los Angeles, CA 90051
    Attn: S. Cunningham

Southern Union Gas Company
Fidelity Union Tower Building
Room 1537
1507 Pacific Avenue
Dallas, TX 75201
    Attn: J. O. Carnes

Southern Union Gas Company
723 Silver SW
Albuquerque, NM 87103
    Attn: B. D. Daugherty

Sundstrand Electric Power
4747 Harrison Avenue
Rockford, IL 61101
    Attn: A. Warren Adam

Carroll V. Kroeger, Sr.
Director, Tennessee Energy Office
Suite 250
Capitol Hill Bldg.
Nashville, TN 37219

Watt Engineering Ltd
RR 1, Box 183 1/2
Cedaredge, CO 81413
    Attn: A. D. Watt

Texas Electric Service Co.
P. O. Box 970
Fort Worth, TX 76101
    Attn: Jack A. Harris
          Marketing Services Manager

Commanding General
White Sands Missile Range, NM 88002
    Attn: STEWS-TE-NT
          Marvin Squires

| | | |
|---|---|---|
| 1100 | C. D. Broyles, | |
| | Attn: 1110 | J. D. Kennedy |
| | 1120 | G. E. Hansche |
| 1300 | D. B. Shuster | |
| 1310 | A. A. Lieber | |
| 1320 | M. L. Kramm | |
| 1325 | W. N. Caudle | |
| 1330 | R. C. Maydew | |
| 1340 | T. B. Lane | |

DISTRIBUTION: (Cont.)

1343 H. C. Hardee
1344 R. T. Othmer
1400 A. Y. Pope
2300 L. D. Smith
2320 K. Gillespie
      Attn: 2324 L. W. Schulz
2541 G. W. Gobeli
3622 T. P. Conlon, Jr.
3700 L. S. Conterno
3720 L. E. Fuller (3)
      Attn: 3732 E. G. Dylo
5000 A. Narath
      Attn: 5100 J. K. Galt
5110 F. L. Vook
5130 G. A. Samara
5150 J. E. Schirber
5200 E. H. Beckner
5231 J. H. Renken
5420 J. V. Walker
5700 J. H. Scott
5710 G. E. Brandvold
5711 R. P. Stromberg
5712 J. A. Leonard (100)
5715 R. H. Braasch
5718 M. M. Newsom
5719 D. G. Schueler
5730 H. Stoller
5740 V. L. Dugan
5800 R. S. Claassen
      Attn: 5820 R. L. Schwoebel
5830 M. J. Davis
      Attn: 5834 D. M. Mattox
5840 D. M. Schuster
      Attn: 5842 R. C. Heckman
              5844 F. P. Gerstle
              5846 E. K. Beauchamp
8100 L. Gutierrez
8180 C. S. Selvage
      Attn: 8184 A. C. Skinrood
9300 L. A. Hopkins
9330 A. J. Clark, Jr.
      Attn: 9336 J. V. Otts
9336 L. V. Otts
9340 W. E. Caldes
      Attn: 9344 J. L. Mortley
9400 H. E. Lenander
9410 R. L. Brin
      Attn: 9412 R. K. Petersen
9515 J. T. Hillman
9700 R. E. Hopper
      Attn: 9740 H. H. Pastorius
              9750 R. W. Hunnicutt
6011 G. C. Newlin
3140 C. A. Pepmueller (5)
8266 E. A. Aas (2)
3151 W. L. Garner (3)
      For ERDA/TIC (Unlimited Release)